

ZÁPADOČESKÁ UNIVERZITA V PLZNI
FAKULTA STROJNÍ

DIPLOMOVÁ PRÁCE

ZÁPADOČESKÁ UNIVERZITA V PLZNI

FAKULTA STROJNÍ

Studijní program: N 2301 Strojní inženýrství
Studijní zaměření: 2302T019 Stavba výrobních strojů a zařízení

DIPLOMOVÁ PRÁCE

Design of inner condenser - heat exchanger for R744 refrigerant

Autor: **Bc. Martin Myslikovjan**
Vedoucí práce: **Doc. Ing. Václava Lašová PhD.**

Akademický rok **2017/2018**

Declaration of Own Work

I hereby declare that this master thesis is completely my own work and I used only the cited sources.

Pilsen:

.....

Author signature

Autorská práva

Podle zákona o právu autorském. č.35/1965 Sb. (175/1996 Sb. ČR) § 17 a Zákona o vysokých školách č. 111/1998 Sb. je využití a společenské uplatnění výsledků diplomové práce, včetně uváděných vědeckých a výrobně-technických poznatků nebo jakéhokoliv nakládání s nimi možné pouze na základě autorské smlouvy za souhlasu autora a Fakulty strojní Západočeské univerzity v Plzni.

Acknowledgement

I would like to thank to my thesis supervisor Doc. Ing. Václava Lašová, PhD. and my consultant Ing. Jan Forst for assistance, time and valuable remarks.

ANOTAČNÍ LIST DIPLOMOVÉ PRÁCE

AUTOR	Příjmení Myslikovjan	Jméno Martin
STUDIJNÍ OBOR	2302T019 „Stavba výrobních strojů a zařízení“	
VEDOUcí PRÁCE	Příjmení (včetně titulů) Doc, Ing. Lašová PhD.	Jméno Václava
PRACOVIŠTĚ	ZČU - FST - KKS	
DRUH PRÁCE	DIPLOMOVÁ	BAKALÁŘSKÁ
NÁZEV PRÁCE	Navrh optimální designové definice výměníku - vnitřního kondenzátoru pro chladivo R744	

FAKULTA	Strojní	KATEDRA	KKS	ROK ODEVZD.	2018
----------------	---------	----------------	-----	--------------------	------

POČET STRAN (A4 a ekvivalentů A4)

CELKEM	105	TEXTOVÁ ČÁST	76	GRAFICKÁ ČÁST	29
---------------	-----	---------------------	----	----------------------	----

<p style="text-align: center;">STRUČNÝ POPIS (MAX 10 ŘÁDEK)</p> <p>ZAMĚŘENÍ, TÉMA, CÍL POZNATKY A PŘÍNOSY</p>	<p>Diplomová práce obsahuje úvod do problematiky tepelných výměníků autoklimatizace. V praktické části je popsán návrh výměníku – „Inner gas cooler“ pro chladivo R744 (CO₂)</p>
<p style="text-align: center;">KLÍČOVÁ SLOVA</p> <p style="text-align: center;">ZPRAVIDLA JEDNOSLOVNÉ POJMY, KTERÉ VYSTIHUJÍ PODSTATU PRÁCE</p>	<p style="text-align: center;">Výměník tepla, autoklimatizace, FEM, R744</p>

SUMMARY OF DIPLOMA SHEET

AUTHOR	Surname Myslikovjan	Name Martin
FIELD OF STUDY	2302T019 „Design of manufacturing machine and equipment“	
SUPERVISOR	Surname (Inclusive of Degrees) Doc, Ing. Lašová PhD.	Name Václava
INSTITUTION	ZČU - FST - KKS	
TYPE OF WORK	DIPLOMA	BACHELOR
TITLE OF THE WORK	Design of inner condenser - heat exchanger for R744 refrigerant	

FACULTY	Mechanical Engineering	DEPARTMENT	KKS	SUBMITTED IN	2018
----------------	------------------------	-------------------	-----	---------------------	------

NUMBER OF PAGES (A4 and eq. A4)

TOTALLY	105	TEXT PART	76	GRAPHICAL PART	29
----------------	-----	------------------	----	-----------------------	----

BRIEF DESCRIPTION TOPIC, GOAL, RESULTS AND CONTRIBUTIONS	This thesis contains an introduction to the problems heat exchangers of car air – conditioning. The main purpose of this work is design of Inner gas cooler - Heat exchanger for R744 refrigerant.
KEY WORDS	Heat exchanger, Vehicle A/C, FEM, R744, Heat pump

Content

1	Introduction	13
2	Valeo company presentation	14
3	Physical description of A/C system	15
3.1	Introduction	15
3.2	Basic thermal cycle.....	15
3.3	The cooling cycle.....	17
3.3.1	Diagram description	17
3.3.2	Basic cooling cycle.....	18
3.3.3	Complex cooling cycle description	19
3.3.4	Real cooling cycle description	21
3.4	Heat calculation of the main parameters in the cycle	22
3.4.1	Evaporator	22
3.4.2	Compressor.....	23
3.4.3	Condenser.....	24
3.4.4	TXV - thermo expansion valve (throttle).....	25
3.4.5	COP – Coefficient of performance.....	25
4	A/C components in the vehicle layout	26
5	CO ₂ as a refrigerant	28
5.1	Refrigerant used in car A/C – historical overview	28
5.2	Benefits of CO ₂ refrigerant	29
5.3	Comparison of CO ₂ vs. R134a.....	30
5.3.1	Thermo dynamical cycle comparison	30
5.3.2	COP comparison	30
5.3.3	CO ₂ thermodynamic cycle in supercritical zone	33
5.3.4	Heat transfer coefficient, density, saturation pressure comparison.....	34
5.4	Conclusion	36
6	Heat pump technology	37
6.1	Idealised circuiting	37
6.2	Real vehicle circuiting	38
7	Heat exchangers	40
7.1	Heat exchangers basic calculation.....	41
7.1.1	Heat balance equation	41
7.1.2	Equation of heat transfer (Newton’s law of cooling).....	42

7.2	HEAT TRANSFER FROM FINNED SURFACES	45
8	Convection theory	48
8.1	Nusselt number - Nu	48
8.2	Prandtl number - Pr	48
8.3	Reynolds number - Re	51
8.4	Heat transfer enhancement of heat exchangers	53
9	Aluminium brazed heat exchangers	55
9.1.1	Advantages of Aluminium Heat exchangers.....	55
9.1.2	Design of Aluminium heat exchangers	55
9.1.3	Aluminium brazed heat exchangers manufacturing.....	57
9.1.4	Aluminium brazed heat exchangers material	60
10	Task specification: Inner gas cooler requirements	63
11	Available Heat exchangers research	65
11.1	LUCIE - Evaporator.....	65
11.2	R744 Evaporator	66
11.3	R744 – Outer cooler.....	68
11.4	Decision matrix	68
12	R744 – Evaporator redesign	69
13	FEM – Mechanical robustness of R744 evaporator	72
13.1	Material inputs	73
13.2	Mechanical calculation	74
13.2.1	Tank sub-assembly	74
13.2.2	Flat tube.....	76
13.2.3	Connector sub-assembly	78
13.2.4	Pipe.....	80
13.2.5	FEM summary.....	81
14	IGC design.....	82
14.1	Tank design.....	82
14.2	Flat tube design	85
14.3	Real mechanical test	85
14.3.1	Burst test.....	86
14.3.2	Pressure cycle test	87
14.3.3	Mechanical test conclusion	88
15	Inner gas cooler geometry optimisation in terms of heating performance.....	89
15.1	Dymola Interface and inputs definition	89

15.2	Dymola Calculation	91
15.3	15.3 Prototypes build	94
16	Heat performance and air temperature unbalance measurement	96
16.1	Testing device description	96
16.2	The measurement procedure	98
16.3	Heat rejection performance evaluation	98
16.4	Air temperature unbalance (dT) evaluation	99
16.5	Prototype samples measurement results	100
16.6	Measurement conclusion	101
17	Possible steps of other development	102
18	Conclusion.....	103
Sources:		104
List of appendices:		105

List of symbols and abbreviations

Symbols

Symbol	Name	Unit
a_t^k	Specific isotropic work consumed by the compressor	J/Kg
c	Specific heat capacity	J/Kg.K
COP	Coefficient of performance	-
D_h	Hydraulic diameter	m
dP	Air pressure drop	Pa
dT	Temperature unbalance	°C
E	Young modulus	Gpa
h	Specific enthalpy	J/Kg.K
k	Overall heat transfer coefficient	$W.m^{-2}.K^{-1}$
l	Latent heat	J/Kg
L_c	Characteristic length	-
m	Mass flow	Kg/h
M_{ref}	Refrigerant mass flow	kg / h
MA	Air mass flow	kg /h
Nu	Nusselt number	-
P	Pressure	bar
Pk	Consumption of adiabatic coolant compression	W
Pr	Prandtel number	-
PRIGI	Pressure refrigerant inner gas cooler inlet	bar
PRIGO	Pressure refrigerant inner gas cooler inlet	bar
Q_0	Cooling performance	W
q_0	Specific cooling capacity	J/Kg.K
Q_k	Condenser heat rejection	W
q_k	Specific heat energy rejected by condenser	J/Kg.K
R	Thermal resistance	K/W
Re	Reynolds number	-
Rm	Ultimate strength	MPa
$RP_{0,2}$	Yield strength	MPa
s	Specific entropy	J/Kg.K
S	Surface	m^2
T	Temperature	°C
TAIRI	Temperature air Inner gas cooler inlet	°C
TRIGI	Temperature refrigerant inner gas cooler inlet	°C
TRIGO	Temperature refrigerant inner gas cooler outlet	°C
v	Velocity	$m.s^{-1}$
α	Convection heat transfer coefficient	$W/m^2.K$

Symbol	Name	Unit
η	Kinematic viscosity	$\text{m}^2 \cdot \text{s}^{-1}$
μ	Dynamic viscosity	$\text{Kg} \cdot \text{m}^{-1} \cdot \text{s}^{-1}$
ρ	Volumetric mass density	kg/m^3
ϕ	Mutual flow coefficient	-
λ	Thermal conductivity	$\text{W} \cdot \text{m}^{-1} \cdot \text{K}^{-1}$

Abbreviations

Abbreviation	Meaning
IGC	Inner gas cooler
CO ₂	Carbone dioxide
R744	Refrigerant - Carbone dioxide
A/C	Air conditioning
HVAC	Heat ventilation and air conditioning
PTC	Positive temperature coefficient - heater using this physical phenomenon
HEX	Heat exchanger
RnD	Research and development
R134a	Type of refrigerant
R1234yf	Type of refrigerant
OCR	Oil circulation rate
TXV	Thermo expansion valve
GWP	Global warming potential
HP	Heat pump
LMTD	Log mean temperature difference
NTU	Number of transient unit
CAB	Controlled atmosphere brazing
clad	Brazing material
Burst test	Static pressure test
Pressure cycle	Fatigue pressure test
LUCIE	Evaporator type
LLA	Long life alloy
FP	Fin pitch
FEM	Final element method

1 Introduction

So called „Dieselgate“ fully showed the limits of car makers in reduction of combustion engines emissions which is required worldwide. For many years it has been discussed that decreasing world reserves of oil will lead to the end of combustion engines history. Out of this new phenomenon of our age – Tesla Company and its success showed possible future of personal transport – electrical vehicles. In response to that almost all of the world car makers started huge investment of resources into development of this new technology - the race on the field of electrical vehicles has started.

There are two main factors which limit electrical vehicles. The first one is non-existing battery charging infrastructure. The second one is electric car range. To prolong car range the development mainly focuses on increasing capacity of batteries used in electrical vehicles but also other factors are taken into account. One of this factor is to reduce energy consumption of passenger comfort systems such as heating and air conditioning (covered by term in common usage: HVAC - Heating ventilation and air conditioning) which actually steal significant amount from possible car range. Especially heating operation is problematic for electrical cars compared to combustion engine cars. While the combustion engines cars use for cabin heating heat exchangers where the coolant is heated by waste heat produced by engine for free, the electrical cars must use for heating their battery power. The most common system for electric car heating is PTC (positive temperature coefficient) heater. This is fully electrical component which directly changes electrical power to heat power with pure efficiency. That makes car range very low in winter period. There is an alternative to PTC. Heat pump system which is already fully established in the field of building heating seems to be solution how to improve heating efficiency and prolong the car range. In race for HVAC efficiency various ways are investigated and there is special focus on refrigerants. Amongst all refrigerants used, the R744 / CO₂ (carbon dioxide) seems to be the best option in terms of efficiency but there is lot of work in terms of components development as this is completely new solution for automotive industry.

This diploma thesis deals with design development of Inner gas cooler – heat exchanger for car using R744 refrigerant heat pump system. In the theoretical chapters there are described the physical function of the cooling cycle and the heat pump and further traditional HVAC components are introduced. The comparison between R744 and conventional refrigerants is done to explain R744 benefits. Theoretical chapters describe physical characteristics of heat exchangers and also heat convection theory. The main equations of heat convection theory will be explained as they are important for software which is used for heat exchangers designing in this thesis. The theoretical part of the thesis also describes material and components used in aluminium brazed heat exchangers.

Practical part is focused on evaluation of feasibility to use some of current heat exchangers components and their optimisation. This is done by FEM (finite elements method) and 1D thermal calculator.

Based on the results of FEM and 1D functional prototypes are built and tested. All observations and results are recorded in this thesis. The outcome of the thesis is proposal of optimal solution for heat exchanger which could be used for electrical vehicles.

2 Valeo company presentation

The presented thesis describes the project which was assigned to me by the Research and development department (RnD department) of Valeo výměky tepla k.s (ZebraK). This company to be briefly described in few following paragraphs.

The Valeo is international automotive group focused to development, production and sales of components, integrated systems and modules for cars and trucks. In the Czech republic are three plants with associated offices for product and its industrialization development (ZebraK, Humpolec, Rakovnik) and one office fully dedicated for development vehicles intelligent control systems in Prague.

Valeo výměky tepla k.s - ZebraK is the branch of Valeo company and focus to development and production of Heat exchangers to vehicles HVAC units for passenger comfort and well - being. The main products are actually evaporators but production of EGR (Exhaust Gas Recirculation) coolers already started and Valeo ZebraK feel big opportunity in product of family eletrical cars heat exchangers.

Valeo výměky tepla k.s – ZebraK has actually 880 employees, the company supply 19 caremakers and yearly production is 6.8 million of heat exchangers. The RnD departmentowns Material and corrosion laboratory, Mechanical and heat performance laboratory, Metrological laboratory and Prototype shop for prototypes assembly.



Figure 2-1: Valeo ZebraK product portfolio



Figure 2-1: Valeo ZebraK – main indicators

3 Physical description of A/C system

3.1 Introduction

The energetics devices as Air conditioning (A/C) and Heat pumps are actually widely spread in many technical applications. A/C is today common equipment for most of the new cars and with the introduction of electrical vehicles also Heat pump systems seems to be way how to secure heating of vehicle cabin at acceptable level power consumption.

In this chapter to be briefly explains physical basis of A/C – Heat pump function. A/C components used in vehicles to be described as well. Then comparison between actually most common used refrigerant in vehicles - R134a and „rediscovered“ refrigerant R744 (CO₂) to be done where will be focused to benefit of R744 as this is refrigerant used for heat exchanger which will be designed in practical part of this thesis.

3.2 Basic thermal cycle

The A/C circuit used in cars is generally identical as the cooling circuits used in other industries. The A/C circuit is mostly theoretically explained on the example of the reverse operation of the heat engine. The main difference between the heat engine and the cooling machine is that for heat engine is heat recovered from hot medium and this heat is used for production of work. On contrary for cooling machine the work is fed into the system in sense to transfer heat from the colder medium to warmer as according to the second law of the thermodynamics, the heat cannot spontaneously move from a colder medium to warmer.

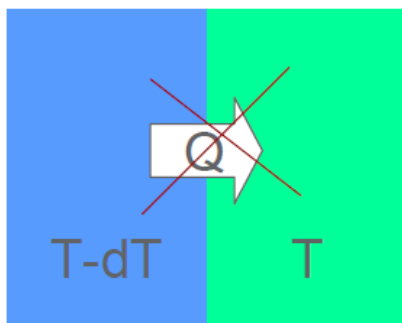


Figure 3-1: Vizualization of 2nd law of Thermodynamics [1]

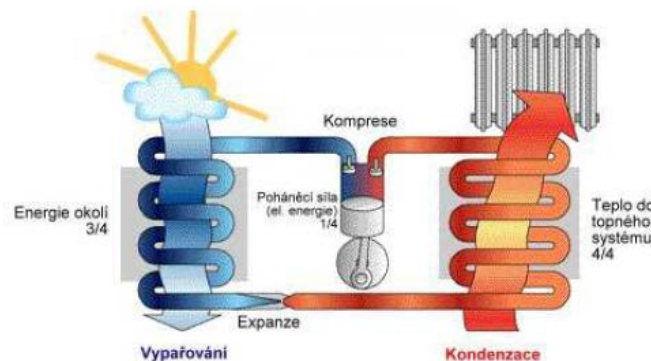


Figure 3-2: A/C cycle [1]

The work is brought into circuit by compressor, where the refrigerant is pumped to a higher pressure level (compressed) and then released into the condenser. There is an interaction (heat exchange) between cooling medium inside the condenser (coolant) and the medium outside of the condensers (air). In the condenser is rejected latent heat and condensation process is on-going. Than condensed refrigerant passes through the expansion valve into the evaporator where at lower pressure and lower temperature it receives heat from the environment and evaporates. The boiling point of the refrigerant corresponds to the evaporator pressure. Then the refrigerant continues to the compressor again and the cycle is repeated. The cooling circuit is divided to a low-pressure and a high-pressure branch where the individual pressures in the low and high pressure branches depend on the type of used

refrigerant. Lower than atmospheric pressure (1 bar) is not particularly suitable due to risk of air entrance to into the circuit, if the leaks occur. Liquid refrigerant flows from the higher pressure vessel (condenser) into the evaporator with a low pressure. The flow control to ensure that the refrigerant always enters the compressor in the gas phase is provided by the expansion valve, where the compressor is throttled by compressing the compressed energy.[3]

From the physical point of view are basic A/C function explained on the example of Carnot cycle. Carnot cycle has the maximum possible efficiency for given border temperatures T_{\max} and T_{\min} . It consists of two isoentrops (1 - 2) and (3 - 4) together with two isotherms (2-3) and (4-1) (Figure 3-3). During isothermal compression (4 - 1), the heat enters to the system. This heat essentially determines the final cooling capacity of the device. Adiabatic compression (1 - 2) is followed by increasing the pressure and temperature of the medium. Medium is pumped to a higher pressure level and it reaches the maximum temperature T_{\max} . During isothermal compression (2 - 3), is heat rejected to surroundings. The entire circulation is then closed by adiabatic expansion (3 - 4) in which it returns to the original temperature level T_{\min} . [2]

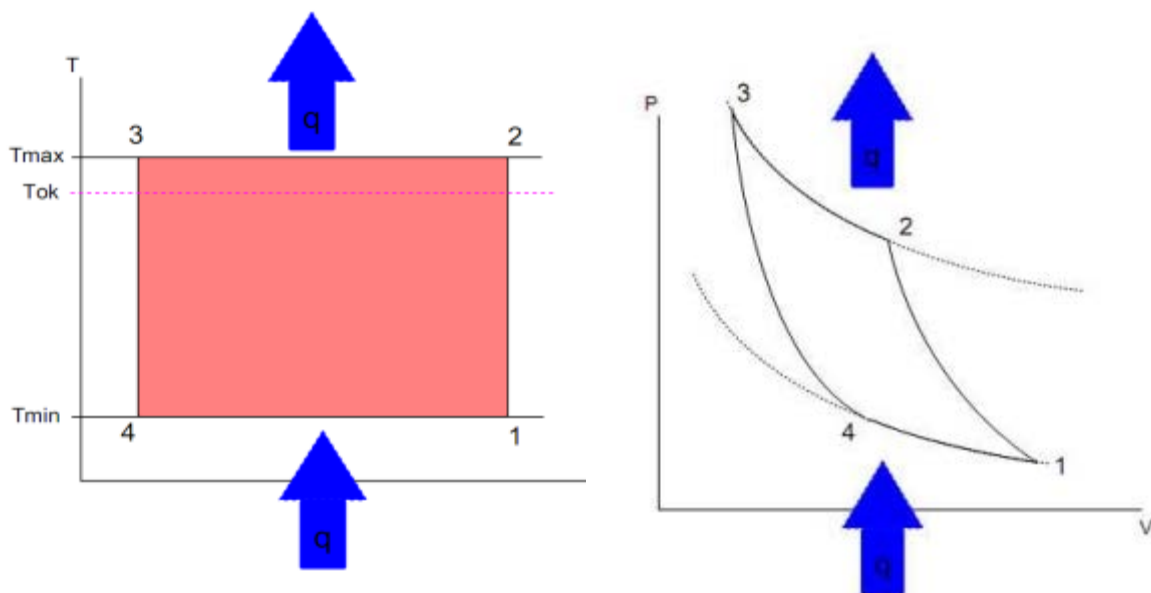


Figure 3-3: Carnot cycle [2]

3.3 The cooling cycle

3.3.1 Diagram description

The thermal $\log P - h$ diagram is used in cooling description. First, an explanation of how the diagram is built up is given, and then its use is described. Figure 3- 4 shows the principle of a $\log P-h$ diagrams, and indicates the refrigerant's various thermodynamic states. This diagram can be seen as a map of the refrigerant. The area above and to the left of the saturation line for liquid (A-CP in Figure 3-4) is the area where the refrigerant is sub-cooled, i.e. the temperature is lower than the saturation temperature for the pressure range in question. The area above and to the right of the saturation line for gas (CP-B in Figure 3-4) is the area where the gas is superheated, or overheated, i.e. the gas has a higher temperature than the saturation temperature at that pressure. The area below the saturation lines for liquid and gas (A-CP-B in Figure 3-4) represents the conditions where the refrigerant can change its state of aggregation from liquid to gas or vice versa. Hence, there is a mixture of gas and liquid. The practical meaning of the critical point (CP) is that at temperatures higher than this, the refrigerant cannot be condensed, no matter how high the pressure. Therefore, compression refrigeration systems normally operate at temperatures below the critical one. Lines of constant temperature (isotherms) are vertical in the sub-cooled liquid region, horizontal (i.e. parallel to the constant pressure lines) in the liquid + vapour mixture region, and drop steeply towards the enthalpy axis in the superheated gas region (see Figure 3-5). The constant pressure lines (isobars) are parallel to the x-axis. [5]

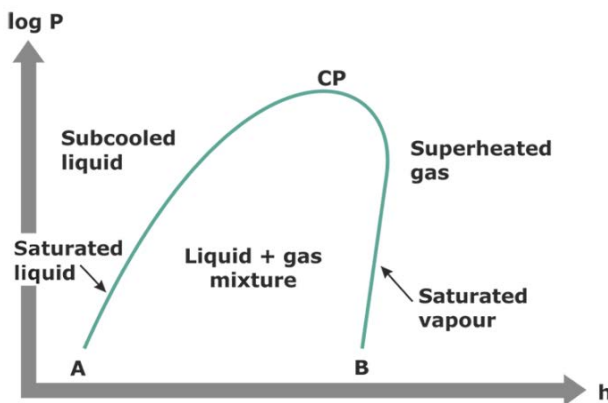


Figure 3-4: $\log P-h$ diagram description [5]

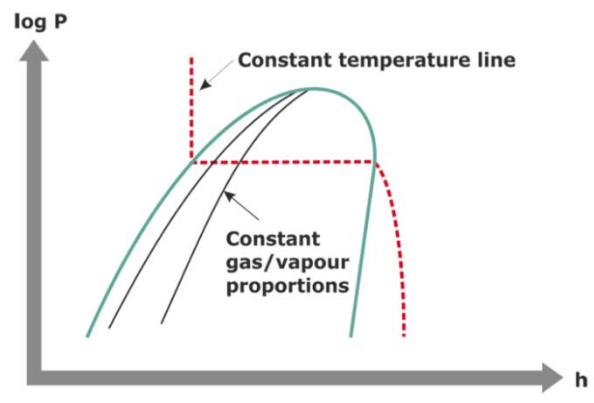


Figure 3-5: $\log P-h$ diagram with isotherm line [5]

The T-s diagram can also be seen in refrigeration technology. Its characteristic shape and typical the state variables are shown in Figure 3-6.

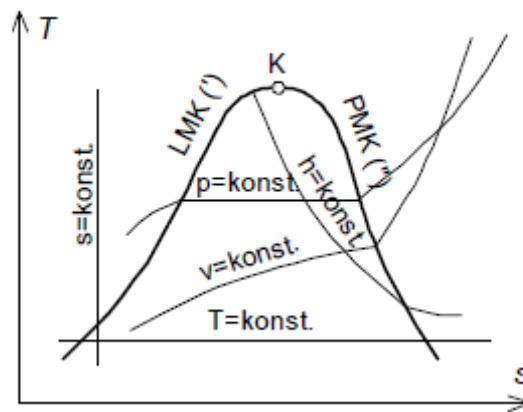


Figure 3-6: T- s diagram with isotherm line [5]

3.3.2 Basic cooling cycle

Usually the cooling cycle as well automotive air condition cycle is modelled with help of reversed Clausius - Rankin's cycle. Clausius – Rankin cycle is one of the most used cycle with medium phase change. This cycle in no reversed version is used for modelling of steam turbine function. For better visualization, the cycle is displayed mostly in log P-h diagram (Pressure – specific enthalpy) and sometimes also in T – s (Temperature – specific entropy) diagram).

On the initial phase of the cycle the heat is removed from surrounding (in our case the air) to the evaporator. The coolant enters to the evaporator the in the wet steam state and when it completely evaporated it receives a large amount of heat from the cooled ambient (air) (section 4 - 1). Slightly superheated steam then enters the compressor, where it is ideally pressed adiabatically to the pressure p_2 (1 - 2). The high pressure steam passes through a condenser in which is rejected latent heat and steam phase is changed to liquid phase (2 to 3). To increase the cooling power, the so-called sub cooling of the liquid emerging from the condenser (3'-3) is used. This move the point in which is doing gas throttling more to the left and as a consequence it leads to increase of the specific enthalpy difference $h_1 - h_4$. The slightly sub cooled liquid then loses its compressed energy when passing through the expansion (throttling) valve where coolant is partially liquefied and cooled down. Than the coolant is returned to the evaporator (3-4) and cycles is repeated. The temperature in the evaporator must be as low as possible, but at the same time it must not freeze, ie approximately 0°C . Cooling performance is determined by the enthalpy difference.

This fundamental process could be described by following thermodynamic process:

(1-2): The compression is performed at constant entropy.

(2-3): The condensation is performed at constant pressure and so it follows the isobars.

(3-4): The lowering of the pressure is performed at constant specific enthalpy (h).

(4-1): The evaporation is performed at a constant pressure and so it follows the isobars, i.e. the pressure at; states 1 and 4 = the evaporator pressure (temperature). State 1 is determined by the temperature of the gas leaving the evaporator.

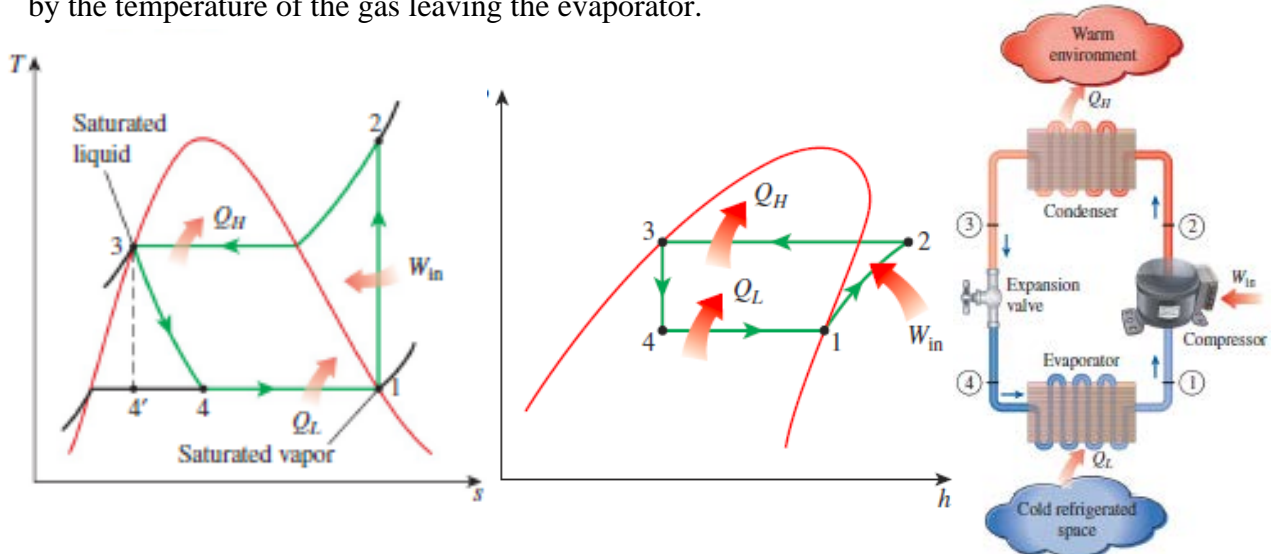


Figure 3-7: Reversed Clausius – Rankin reversed cycle in T-s, P-h diagram, [15]

3.3.3 Complex cooling cycle description

It's important previous description was considerably simplified. In reality the pressure drops (dP) occurs in the evaporator also condenser and also dP in piping must be considered. There not must considered also mechanical and electrical losses in the compressor. The consequences are increased operational and maintenance expenses. However, some measures can be taken to minimize the costs.

In the fundamental cycle description, the gas entering the compressor was assumed as a dry and saturated. In reality, the gas is overheated as described in Figure 3-8 (point 1.2). The overheating is the difference between the temperatures at points 1.1 and 1.2 in the figure and is done in the end of the evaporator. There is a practical demand to allow the refrigerant vapour to become superheated to prevent the carry-over of liquid refrigerant into the compressor, where it may cause severe damage due to its incompressibility. It may also contaminate the lubricants. The level of superheating should be kept on a minimum level to minimize both the work to be done by the compressor and the necessary heat transfer surface in the evaporator.

In the fundamental process, the liquid leaving the condenser was just on the saturation line for liquids. The pressure drop in the pipes, filters, etc., before the expansion valve is negligible, but still causes "flash gas", i.e. vaporization of a small part of the liquid. The

condensed liquid is therefore sub-cooled to a temperature below that of the saturation temperature corresponding to the condenser pressure, for two reasons: the cooling capacity of the refrigeration process is increased and the risk of gas bubbles in the flow fed to the expansion valve is avoided. (Gas bubbles in the inlet flow to the expansion valve disrupt the regulation mechanism.) The sub-cooling is the difference between the temperatures at points 3.1 and 3.2 in picture: , and is generated in the condenser or in a separate heat exchanger after the condenser. In the real refrigeration process, compression does not follow the lines of entropy – Figure 3-8 as it does in the ideal, fundamental process. This means that the compression work increases. The ratio of the theoretical to the real compression work is called the isentropic efficiency. [5]

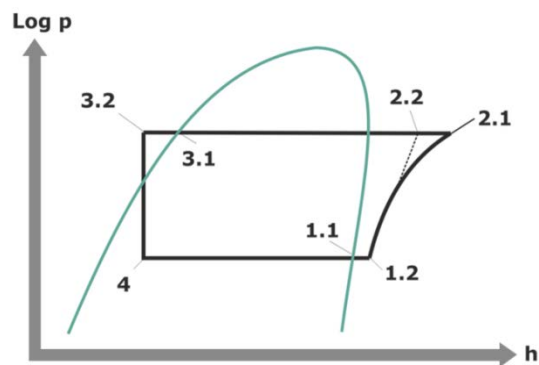


Figure 3-8: Complex cooling cycle – pressure drops in HEX's not taken in to account [5]

3.3.4 Real cooling cycle description

The cycle described by Figure 3-9 is already close to the reality but some influences was not considered still. Firstly (as was already mentioned) there are pressure drops (dP) in both heat exchangers (evaporator, condenser) in the cycle and so condensation (evaporation) is not fully isobaric. In the real A/C system is not only pure refrigerant but the mixture of refrigerant and the oil as is necessary to lubricate movable parts of compressor. The oil influences to the cycles are described in the Figure 3-9 and table 3-10. Now we finally can say that cycle is fully described.[8]

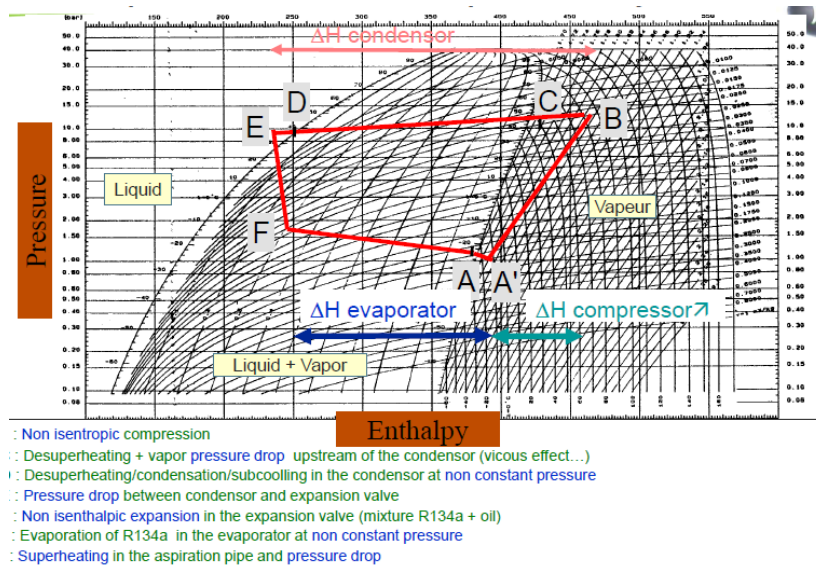


Figure 3-9: Real cooling cycle [8]

IMPACT	COMMENT
- Oil properties	Ensure the miscibility of the oil in the refrigerant to secure the return of oil in the compressor
- Pressure drop increase	oil film on the walls / increase of viscosity of the mixture
- Heat transfer limitation	Desuperheating zone + condensation (condenser) Superheating zone (Evaporator)
- Effective refrigerant flowrate	$Q_{R134a} = (1 - OCR) Q_{measured}$
- Reduction of the refrigerant flowrate (Deformation of the theoretical cycle)	Expansion is an isenthalpic phenomenon, so during expansion, oil is cooled by evaporation of a certain quantity of liquid R134 $P_{pipe_effective} = (1 - OCR) Q_{measured} (\Delta H_{EV} - OCR C_{p,oil} (T_{e-Ts} - T_{e-EV}))$

Table 3-10: Oil influence to cycle [8]

As was showed on the previous page amount of oil in the system significantly influences cycle and also performance of each single component. Due to this the amount of oil must in the A/C loop must be recorded and quantified. Due to this the refrigerant engineers work with term OIL CIRCULATIO RATE (OCR). For OCR the equation below is valid.[8]

$$OCR = \frac{\text{oil flowrate}}{\text{total flowrate}}$$

3.4 Heat calculation of the main parameters in the cycle

3.4.1 Evaporator

Supplying the heat flow (heat removed) Q_0 from the cooled environment to refrigerant under the isobaric isothermal process in which the refrigerant is in the state wet vapour ($x < 1$) (4) and completely vaporizes and changes into the fully saturated vapour ($x=1$) (1).

$$dq = dh + da_t = dh - v dp \quad | dp = 0$$

$$\int_4^1 dq = \int_4^1 dh$$

$$q_0 = h_1 - h_4$$

$$\dot{Q}_0 = \dot{m} \cdot (h_1 - h_4)$$

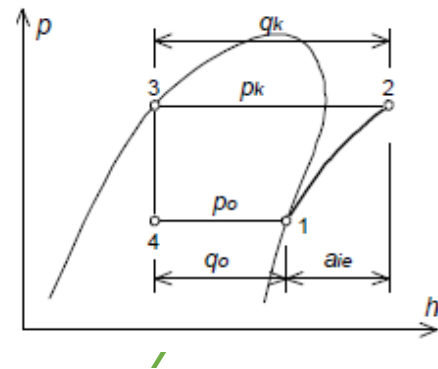


Figure 3-11: Log P-h diagram – focus to evaporator

Q_0 – Cooling performance [W]

This is the heat performance (heat output) of the evaporator

q_0 – Specific cooling capacity [J/Kg]

It represents the amount of heat that holds up to 1 kg of refrigerant, which changes its state from the wet steam state at the vaporizer inlet to the saturated steam on output.

$$q_0 = \frac{\dot{Q}_m}{\dot{m}} = h_1 - h_4 \vee q_m = l \cdot (1 - x_4) = (h_1 - h_5) \cdot (1 - x_4)$$

Where l is a specific latent heat [9]

3.4.2 Compressor

The purpose of the compressor is suction of saturated refrigerant under saturation pressure and temperature (p_0 and t_0). Compressor also compress the exhaust refrigerant vapour to the p_k pressure at which it is running condensation at a temperature higher than the highest temperature of cooled ambient (to heat transfer could run)

Specific isotropic work of the compressor is expressed by the following equation:

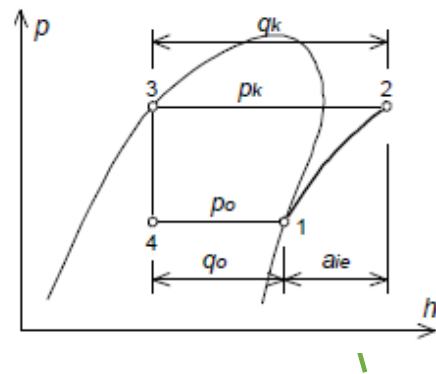


Figure 3-12: Log P-h diagram – focus to compressor

$$dq = dh + da_t \quad | \quad dq = 0$$

$$\int_1^2 da_t = - \int_1^2 dh = \int_2^1 dh$$

$$a_t^K = h_1 - h_2$$

$$P^K = \dot{m} \cdot a_t^K$$

a_t^k – specific isotropic work consumed by the compressor [J/Kg]

The adiabatic work of refrigerant compression in the compressor that passes as heat energy into the refrigerant.

P^k - Consumption of adiabatic coolant compression [W] [9]

3.4.3 Condenser

The condenser is a heat exchanger where the heat exchange takes place between the compressed refrigerant vapour and coolant and thereby condenses coolant vapours. Outlet the heat flow Q_k from the refrigerant to the cooling substance takes place under constant pressure

$$dq = dh + da_t = dh - v dp \quad | dp = 0$$

$$\int_2^3 dq = \int_2^3 dh$$

$$q_k = h_3 - h_2$$

$$\dot{Q}_k = \dot{m} \cdot (h_3 - h_2) = \dot{m} \cdot q_k$$

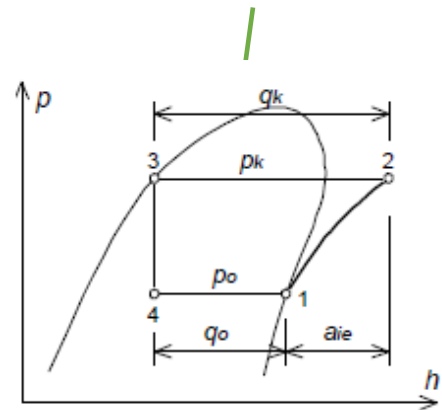


Figure 3-13: Log P-h diagram – focus to condenser

q_k – Specific heat energy rejected by condenser [KJ/kg]

It represents the amount of heat that holds up to 1 kg of refrigerant, which was brought in refrigerant by evaporator (q_0) and following compressor work $q_k = q_0 + a_k$

Q_k - This is the heat rejection performance (heat output) of the condenser [W]

On base Energy Conservation Act for a closed cycle implies that the energy brought into circulation (per unit of time) is equal to the energy from the cycle rejected: $Q_k = Q_0 + P^k$ [6].

3.4.4 TXV - thermo expansion valve (throttle)

The purpose of TXV is to reduce the refrigerant pressure from the condensation pressure (p_k) to the vaporization pressure (p_o) in the evaporator. Throttling is done in part in which flow rate is resistance equal to the pressure difference ($p_k - p_o$). This is caused by a significant reduction of the valve flow cross section.[9]

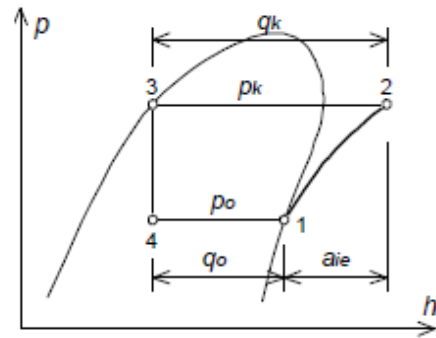


Figure 3-14: Log P-h diagram – focus to TXV [6]

As there is no heat exchange with surroundings $dq = 0$

Also no work is performed $da_t = 0$

Based on previous assumption following equation below is valid:[9]

$$0 = \int_3^4 dh$$

$$0 = h_4 - h_3$$

$$h_4 = h_3$$

3.4.5 COP – Coefficient of performance

The coefficient of performance – COP or ε (is used in the Czech literature) is a ratio of useful heating or cooling provided to work required. Higher COP is equal to lower operating costs and so goal of every A/C system designer is to reach the highest COP as is possible. The COP usually exceeds 1 and 2 types of COP are determined:

$$1) \text{ COP}_{\text{heat}} = \frac{T_1}{T_2 - T_1} = \frac{q_k}{a_k^t}$$

$$2) \text{ COP}_{\text{cool}} = \frac{T_2}{T_2 - T_1} = \frac{q_o}{a_k^t}$$

4 A/C components in the vehicle layout

The condenser is located in the front module of the car (mask), usually in front of the car front radiator-engine cooler (only used for car with standard combustion engine). For cars with combustion engine the compressor is located close to a car engine because it is driven by a engine belt. Whereas electrical cars use compressor with independent electrical engine.

The expansion valve is located behind the wall that separates the crew from the engine (firewall) and is mounted on the evaporator tubes, which is placed in the plastic box (HVAC) behind that wall. The HVAC also includes heating, air flow control valves, and then a fan that fumes through the evaporator, or the heater into the car cabin.

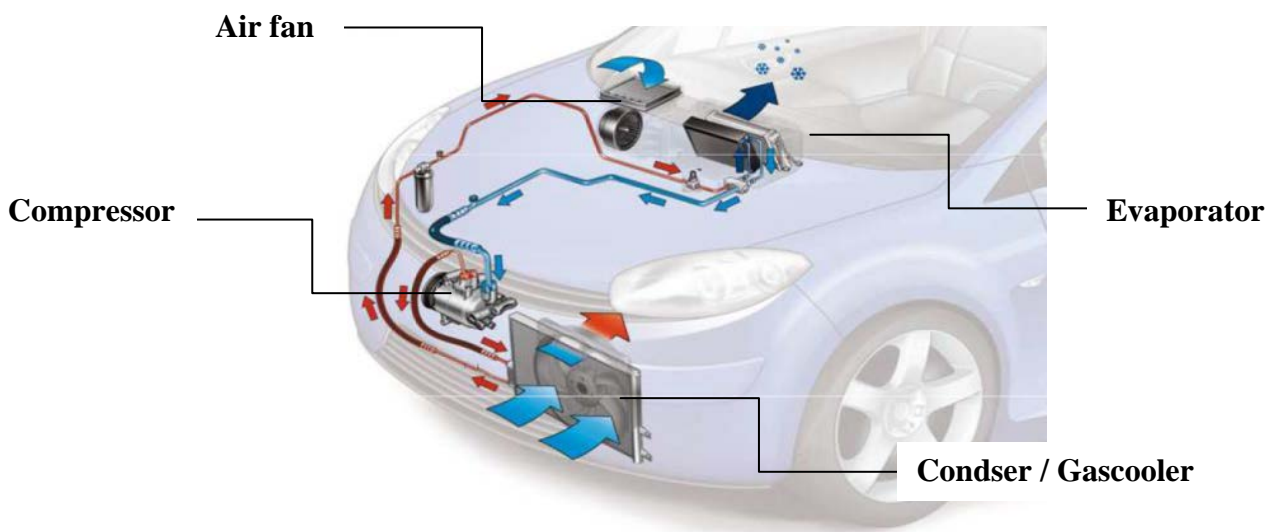


Figure 4-1: A/C components Car layout [8]

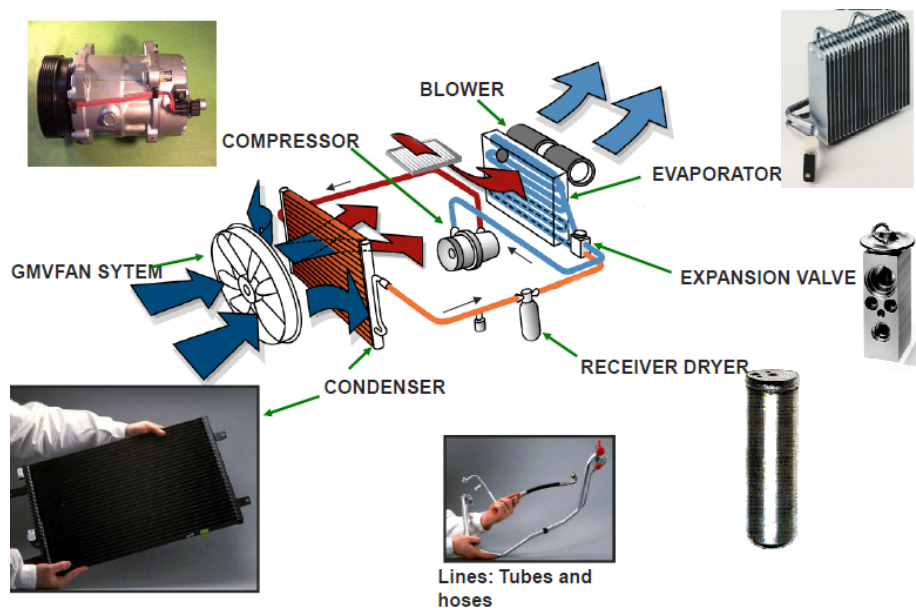


Figure 4-2: A/C coponents description [8]

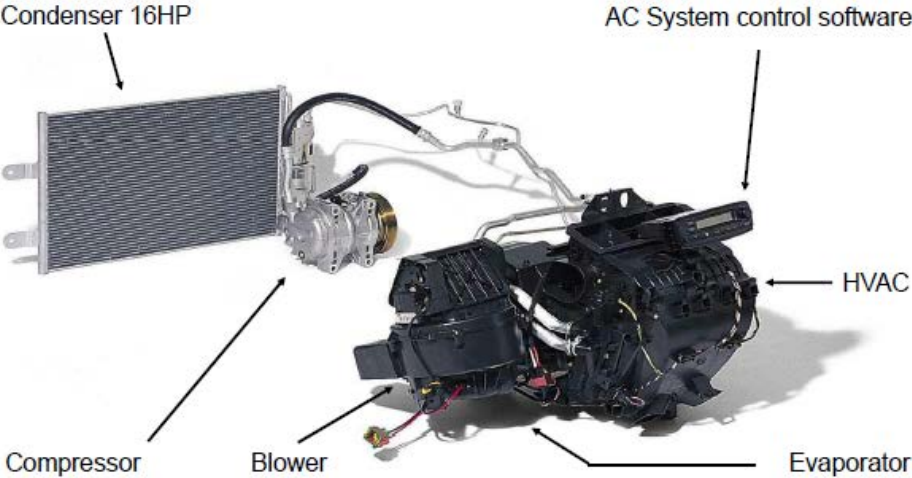


Figure. 4-3: Photo of real A/C components[8]

5 CO₂ as a refrigerant

5.1 Refrigerant used in car A/C – historical overview

In the early days of refrigeration the two refrigerants in common use were ammonia and carbon dioxide (CO₂). However both of them were problematic. Ammonia is toxic and CO₂ requires extremely high pressures (from around 30 to 200 bars!) to operate in a refrigeration cycle, and since it operates on a trans critical cycle the compressor outlet temperature is extremely high (around 160°C). When Freon 12 (dichloro-difluoromethane) was discovered it totally took over as the refrigerant of choice. It is an extremely stable, non-toxic fluid, which does not interact with the compressor lubricant, and operates at pressures always somewhat higher than atmospheric, so that if any leakage occurred, air would not leak into the system, thus one could recharge without having to apply vacuum. [10]

Unfortunately when the refrigerant does ultimately leak and make its way up to the ozone layer the ultraviolet radiation breaks up the molecule releasing the highly active chlorine radicals, which help to deplete the ozone layer. Freon 12 has since been banned from usage on a global scale, and has been essentially replaced by chlorine free R134a (tetrafluoroethane) - not as stable as Freon 12, however it does not have ozone depletion characteristics. R134a has been for a relatively long time used by all cars manufacturer as HVAC refrigerant without problems. [10]

Recently, however, the international scientific consensus is that Global Warming is caused by human energy related activity, and various man made substances are defined on the basis of a Global Warming Potential (GWP) with reference to carbon dioxide (GWP = 1). R134a has been found to have a GWP of 1300 and has been banned in Europe for all new cars manufactured after 2017. [10]

Chemical companies DuPont and Honeywell have in joint venture developed a refrigerant that meets the requirements of the European Commission's regulations. This refrigerant name is R-1234yf and its GWP = 4 which is a significant improvement to the R-134a. The pressure in cycles are very similar to R-134a, and the advantage is also the fact that the amount of coolant in the cooling circuit is about 5% lower vs. R-134a. What is the biggest benefit of R-1234yf is that due to close chemical and physical properties it is possible to use (with really small modification) all A/C components (Heat exchangers, compressors, A/C lines etc.) which was originally used for R-134a refrigerant. This was really welcomed by all car manufacturers which could simply carry over all this components and so prevent to finance costly development of new A/C components. [10]

The problem rise with its hazard classification. The R-1234yf refrigerant is classified as "heavily flammable ". Due to this there was quite hot discussion between care refrigerant experts where one group declared flammability of R-1234yf as a big risk in case of car crash as car crew could be in danger by fire.

This is a significant negative factor for safety and its use in automobiles. However, within the prescribed tests, this refrigerant was not classified as unsuitable in automotive air conditioners and is actually used for all the new cars (if the R744 technology is not used). Anyway this coolant is "suspicious" and strongly focused especially by German car makers

which together with their suppliers made a strong effort to find replacement for R-1234yf. [10]

5.2 Benefits of CO₂ refrigerant

Due to the reasons described before the new topic is to return carbon dioxide as a refrigerant. The previous two major problems of high pressure and high compressor temperature are found in fact to be advantageous. The very high cycle pressure results in a high fluid density throughout the cycle allowing miniaturization of the systems (heat exchangers, pipes etc.) for the same heat pumping power requirements. Furthermore the high outlet temperature will allow instant defrosting of automobile windshields. Other parameter which must not be forgotten is much lower price of CO₂ refrigerant vs. R-1234yf.

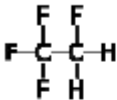
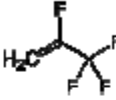

Refrigerant	R-134a	R-1234yf	R-744
Formula			
Name	1,1,1,2-Tetrafluoroethane	2,3,3,3-tetrafluoropropène	CO ₂
Type	Hydro Fluoro Carbone (HFC)	Hydro Fluoro Olefin.	Natural
Mass	102 g/mol	112 g/mol	44 g/mol
Critical T°	101 °C	95°C	31°C
Flammability	Non Fammable	Low Fammable	Non Fammable
GWP	1430	4	1

Figure 5-1: Comparison of refrigerans properties [8]

5.3 Comparison of CO₂ vs. R134a

5.3.1 Thermo dynamical cycle comparison

In the Figure 5-1 was presented basic properties of all three refrigerants. But to understand differences of CO₂ refrigerant (potential car refrigerant) vs. R134a – refrigerant used in the CAR nowadays to be good to show their operating conditions. Typical operating conditions are showed on the Log P-h diagram. For direct comparison to be evaporation temperature set up for both cycles to $T = 5\text{ }^{\circ}\text{C}$

AC Mode Cycle for $T_{\text{evaporation}} = 5\text{ }^{\circ}\text{C}$

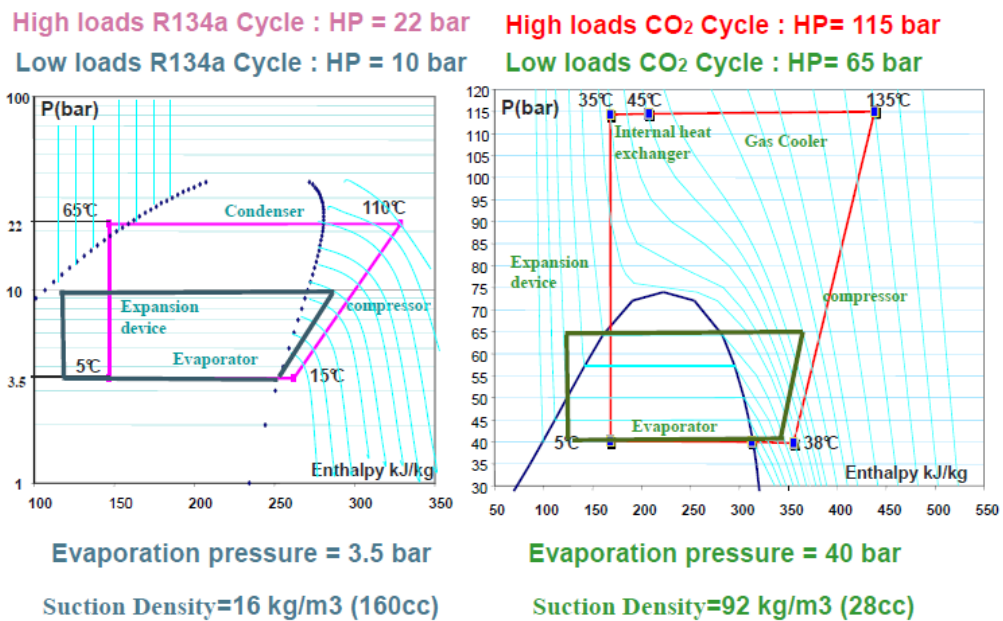


Figure. 5-2: Comparison of refrigerants properties [8]

From the comparison is visible significant differences of evaporation pressure to reach evaporation temperature $^{\circ}\text{C}$ – 3.5 bar for R-134a vs. 40 bar for CO₂. Also this cause 22 bars for high loads condensation – R134a vs. 115 bars for high pressure heat exchanger for CO₂. Higher temperature and pressure leads to different values of refrigerant density and viscosity as well. From this is clear that for CO₂ A/C system the heat exchangers cannot be simply carry over from R134a system as they are not dimensioned for such a high pressure and refrigerant physical properties. The new type of heat exchangers for CO₂ refrigerant must be developed.

5.3.2 COP comparison

From the diagram (Figure 5-2) is also visible that dP which to be compensated by compressor is also such a significantly higher for CO₂. However the specific work consumed by the compressor a_t^k (see chap. 1.4) which express power necessary to bring to the system is only a slightly higher for system worked with CO₂. It can be also read that q_0 – Specific cooling capacity and q_k – Specific heat energy rejected by condenser (gas cooler for CO₂ – to be explained later) is in favour to CO₂ system. This all summarised imply better COP for CO₂ for given conditions. The research which was done in this topic confirmed better COP for CO₂ vs. standard R134a for most of conditions - ambient temperature (Figure 5-3). This

tendency is significant especially if the ambient temperature goes below 15 °C which makes CO₂ refrigerant clear choice for refrigeration systems which works predominantly in heat pump mode.

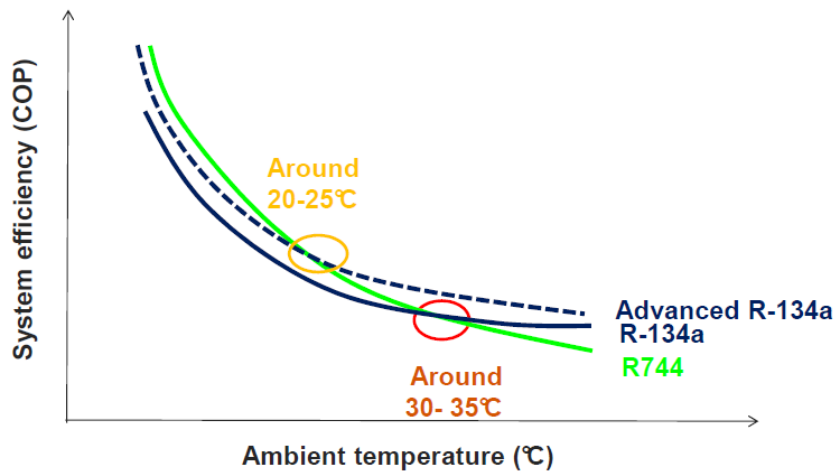


Figure 5-3: COP comparison[8]

To understand COP improvement for CO₂ and why CO₂ thermodynamic cycle works with a such high pressure helps research realised as bacalor thesis realised as West Bohemian university by Jan Fuks under supervision of Prof. Ing. Radim MAREŠ, CSc.[11]

In the thesis is explained that occurrence of the local maximum of COP depending on high pressure side but there is not direct dependency.

While the specific cooling capacity q_{pr} increase together with the high pressure, for COP is this not valid in all cases. Specific cooling capacity depends on the difference of the enthalpy h_1 and h_3 . This difference increases almost always with increasing pressure. (Exceptions would be only high pressures when the isotherms begin in the p-h diagram with increasing pressure pushing to the right, so the enthalpy h_3 then grows, but this area of the graph is we will not deal). However the COP examines the ratio q_{pr} / a_{12} and this ratio is increased by conditions other than simple rising of pressure in high pressure side.

In this case the shape of two curves is decisive. Firstly, it depends on the shape of the T3 isotherm and, on the other hand, the shape of the adiabatic connecting points 1 and 2 in the p-h diagram. Initial growth of COP with the increasing pressure in high pressure side is caused by a small, gradual slope of the isotherm T3 curve in p-h ($s_1 = s_2 = \text{const.}$) at a given pressure above the adiabatic stroma. The original cycle indicated by blue (1, 2, 3, 4, 1) changed by increasing the pressure in high pressure side to “red cycle” (1, 2', 3', 4', 1').

By comparison of original blue and red cycle is visible that to original compressor work – a (1-2) has been added Δa (2-2') and for original specific cooling capacity (in the other words heat bring to the system) q_{pr} (4-1) has been added Δq (4-4'). At first view, is visible that heat introduced to the system gained much more than work of compressor. This effect is desirable for us as it increases a COP.[11]

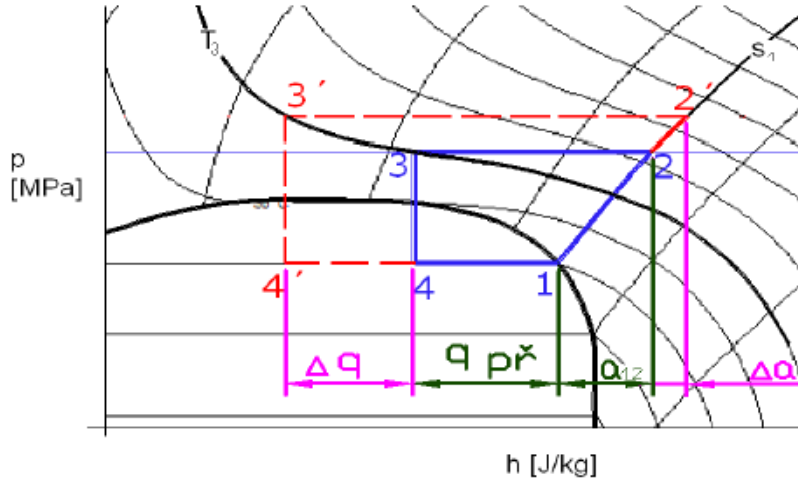


Figure 5-4: Log p-h diagram with low load in high pressure side [11]

However, if we exceed the pressure above a certain limit, the isotherm of T_3 at point 3 (see figure 5-5). If we continue to increase the pressure above, enthalpy h_2 will be faster increase the enthalpy h_3 slower, thus increasing the required size faster work and slowly increase the heat brought into circulation. This results in a decrease in COP at high pressure side. [11]

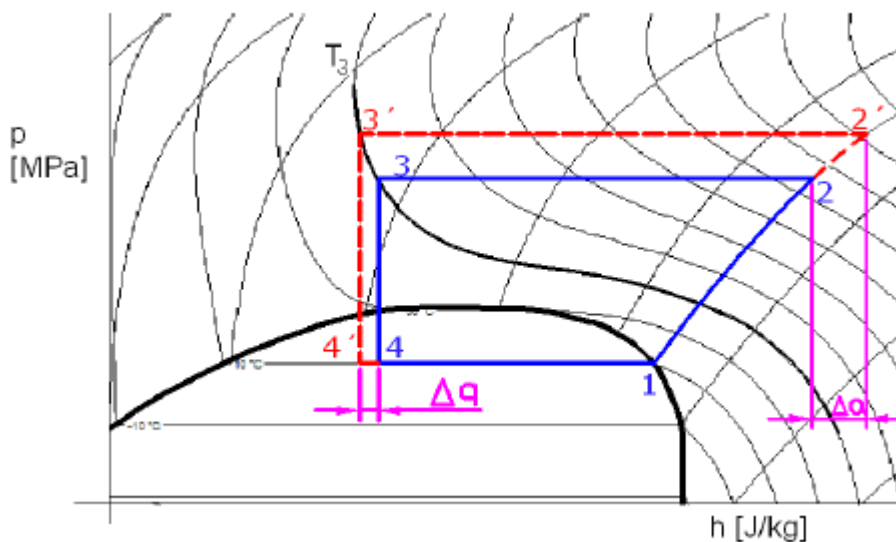


Figure 5-5: Log p-h diagram with too high load in high pressure [11]

5.3.3 CO₂ thermodynamic cycle in supercritical zone

The other important difference is that for CO₂ refrigerant the cycle is in its high pressure side realised in supercritical zone for given example (Figure 5-6) and so no condensation is done. The CO₂ medium is in supercritical state only cooled and thus the exchanger is called simply **gas cooler** (figure 5-6).

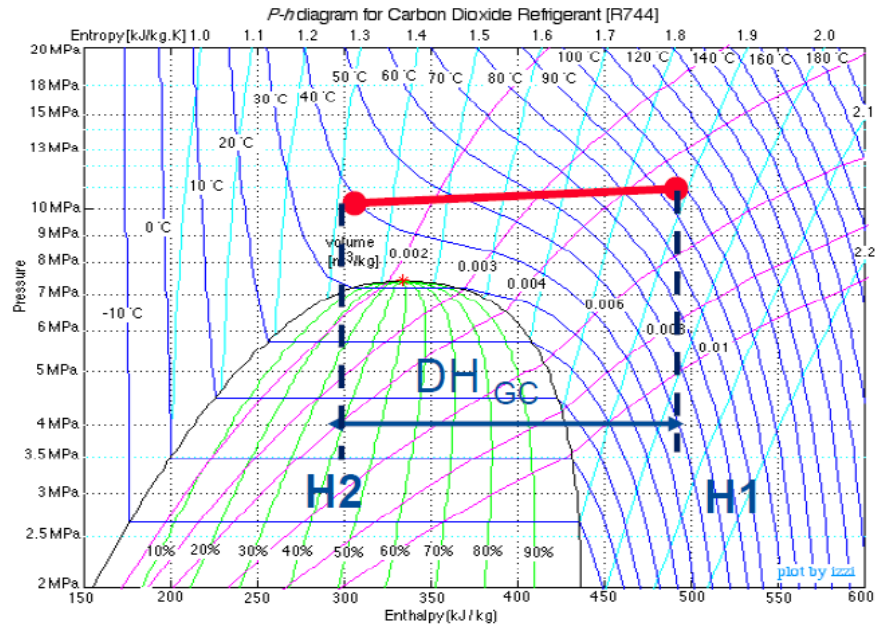
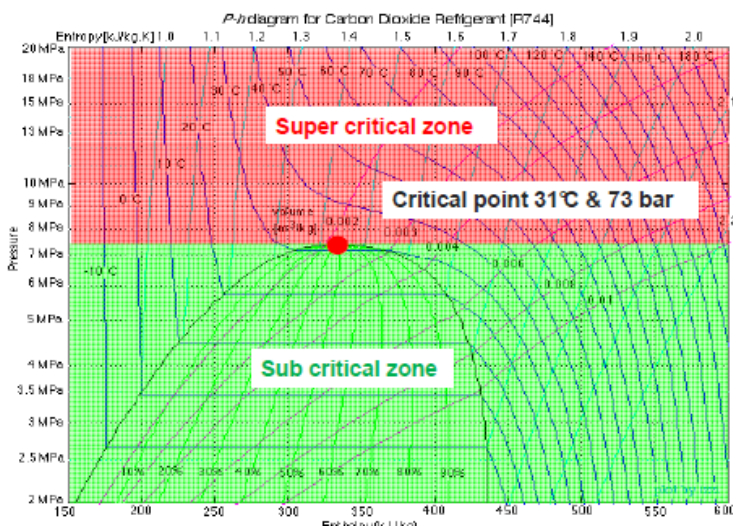


Figure 5-6: The Gas cooler allows to feed the expansion device with cool supercritical refrigerant. [8]

A supercritical fluid is any substance at a temperature and pressure above its critical point (Figure 5-7) where distinct liquid and gas phases do not exist.



Must consider the critical point when using carbon dioxide
 – Critical point is when liquid and vapour phases reach the same density

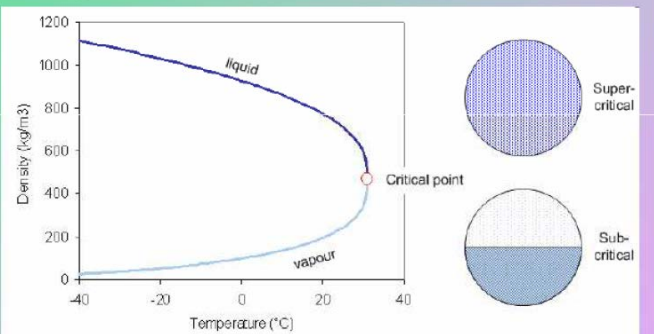


Figure 5-7: log P-h diagram – focus to supercritical zone [8]

Anyway it's important to say that for different ambient condition (low loads) CO₂ system could work below supercritical point (as standard refrigerants) and so heat exchanger realise this work as pure condenser as phase change take a place (Figure 5-8)

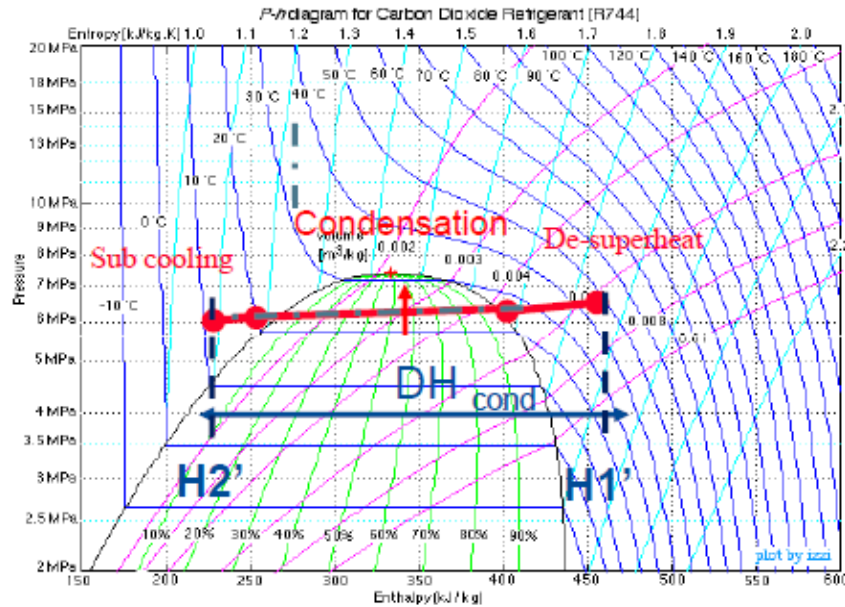


Figure 5-8: The Gas cooler allows to feed the expansion device with liquid refrigerant [8]

5.3.4 Heat transfer coefficient, density, saturation pressure comparison

The heat transfer coefficient α is the dependency between the heat flux and the thermodynamic driving force for the flow of heat. It is used in calculating the heat transfer, typically by convection or phase transition between a fluid and a solid. Heat transfer coefficient equation is derived from the following assumption.

The heat flux from the wall to the surrounding fluid depends on the temperature difference between the wall temperature and ambient temperature on the fluid properties of the fluid and the type of the fluid flow. The two last mentioned conditions are taken into account by the coefficient of heat transfer α in the following equation. This equation is the equation of Newton's empirical law.

$$\dot{Q} = S \times \alpha \times \Delta T$$

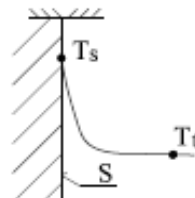


Figure 5-9: The temperature change in the fluid into which the heat transmits from the wall [4]

If the equation is divided by the surface S , which transmits the heat to the surroundings we get the equation for the heat flux.

$$q = \alpha \times \Delta T$$

From this equation is expressed:

$$\alpha = \frac{q}{\Delta T} \left[\frac{W}{m^2 K} \right]$$

On the Figure 5-10 is showed the dependency of heat transfer coefficient on vapour quality during evaporation process. For R-134 the heat transfer coefficient increase when vapour quality increase. For CO_2 refrigerant is this valid vice versa. What is important to remember is that heat transfer coefficient of the R744 is always better than the R-134a one during the evaporation process.[8]

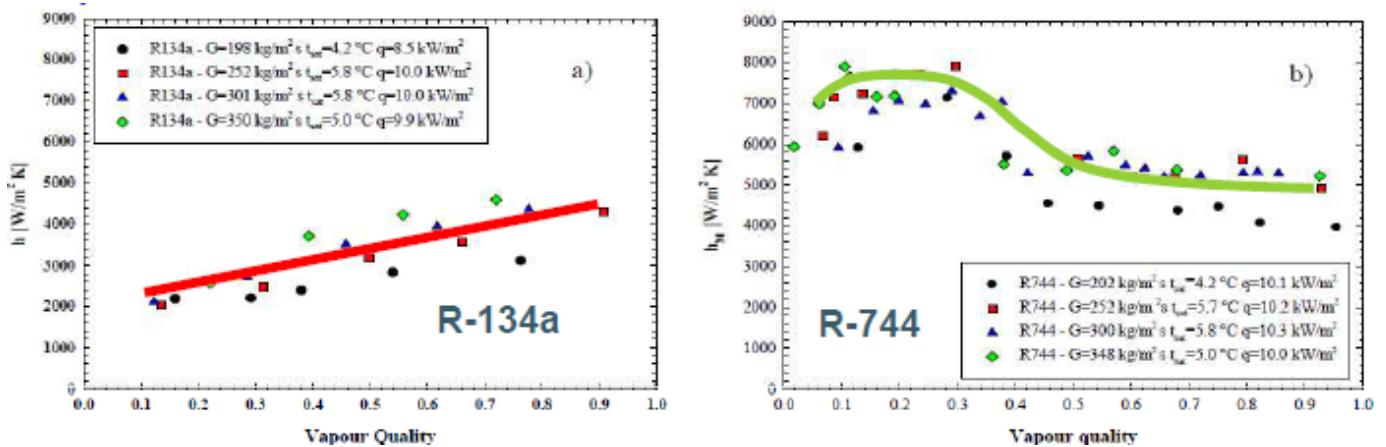


Figure 5-10: The dependency of heat transfer coefficient on vapour quality for R-134 and CO_2 refrigerant [8]

For the high pressure side of the cycle the heat transfer coefficient of the R744 depends on the HP and the temperature during the gas cooling process as describes Figure 5-11.

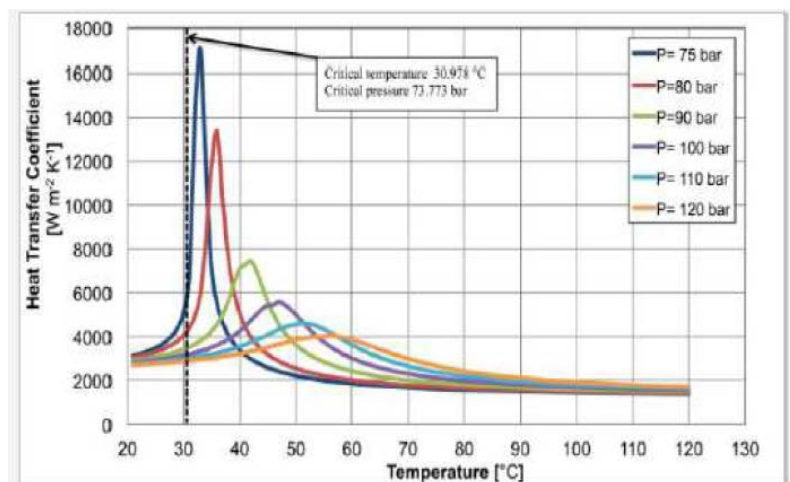


Figure 5-11: The dependency of heat transfer coefficient on pressure and temperatur of CO_2 refrigerant [8]

As the other refrigerant parameter to be focused density as density influenced geometrical dimension the components used in A/C system (Swept volume of compressor,

cross section of heat exchangers, cross section of A/C pipes etc.). From the Figure 5-12 is visible that R744 density is much higher vs. R134a density. This cause much smaller Compressor swept volume (28cc vs. 160cc) and also less pressure drop and also smaller hydraulic diameter could be used in the A/C system.

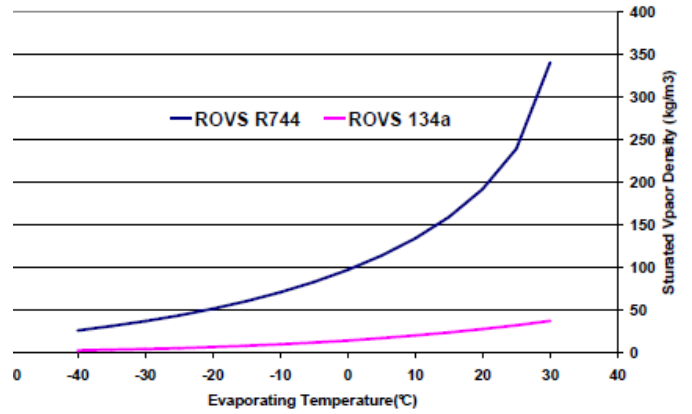
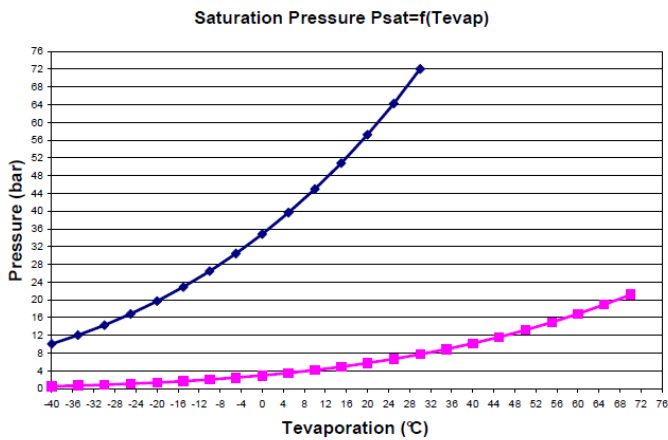


Figure 5-12: Saturation temperature / Saturation pressure – R744 vs. R134a comparison

Figure 5-12: Dependency of Saturated vapor density on Evaporating temperature - R744 vs. R134a comparison

5.4 Conclusion

Referring to information listed above benefits of carbon dioxide used as refrigerant are significant. The higher density which leads to less dP allows miniaturization of components in CO₂ system vs. R134a (cross section, compressor swept volume etc.). The higher heat thermal coefficient leads to better heat exchange. There is special interest focus to COP which is significantly higher for carbon dioxide (for most of cases) which made it object of interest by electrical vehicle manufacturers because it's use leads to reduction of vehicles battery energy consumption vs. when R134a / R1234yf is used. As this energy could be used to increase car vehicle range (is for electric cars especially appreciate) make this liquid the refrigerant of choice.

The higher working pressure is disadvantage of course as the components for A/C system working with carbon dioxide must be more mechanical resistant and so it's necessary to develop them. Also is necessary mentioned that due to high operation pressure is CO₂ more sensitive for fluid leakage. If the higher leakage will happen this is serious danger for cabin crew as CO₂ in cabin could cause Health problems or even crew fainting.

6 Heat pump technology

6.1 Idealised circuiting

To introduce the basic principal of the heat pump to be started from traditional A/C loop. The cabin is cooling by extract the calories from the evaporator. The refrigerant captures energy from the cabin air and from the compressor. All the energy is transferred by outside with the condenser. In the evaporator the energy is growing and after compressor put the pressure the energy continues grows. The refrigerant is now on high pressure and high temperature after the gas is condensed near the ambient temperature in the front condenser the energy is transferred to the outside air. The power transfer to the outside is equal to the power extracted from the cabin plus the power of the compressor.

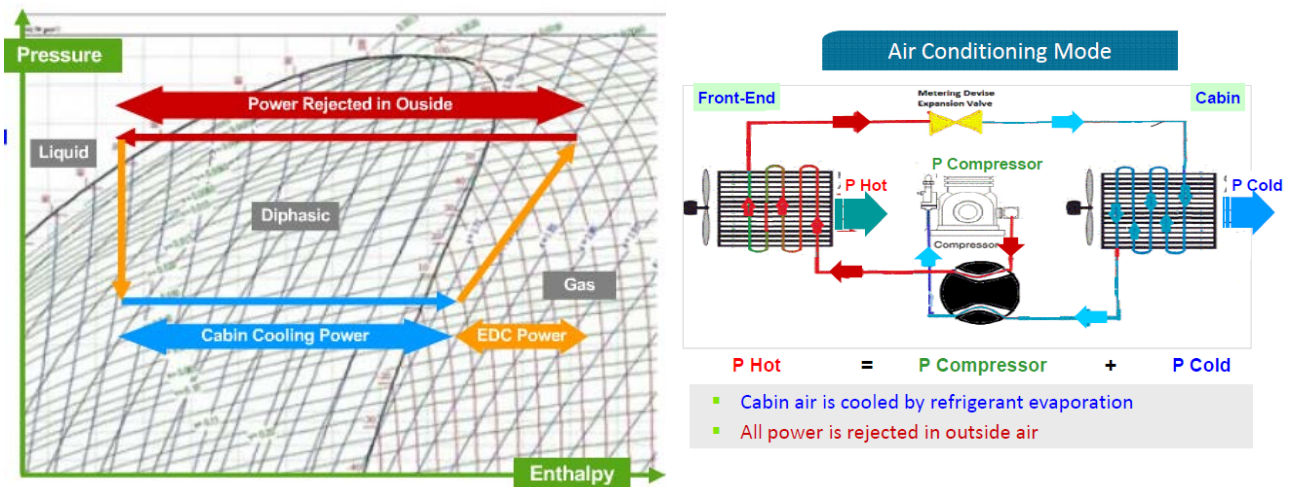


Figure 6-1: A/C mode [8]

In the heat pump mode it's done by opposite way. By inverting the circuiting routing using a forwarding valve. By forwarding valve the condenser becomes evaporator. The ambient temperature is used to evaporate. With the compressor we can compress the vapour to certain degrees and now the hot gas condensate in the HVAC to warm the cabin air. After there is the expansion valve to cool down refrigerant before to heading front exchanger to extract free heat from outside air.

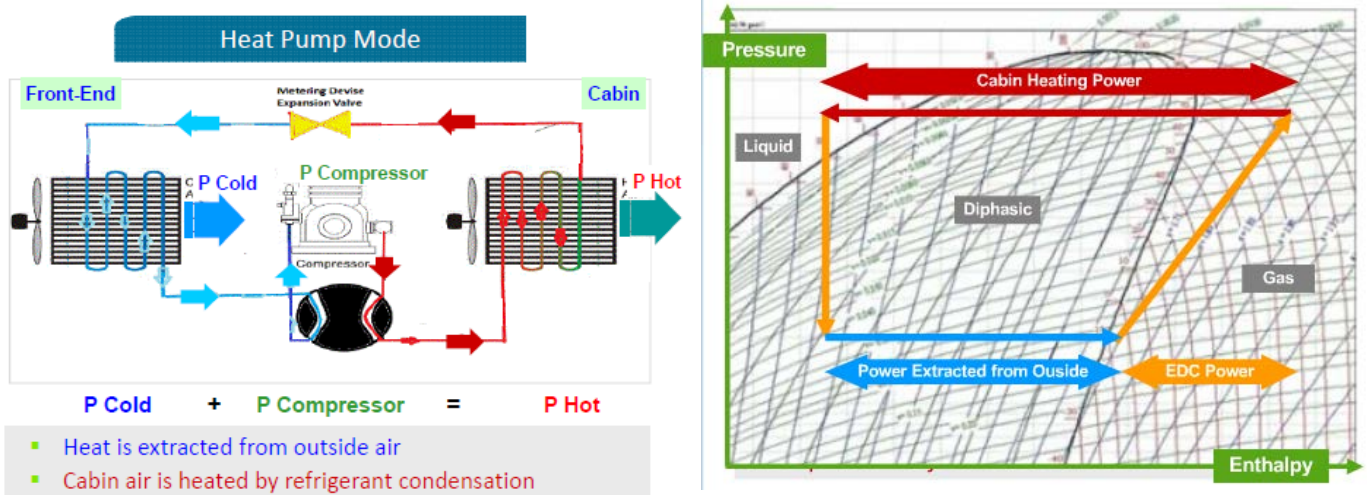


Figure 6-2: Heat pump mode [8]

As we are now in the heat pump mode. The power which is the heating cabin is equal to the power consumed by compressor plus energy coming from outside for free. The heating power giving to the cabin is higher than compressor power. It's possible to have COP = 2. It means that the energy coming from the outside is matching to the energy of compressor. So it's delivering two times compressor power.

6.2 Real vehicle circuiting

About the physical principle the air conditioning (A/C) loop and the heat pump are the same - both vapour compression cycles. But in automotive case this couldn't work. We need dehumidify the air and thus is necessary to have in the same time heating and cooling capacity. But the previous architecture when we go from cold to hot - where the evaporator becomes hot and vapours to be sent to the cabin we face the risk of dehumidification issue as there is no way how to dehumidify. So it's necessary to have in the cabin two heat exchangers - one dedicated to cool and one additional heat exchanger dedicated to heat. The front - end exchanger has two functions: In the summer it's the condenser in the winter evaporator. In winter we have much lower pressure drop compare to air conditioning mode so we have much more pressure drop constraints to front-line. The compressor shall be able operate with higher pressure ratio.

In the Figure 6-3 is the concrete example of the direct heat pump architecture. In A/C mode one of expansion valve is activated just before the evaporator. The inner condenser is by-passed to avoid heat pick upped.

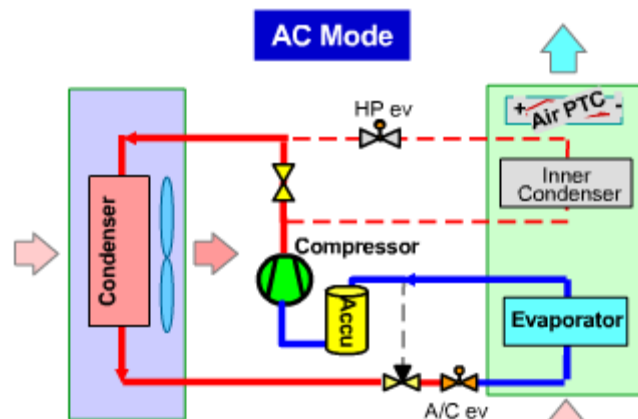


Figure 6-3: A/C mode [8]

In the heat pump mode one of expansion valve was activated before front - end exchanger and this is the evaporator who is by-passed.

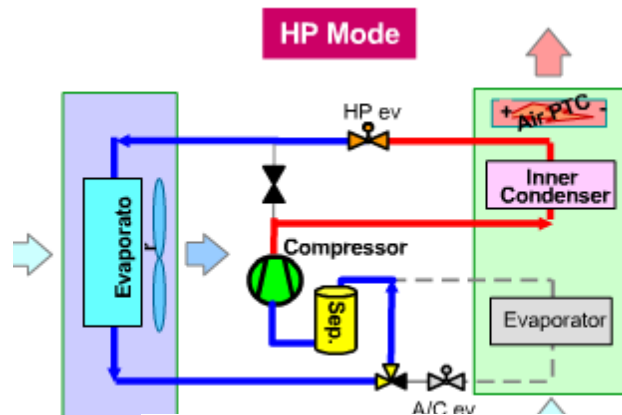


Figure 6-4: HP mode [8]

The dehumidification mode is close to A/C mode but we use the both HVAC heat exchangers: the inner condenser and the evaporator. The dehumidification function is much more tricky compare to current A/C system because of strong coupling between cooling and heating power. At high temperature above 15degrees °C we need extract heating power access on the front – end. At low temperature below 5 degrees C we need to catch additional power by add other electrical heater (Air PTC). The balance of circulating refrigerant in all modes is very tricky leading significantly extra charge compare to traditional A/C loop. The circuiting is more complex compare to simple A/C loop with much more lines and connectors. System development shall focus on three topics. Security of balance of refrigerant charge an electric driven compressor. Manage the system to prevent icing. Ensure smooth switch from one mode to the other.

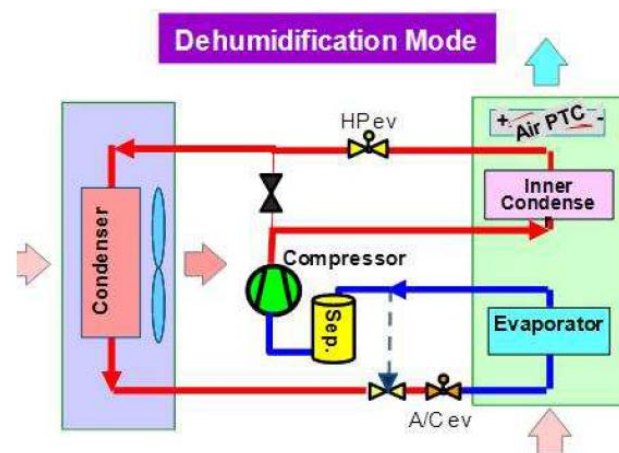


Figure 6-5: Dehumidifaction mode [8]

7 Heat exchangers

Heat exchangers are devices that enable the exchange of heat between two fluids at different temperatures while prevent them from mixing with each other. Heat exchangers are commonly used in practice in a wide range of applications, from heating and air-conditioning systems in automotive. Heat exchangers differ from mixing chambers in that they do not allow the two fluids involved to mix. [12]

Heat exchangers should meet the following requirements:

- High thermal efficiency
- Low pressure drop on flow media
- High reliability and durability
- Safety
- The resistance of the materials used to the operating media
- Easy maintenance and service
- Minimizing dimensions
- Simple production
- Low purchase price

There is lot of types of heat exchangers classifying but due to limited space of this thesis only **classification acc. to arrangement of the media flows** to be mentioned. In the shorten version of this classification heat exchangers are divided to:

- **Co-flow heat exchanger**
- **Counter- flow heat exchanger**
- **Cross – flow heat exchanger**

The choice of the particular arrangement depends on the desired efficiency of the exchanger, allowed thermal stresses and required temperatures at the exchanger inlets and outlets. However co-flow heat exchanger is not used in industrial application due to his theoretical lower efficiency (demonstrated by LMTD method).[13] All the layout types are schematically shown in Figure 7-1.

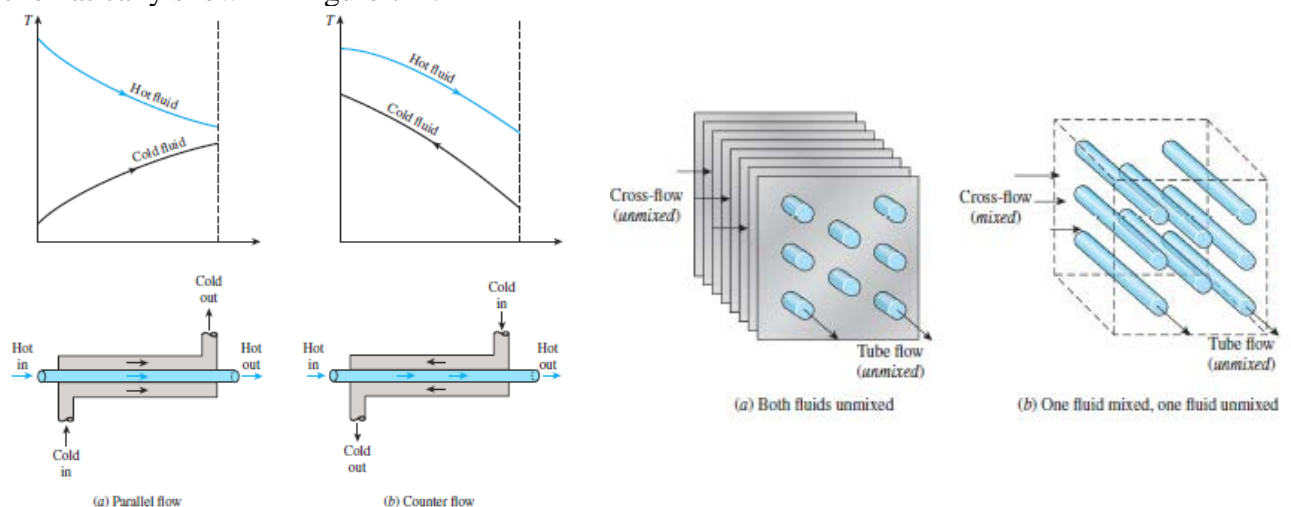


Figure 7-1: Paralel flow, counter flow, cros flow HEX [13]

7.1 Heat exchangers basic calculation

Heat exchangers are commonly used in practice, and an engineer often finds a position to select best heat exchanger for two following tasks: 1. To find heat exchanger that will achieve a specified temperature change in a fluid stream of known mass flow rate 2. To predict the outlet temperatures of the hot and cold fluid streams in a specified heat exchanger.

There are two main methods used in the analysis of heat exchangers. First one is the log mean temperature difference (or LMTD) method. This method is best suited for the first task. The second one is the effectiveness–NTU (the number of transfer units) method for the second task. Only the first method to be explained due to limited space of this thesis. But first there to be presented some general considerations.

Heat exchangers usually operate for long periods of time with no change in their operating conditions. Therefore, they can be modelled as steady-flow devices. As such, the mass flow rate of each fluid remains constant, and the fluid properties such as temperature and velocity at any inlet or outlet remain the same. Also, the fluid streams experience little or no change in their velocities and elevations, and thus the kinetic and potential energy changes are negligible. The specific heat of a fluid, in general, changes with temperature. But, in a specified temperature range, it can be treated as a constant at some average value with little loss in accuracy. Axial heat conduction along the tube is usually insignificant and can be considered negligible. Finally, the outer surface of the heat exchangers assumed to be perfectly insulated, so that there is no heat loss, and any heat transfer occurs between the two fluids only. The idealizations stated above are closely approximated in practice, and they greatly simplify the analysis of a heat exchanger with little sacrifice from accuracy. Therefore, they are commonly used. Under these assumptions, the first law of thermodynamics requires that the rate of heat transfer from the hot fluid be equal to the rate of heat transfer to the cold one. This express Heat balance equation explained below:

7.1.1 Heat balance equation

$$\dot{Q}_b = \dot{m}_1 \cdot c_1 \cdot (t_{11} - t_{12}) \cdot \eta = \dot{m}_2 \cdot c_2 \cdot (t_{21} - t_{22})$$

where

\dot{Q}_b	[Kw]	heat flux
\dot{m}_1, \dot{m}_2	[kg.s ⁻¹]	mass flow of heating and heated fluid
c_1, c_2	[kJ.kg ⁻¹ .K ⁻¹]	average specific heat capacity of heating and heated substance
t_{11}, t_{12}	[°C]	temperature of heating fluid on inlet and outlet
t_{21}, t_{22}	[°C]	temperature of heated fluid on inlet and outlet

Two special types of heat exchangers commonly used in practice are condensers and evaporators. One of the fluids in a condenser or evaporator undergoes a phase-change process, and the rate of heat transfer is expressed as

$$\dot{Q}_b = \dot{m} \cdot h_{fg}$$

Where \dot{m} is the rate of evaporation or condensation of the fluid and h_{fg} the enthalpy of vaporization of the fluid at the specified temperature or pressure. The other important relation is the Equation of heat transfer.

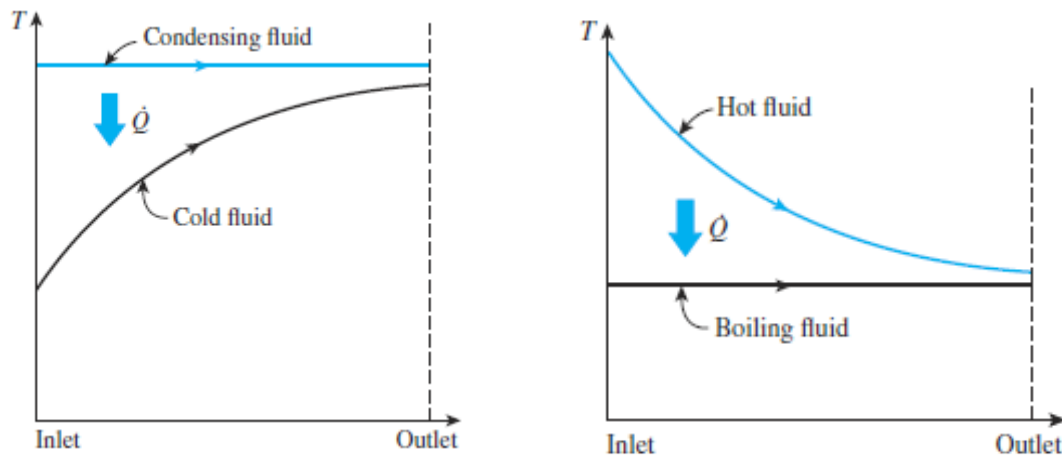


Figure 7-2: Condenser and evaporator. [13]

7.1.2 Equation of heat transfer (Newton's law of cooling)

This is the process of heat transfer from one space where is the first fluid which is separated by a fixed wall to the second space with the second fluid. Only the equation for flat wall is written (as this is case of thesis heat exchanger) but the others are possible (cylindrical wall, cubic wall etc.). Overall heat transfer coefficient k depends on the type of fluid and material used on the heat exchange wall. The mean logarithmic temperature gradient ΔT is determined by the mean method logarithmic temperatures

$$\dot{Q}_k = k \cdot \overline{\Delta T} \cdot S$$

Where:

\dot{Q}_k	[W]	heat flux
k	[W.m ⁻² .K ⁻¹]	overall heat transfer coefficient
$\overline{\Delta T}$	[K]	mean temperature difference
S	[m ²]	heat exchange surface

Overall heat transfer coefficient k depends on the type of fluid and material used on the heat exchange wall. The mean logarithmic temperature gradient ΔT is determined by the mean method logarithmic temperatures.

Mean temperature difference

$$\overline{\Delta T} = \frac{\Delta T_1 - \Delta T_2}{\ln\left(\frac{\Delta T_1}{\Delta T_2}\right)}$$

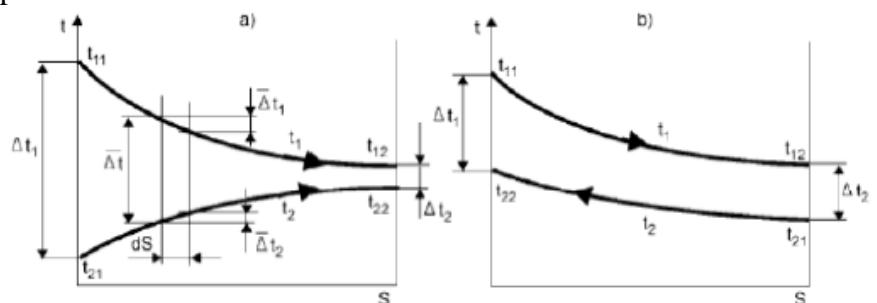


Figure 7-3: LMDT method. [13]

The equation for $\overline{\Delta T}$ is valid for co-flow and counter-flow HEX only. For the more complex (cross, combined) flow is to use the following relationship:

$$\overline{\Delta T} = \varphi \cdot \Delta T_{pre}$$

where

φ	[-]	mutual flow coefficient
ΔT_{pre}	[K]	mean temperature difference of counter-flow HEX

Heat transfer through a flat wall

A heat exchanger typically involves two flowing fluids separated by a solid wall. Heat is first transferred from the hot fluid to the wall by convection, through the wall by conduction, and from the wall to the cold fluid again by convection. Any radiation effects are usually included in the convection heat transfer coefficients. Heat transfer in a heat exchanger usually involves convection in each fluid and conduction through the wall separating the two fluids. In the analysis of heat exchangers, it is convenient to work with an overall heat transfer coefficient K that accounts for the contribution of all these effects on heat transfer. The rate of heat transfer between the two fluids at a location in a heat exchanger depends on the magnitude of the temperature difference at that location, which varies along the heat exchange.

$$\dot{Q} = S \cdot \alpha_1 \cdot (T_{t1} - T_{s1})$$

$$\dot{Q} = S \cdot \frac{\lambda}{\delta} \cdot (T_{s1} - T_{s2})$$

$$\dot{Q} = S \cdot \alpha_2 \cdot (T_{t1} - T_{s1})$$

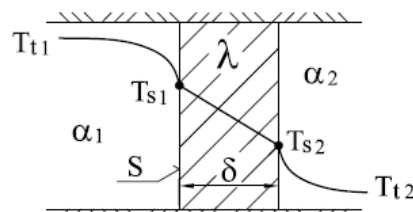


Figure 7-4: Heat transfer through wall [4]

By separating the temperature differences of these three equations on the left and adding up these equations we get the following relationship:

$$T_{t1} - T_{t2} = \frac{\dot{Q}}{S} \cdot \left(\frac{1}{\alpha_1} + \frac{\lambda}{\delta} + \frac{1}{\alpha_2} \right)$$

By expressing the heat flow, we get the following relationship from which the overall coefficient k can be derived

$$\dot{Q} = \frac{(T_{t1} - T_{t2}) \cdot S}{\frac{1}{\alpha_1} + \frac{\lambda}{\delta} + \frac{1}{\alpha_2}} = k \cdot \Delta T \cdot S$$

$$k = \frac{1}{\frac{1}{\alpha_1} + \frac{\lambda}{\delta} + \frac{1}{\alpha_2}} \quad \left[\frac{W}{m^2 K} \right]$$

Thermal resistance concept

Especially English literature works with concept thermal resistance which has its analogy in electrical resistance. This concept to be explained on the heat transfer through wall again which represents 3 thermal resistances in series.

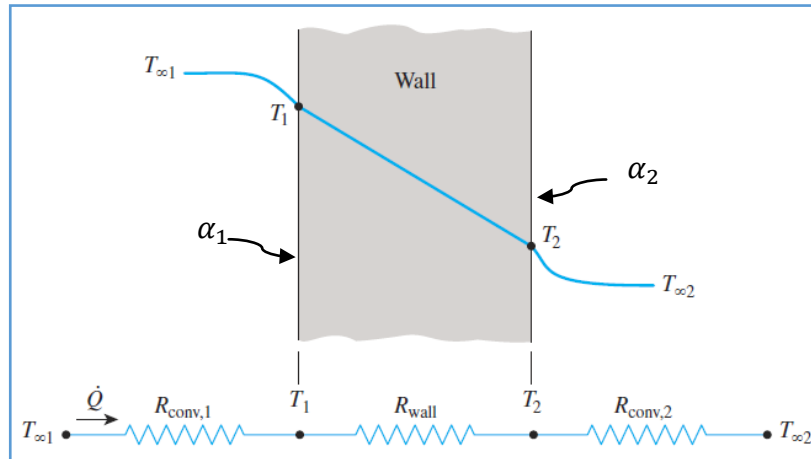


Figure 7-5: Thermal resistance concept. [13]

$$R_{total} = R_{conv,1} + R_{wall} + R_{conv,2} = \frac{1}{\alpha_1 \cdot S} + \frac{\delta}{k \cdot S} + \frac{1}{\alpha_2 \cdot S} \quad [K/W]$$

Expression of Newton's law of cooling

$$\dot{Q}_k = k \cdot S \cdot \Delta T \quad [W]$$

Where

$$k \cdot S = \frac{1}{R_{total}} \quad [W/K]$$

Based on written above following equation is valid:

$$\dot{Q}_k = \frac{\Delta T}{R} = K \cdot S_s \cdot \Delta T = K_i \cdot S_i \cdot \Delta T = K_o \cdot S_o \cdot \Delta T$$

As every heat exchanger has two heat transfer surface areas S_i and S_o , which, in general, are not equal to each other.

$$K_i \cdot S_i = K_o \cdot S_o \text{ but } K_i \neq K_o$$

Therefore, the overall heat transfer coefficient K of a heat exchanger is meaningless unless the area on which it is based is specified! This is especially the case when one side of the tube wall is finned and the other side is not, since the surface area of the finned side is several times that of the unfinned side.

7.2 HEAT TRANSFER FROM FINNED SURFACES

Especially for refrigerant – air heat exchangers there is big discrepancy between convection heat transfer coefficient – α_1 of the refrigerant side and the air side α_2 as the air is worst possible medium for heat exchange. From the equation of heat convection $\dot{Q}_{conv} = S \cdot \alpha \cdot (T_{t1} - T_{s1})$, if the temperature is fixed by design considerations, as is often the case, there are two ways to increase the rate of heat transfer: a) to increase the convection heat transfer coefficient α or to increase the surface area S . Increasing may α_1 require promotes of air flow (speed) but this approach may or may not be possible or is limited in car. The alternative is to increase the surface area by attaching to the surface extended surfaces called fins. Finned surfaces are commonly used in practice to enhance heat transfer, and they often increase the rate of heat transfer from a surface several times.

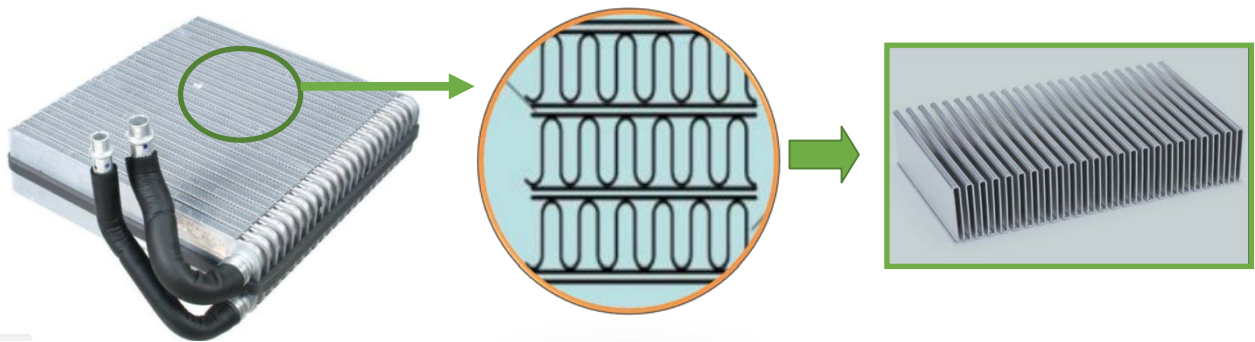


Figure 7-6: a) Finned HEX b) Detail to fin area – each fin between 2 tubes (coolant inside) c) Photo of fin

Fin calculation

Consider the plane of a plane wall at temperature T_b exposed to a medium (air) at temperature T_c . Heat is rejected from the surface to the surrounding medium by convection with a heat transfer coefficient of α (radiation included in coefficient). Heat transfer from a surface area as is expressed as:

$$\dot{Q}_k = \alpha \cdot A_b \cdot (T_b - T_c)$$

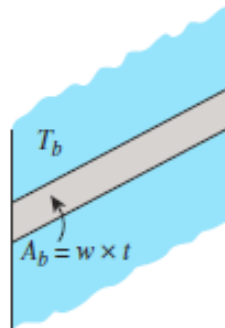


Figure 7-7: Surface without fin. [13]

If fin of constant cross-sectional area A_b and length L that is attached to the surface with a perfect contact and to be purposed infinite thermal conductivity of fin $\lambda \rightarrow \infty$ - the heat

to be transferred from the surface to the fin by conduction and from the fin and to the surrounding medium (air) by convection with the same heat transfer coefficient α .

$$\dot{Q}_k = \alpha \cdot A_{fin} \cdot (T_b - T_c)$$

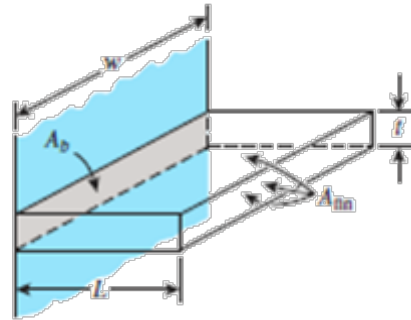


Figure 7-8: Surface with fin. [13]

In reality, however, the temperature of the fin drops along the fin, and thus the heat transfer from the fin is less because of the decreasing temperature difference $T(x) - T_c$. Fin efficiency is defined as:

$$\eta_{fin} = \frac{\dot{Q}_{fin}}{\dot{Q}_{fin,max}} = \frac{\text{Actual heat transfer rate from the fin}}{\text{Ideal heat transfer rate from the fin}}$$

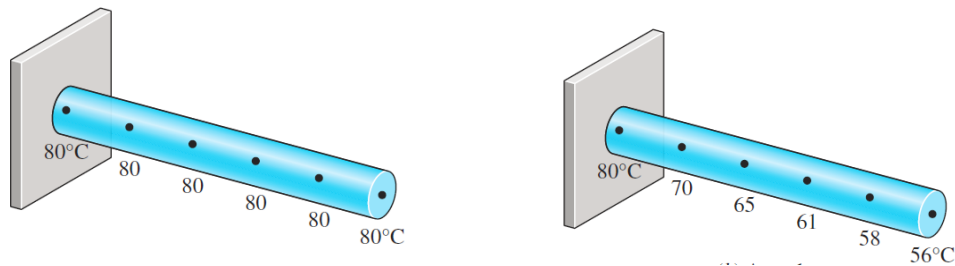


Figure 7-9: Ideal (left) and real temperature distribution in fin. [13]

From the equation above is finally expressed fin heat transfer:

$$\dot{Q}_{fin} = \eta_{fin} \dot{Q}_{fin,max} = \eta_{fin} \cdot \alpha \cdot A_{fin} (T_b - T_c)$$

Where fin efficiency could be found in literature. Rectangular fins efficiency is given by following equation:

$$\eta_{fin} = \frac{\tanh m \cdot L_c}{m \cdot L_c} \quad \text{Where:} \quad m = \sqrt{\alpha / 2\lambda \cdot t} \quad L_c = L + t/2$$

$$A_{fin} = 2w \cdot L_c$$

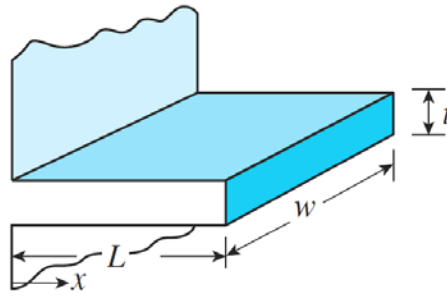


Figure 7-10: Rectangular fin. [13]

As was written above fin is very important part of heat exchanger and there are various fin in the market with different height, thickness and fin pitch. Regarding outer design there are two main types – sinusoidal and square. Square type is more difficult from manufacturing point of view but is favoured due to higher level contact fin with tube which leads to better heat exchange by conduction.

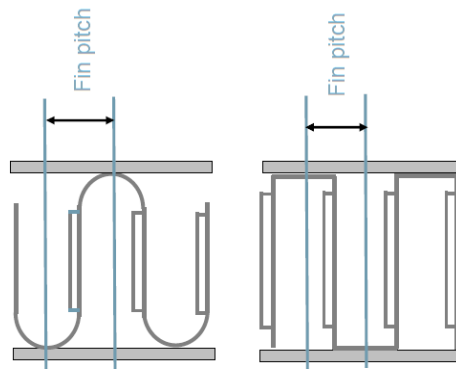


Figure 7-11: Sinusoidal (left) and rectangular fin (right)

8 Convection theory

As the principle of heat exchanger there is heat exchange between two fluids it will be in this part briefly explain the basics of heat exchange mechanisms. Generally there are 3 types of heat exchange: conduction, convection and radiation. In car heat exchangers small part of the total heat comes from the radiation due to HEX fluid low temperature. The conduction is the mechanism of heat transfer through a solid or a quiescent fluid. In the car heat exchangers conduction take place during heat transfer threw HEX wall and also not is decisive as because it is applied in specific processes only. Let's more focus to convection, which is the main HEX mechanism of heat transfer through a fluid in the presence of bulk fluid motion. [13]

8.1 Nusselt number - Nu

Experience showed that convection heat transfer strongly depends on the fluid properties dynamic viscosity μ , thermal conductivity, density ρ , and specific heat C_p , as well as the fluid velocity v . It also depends on the geometry and the roughness of the solid surface, in addition to the type of fluid flow (such as being streamlined or turbulent). In convection studies, it is common practice to dimensionless the governing equations and combines the variables, which group together into dimensionless numbers in order to reduce the number of total variables. It is also common practice to dimensionless the heat transfer coefficient k with the Nusselt number, defined as

$$Nu = \frac{\text{convection heat transfere}}{\text{conduction heat transfere}} = \frac{\alpha \cdot L_c}{\lambda}$$

Where λ is the thermal conductivity of the fluid and L_c is the characteristic length. The Nusselt number represents the enhancement of heat transfer through as a result of fluid motion. The larger the Nusselt number, the more effective the convection.

For most of real application (for example equation used by Dymola software for calculation R744 – inner gas cooler in this thesis) being use the following expression:

$$Nu = C_1 \cdot Re^{C_2} \cdot Pr^{C_3}$$

Where C_1, C_2, C_3 are coefficients which could be obtain only from experiments. Pr and Re to be described in following section [13]

8.2 Prandtel number - Pr

When fluid flows around a solid body, a thin layer of fluid is formed by the viscosity. In this layer, the flow rate of the flowing fluid drops to a zero value on the body surface – no slip condition. This layer with different physical properties from the mainstream is called the boundary layer. This layer may have several forms – velocity and thermal. This is the boundary layer at the surface of the plate in parallel with the fluid flow. The velocity boundary layer is formed so that the fluid has a zero velocity on the body surface and slows down due to viscosity closest surrounding layers. The speed in this layer increases up to the velocity of the main stream w_f . The thickness of the boundary layer δ_x is determined by the distance of the first layer at the velocity w_f from the surface of the wrapped body. The figure

shows that the leading edge is the thickness of the border layers zero. The maximum thickness of the boundary layer is, on the contrary, at the drainage edge. With a long enough surface to run, high fluid flow rates or low viscosity of the fluid, the laminar boundary layer may develop from a certain length in a turbulent (Figure 8-1). There is a transitional area between these areas. The turbulent boundary layer is the boundary influenced by the fluctuations in time, so it is necessary to calculate the mean thickness of the turbulent boundary layer. Criterion for determining laminar transition the boundary layer on the turbulent is the Reynolds number. [20]

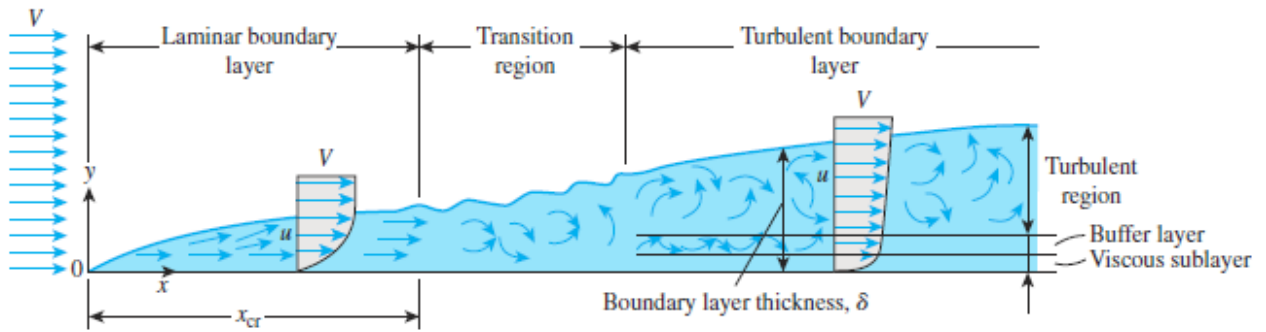


Figure 8-1: Velocity boundary layer establishment on flat plate [20]

Likewise, a thermal boundary layer develops when a fluid at a specified temperature flows over a surface that is at a different temperature (picture). Consider the flow of a fluid at a uniform temperature of T_∞ isothermal flat plate at temperature T_s . The fluid particles in the layer adjacent to the surface reach thermal equilibrium with the plate and assume the surface temperature T_s . These fluid particles then exchange energy with the particles in the adjoining-fluid layer, and so on. As a result, a temperature profile develops in the flow field that ranges from T_s at the surface to T_∞ sufficiently far from the surface. The flow region over the surface in which the temperature variation in the direction normal to the surface is significant is the thermal boundary layer. The thickness of the thermal boundary layer increases in the flow direction since the effects of heat transfer are felt at greater distances from the surface further downstream. The convection heat transfer rate anywhere along the surface is directly related to the temperature gradient at that location. Therefore, the shape of the temperature profile in the thermal boundary layer dictates the convection heat transfer between a solid surface and the fluid flowing over it. In flow over a heated (or cooled) surface, both velocity and thermal boundary layers develop. [13]

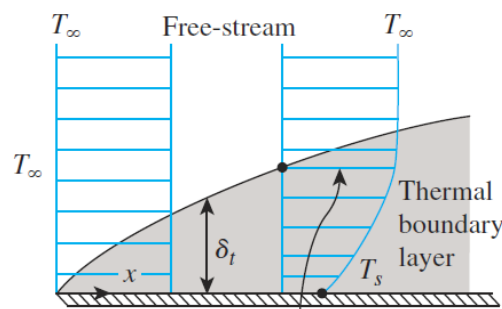


Figure 8-2: Thermal boundary layer establishment on flat plate [13]

Noting that the fluid velocity has a strong influence on the temperature profile, the development of the velocity boundary layer relative to the thermal boundary layer will have a strong effect on the convection heat transfer.

The relative thickness of the velocity and the thermal boundary layers is best described by the dimensionless parameter Prandtl number, defined as:

$$Pr = \frac{\text{Molecular diffusivity of momentum}}{\text{Molecular diffusivity of heat}} = \frac{\mu \cdot C_p}{\lambda}$$

The effect of boundary layer is visible also if to be consider a fluid entering a circular pipe at a uniform velocity. The thickness of this boundary layer increases in the flow direction until the boundary layer reaches the pipe centre and thus fills the entire pipe, and the velocity becomes fully developed a little further downstream. The region from the pipe inlet to the point at which the velocity profile is fully developed is called the hydrodynamic entrance region, and the length of this region is called the hydrodynamic entry length L_h . Flow in the entrance region is called hydro dynamically developing flow since this is the region where the velocity profile develops. The region beyond the entrance region in which the velocity profile is fully developed and remains unchanged is called the hydro dynamically fully developed region. The velocity profile in the fully developed region is parabolic in laminar flow and somewhat flatter or fuller in turbulent flow due to eddy motion and more vigorous mixing in radial direction. [13]

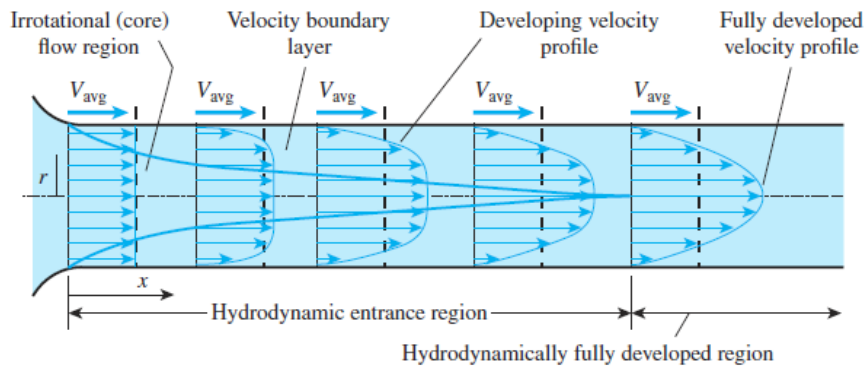


Figure 8-3: Velocity boundary layer in tube establishment

Based on experiments where was focusing variation of local Nusselt number and thus heat exchange ratio along a tube in turbulent flow for both constant surface temperature and constant surface heat flux is visible following conclusions:

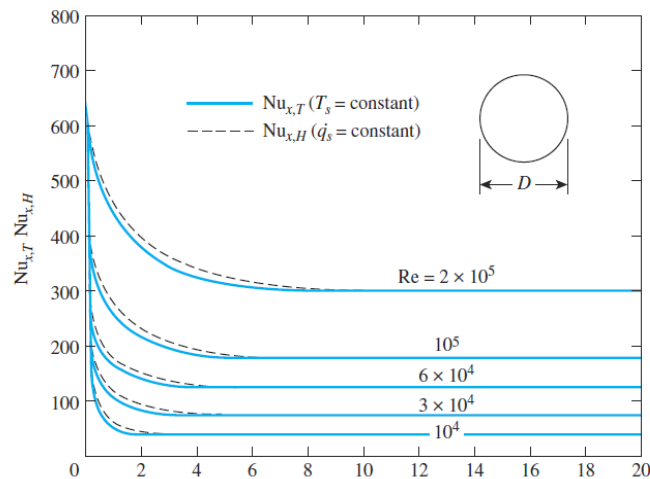


Figure 8-4: Variation of local Nusselt number along a tube in turbulent flow

- The Nusselt numbers and thus the convection heat transfer coefficients are much higher in the entrance region where thermal boundary layer is low.
- The Nusselt number reaches a constant value at a distance of less than 10 diameters, and thus the flow can be assumed to be fully developed for $x > 10D$.
- The Nusselt numbers for the constant surface temperature and constant surface heat flux conditions are identical in the fully developed regions and nearly identical in the entrance regions. Therefore, Nusselt number is insensitive to the type of thermal boundary condition, and the turbulent flow correlations can be used for either type of boundary condition

8.3 Reynolds number - Re

Based on careful inspection of flow in a pipe reveals which was done by scientist has been observed that the fluid flow is streamlined at low velocities but turns chaotic as the velocity is increased above a critical value, as shown in Figure 8-5. The flow regime in the first case is said to be laminar, characterized by smooth streamlines and highly-ordered motion, and turbulent in the second case where it is characterized by velocity fluctuations and highly-disordered motion. The transition from laminar to turbulent flow does not occur suddenly; rather, it occurs over some region in which the flow fluctuates between laminar and turbulent flows before it becomes fully turbulent. Most flows encountered in practice are turbulent. Laminar flow is encountered when highly viscous fluids such as oils flow in small pipes or narrow passages.

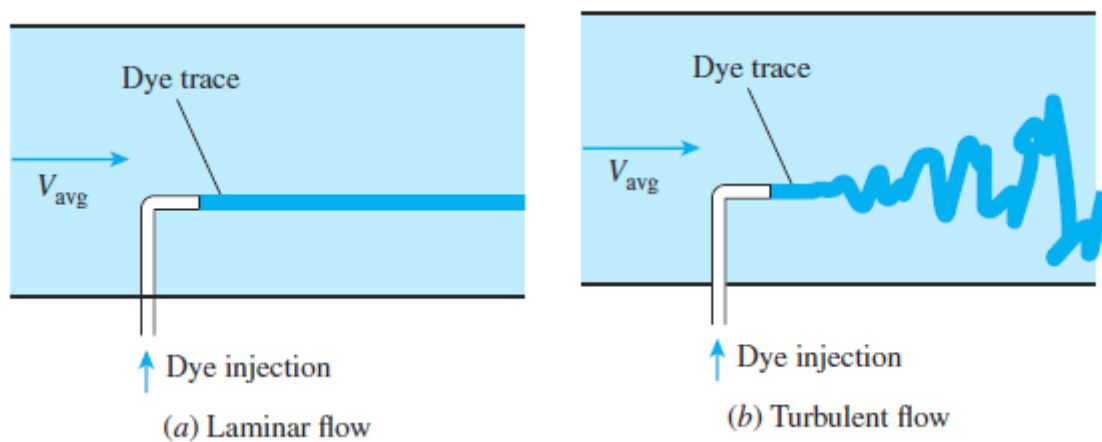


Figure 8-5: Laminar and turbulent flow in pipe [20]

The transition from laminar to turbulent flow depends on the surface geometry surface roughness, flow velocity, surface temperature, and type of fluid, among other things. After exhaustive experiments in the 1880s, Osborn Reynolds discovered that the flow regime depends mainly on the ratio of the inertia forces to viscous forces in the fluid. This ratio is called the Reynolds number which is a dimensionless quantity, and is expressed for external flow as:

$$Re = \frac{\text{Inertia forces}}{\text{viscous forces}} = \frac{v \cdot L_c}{\eta} = \frac{\rho \cdot v \cdot L_c}{\mu}$$

Where v is the upstream velocity (equivalent to the free-stream velocity for a flat plate), L_c is the characteristic length of the geometry, $\eta = \frac{\mu}{\rho}$ is the kinematic viscosity of the fluid. For a flat plate, the characteristic length is the distance x from the leading edge.

The following Reynolds number distribution is shown for piping flow of circular cross-section, where the characteristic dimension L_c corresponds to the diameter of the pipe so called hydraulic diameter - D_h . For flow in non-circular pipelines the so-called equivalent diameter is used as the characteristic dimension:

$$D_H = \frac{4 \cdot A_C}{P}$$

where A_c is the cross sectional area of the tube and P is wetted perimeter. Transition from laminar to turbulent flow also depends on the degree of disturbance of the flow by surface roughness, pipe vibrations and the fluctuations in the flow. Under most practical conditions, the flow in a tube is laminar for $Re < 2300$, fully turbulent for $Re > 10000$ and transitional in between. But it should be kept in mind that in many cases the flow becomes fully turbulent for $Re > 4000$.

8.4 Heat transfer enhancement of heat exchangers

In the previous section has been briefly described the basics of convection heat transfer. Based on showed relations was developed many heat exchangers design updates in sense to improve heat exchange. Two of them to be introduced.

First one is to add shutters – to the HEX spacers (fins) which leads to restart thermal boundary layer and so promotes heat exchange between fluid – air and spacers. On the pictures is comparison of heat exchange ratio between smooth spacer (left) and „shutter“ spacer (right). It is visible that for smooth spacer heat exchange ration decrease threow fin length due to establishing thermal limit layer. For shooter spacer thermal layer restarted in with each lower and so the average value is much higher. This phenomenon is followed by one negative think well and so pressure drop increase due to resistance of air on fin surface.

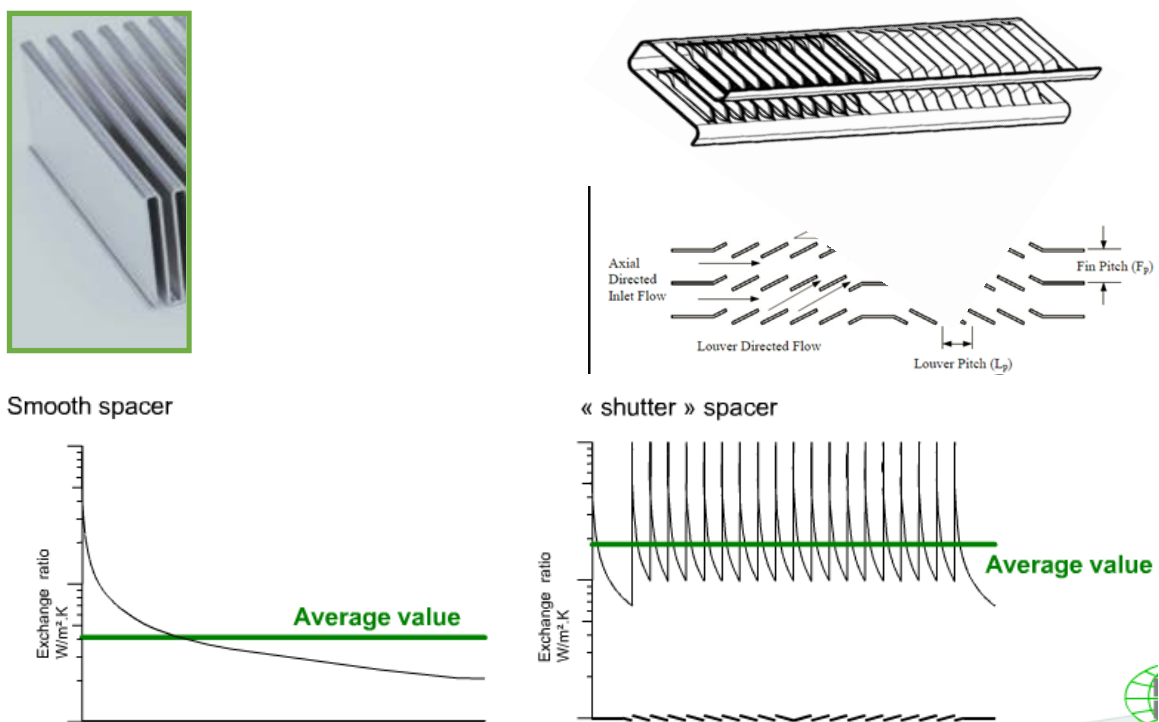


Figure 8-6: Smooth fin and shutter fin heat exchange ratio comparison [13]

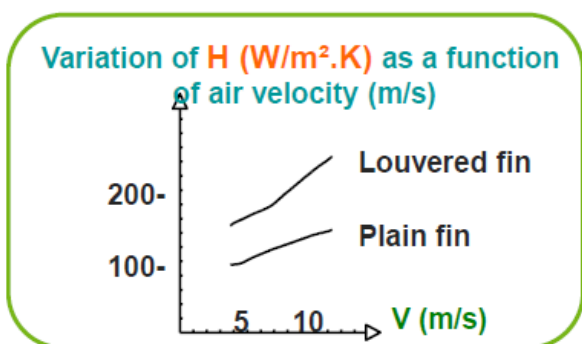


Figure 8-7: Direct comparison of smooth fin and shutter heat exchange coef. [8]

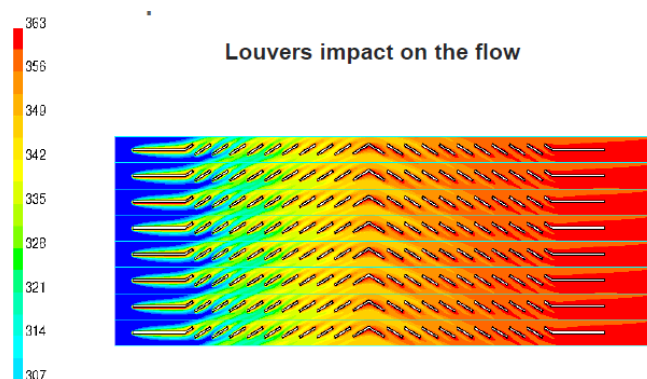


Figure 8-8: Air flow through fin length (CFD) [8]

Experimental measurements which were done by many research teams around the world (for example Ghajar and co-workers [21]) demonstrated that tubes with rough surfaces have much higher heat transfer coefficients than tubes with smooth surfaces. Therefore, tube surfaces are often intentionally roughened, corrugated, or finned in order to enhance the convection heat transfer coefficient and thus the convection heat transfer rate. Heat transfer in turbulent flow in a tube has been increased by as much as 400% by roughening the surface. Roughening the surface, of course also increases the friction factor and thus the power requirement for the pump or the fan. The convection heat transfer coefficient can also be increased by inducing pulsating flow by pulse generators, by inducing swirl by inserting a twisted tape into the tube, or by inducing secondary flows by coiling the tube.[20]

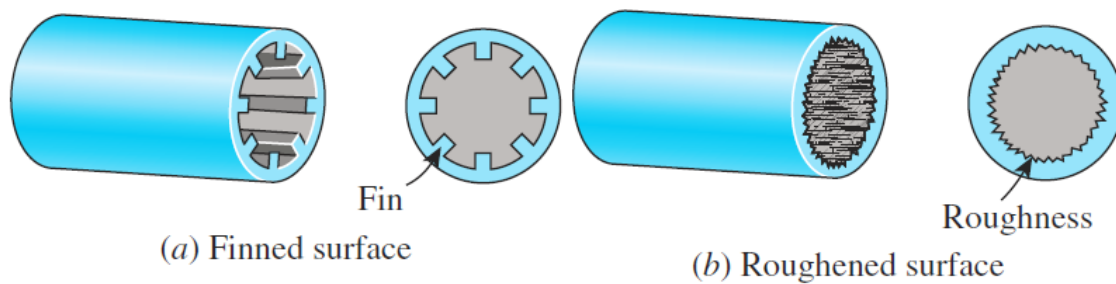


Figure 8-9: Possibilities of tube heat exchange coefficient improvement [20]

9 Aluminium brazed heat exchangers

9.1.1 Advantages of Aluminium Heat exchangers

There two main factors which explain why are Al heat exchangers so used in automotive. The cost savings realized by substituting an expensive raw material, copper, with a less expensive raw material, aluminium, and, the cost savings that are made possible by implementing higher performance products and more efficient fabrication processes. Aluminium offers a number of advantageous material characteristics for heat exchangers:

- Significant potential for lightweight design
- Highly automated, reliable manufacturing process (brazing)
- High thermal conductivity, also when joined by brazing
- Excellent corrosion resistance
- Good formability
- Adequate strength to resist temperature and pressure cycles
- Easy recyclability, i.e. an environmentally friendly solution

	Aluminium	Aluminium	Aluminium	Steel	Stainless Steel	Copper
	Alloy 1050A H14	Alloy 3003 H14	Alloy 6005A T5T6	E36 A52	Z7CN (18-09) 304	Laminate Temper M20
TEMPERATURE or Melting range (°C)	645 / 658	640 / 655	605 / 655	1400 / 1530	1400 / 1450	1083
Volumic Mass (kg.m ⁻³)	2700	2730	2710	7820	7900	8940
Thermal Expansion Coefficient (20 à 100°C) (10 ⁻⁶ .K ⁻¹)	23,5	23,2	23,5	13,5	17,5	17
Thermal Conductivity at 20°C (W/(K.m))	229	155	193	40	15	391
Yield Point (Mpa)	80	140	260	360	230	69
Breaking Strength (Mpa)	115	155	285	550	700	235
Extension (A%)	6	8	12	20	50	45
Elastic Modulus (Mpa)	69000	69000	69500	210000	200000	115000
Brinell Hardness (HB)	35	46	90	155		45

Figure 9-1: Material comparisons. [16]

9.1.2 Design of Aluminium heat exchangers

Although a wide variety of design concepts for aluminium heat exchangers exist, they invariably fall into one of the following categories:

- Tube / fin
- Plate-fin
- Plate-bar
- Extrusion / fin.

However majority of the heat exchangers used in today's automobiles are based on tube / fin designs. [17]

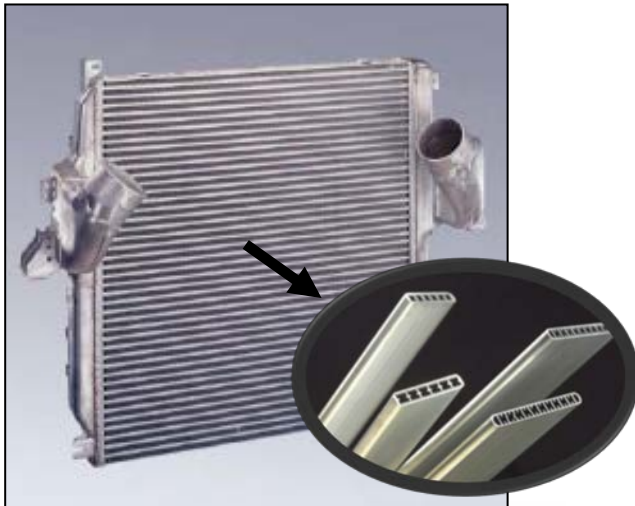


Figure 9-2: Charge air cooler in a tube / fin design (Denso). [16]

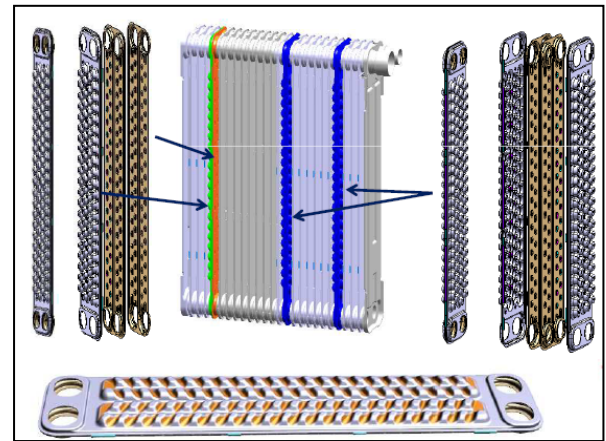


Figure 9-3: Evaporator in a fin / plate design (Valeo). [16]

There are three types of tubes for heat exchanger applications:

- Welded tubes
- Folded tubes
- Extruded tubes and these can be round tubes (RT) or multiport extrusions (MPE).

Welded round tubes can be used in mechanically assembled heat exchangers as liquid lines or as header pipes, e.g. in brazed condensers. Round extruded tubes can be subjected to a drawing operation for further reduction of the wall thickness and a closer control of the geometrical tolerances. MPE tubes are flat tubes with multiple small channels running the length of the tube, i.e. they could be described as one large tube split into multiple smaller parallel ports. The flat geometry of MPE tubes results in reduced aerodynamic drag and an advantageous development of the heat transfer boundary layer leading to larger heat transfer coefficients on the air-side (see chap. 8.2). The enhanced heat transfer of MPE tubes results from the increased ratio of the heat transfer area to the internal volume, and a favourable impact on the coolant flow regime and the dominant heat transfer mechanism.[17]

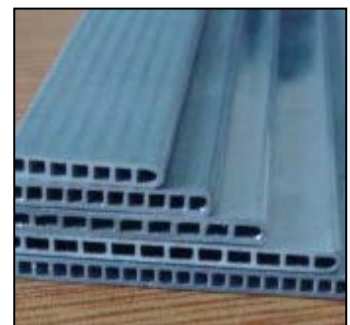
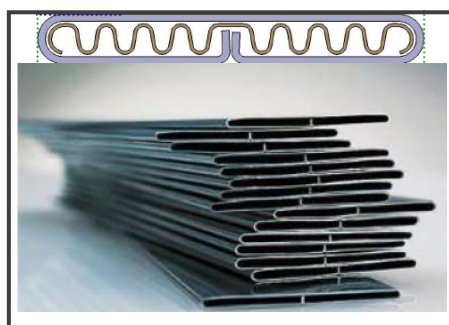


Figure 9-4: Charge air cooler in a tube / fin design (Denso). [16]

9.1.3 Aluminium brazed heat exchangers manufacturing

Brazed aluminium heat exchangers show a metallurgical bond between tube and fin which has a positive impact on several performance measures. Most important is the elimination of the contact resistance between tube and fin leading to significantly improved heat conduction. Different brazing processes have been used commercially to manufacture aluminium heat exchangers:

- Controlled atmosphere brazing (CAB)
- Vacuum brazing
- Salt bath brazing
- Neitz process
- Ni brazing.

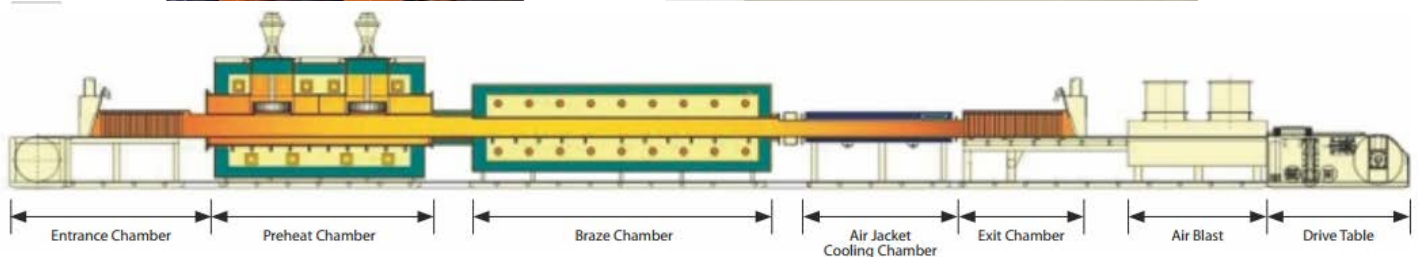
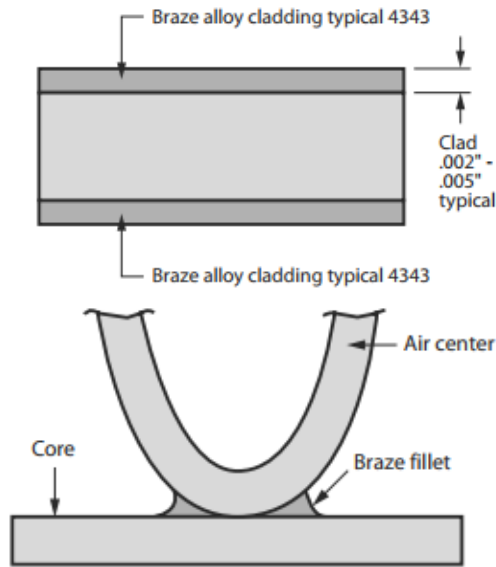


Figure 9-5: Vacuum furnace – left picture / Cab furnace right and bottom picture). [19]

The controlled atmosphere brazing (CAB) process heats a product to brazing temperatures while maintaining uniform temperatures within the product in an oxygen-free nitrogen atmosphere. During furnace brazing, a brazing sheet (Figure 9-7) of aluminium/silicon alloy plate (cladding) is heated to a liquid state and flows to form aluminium joints or fillets. The bond mechanism is that the elements from the core alloy and the filler alloy diffuse at the same time to one another. A sample of a fillet is shown in picture Figure 9-7. As a solder is used Al – Si which melting point is about 30 – 60 °C lower than core alloy (3xxx or 6xxx Al series). There is several ways how to apply solder to bonding material. The most common way is multicladd material when Al-Si is rolled on core alloy – after several steps of rolling and homogenisation annealing material rise.[19]

Diagram in picture 44 shows an Al - Si phase diagram giving reference to the different alloys used for CAB brazing with temperatures of the liquid phase for each.



Al - Si Phase Diagram

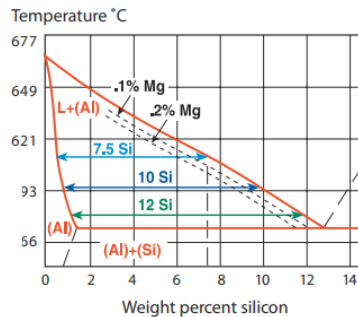


Figure 3

Alloy Melt Range °C	
1350 Liner	646 - 657
3003 CAB Core	643 - 654
3005 AVB Core	638 - 657
6061 Fittings	638 - 652
4343 CAB & AVB Clad	577 - 612
4045 CAB & AVB Clad	577 - 599
4047 CAB & AVB Clad	577 - 582

Figure 9-6: Clad function



Figure 9-7: Clad distribution in alloy. [16]

The manufacturing of brazed heat exchangers using tube and fin components is well established within the automotive heat exchanger industry. Highly-automated assembly and brazing processes suitable for high volume production provide both high throughput and excellent quality leading to heat exchangers comprised of joints made with 100% metallurgical bonding.

Aluminium producers, brazing flux producers and furnace builders actively work together to improve and further develop the brazing processes for better economy and environmental friendliness. A wide range of heat-treatable and non-heat treatable aluminium alloys are available both for tubes and fins. Suitable aluminium materials for brazing applications (coils, sheets and tubes) can be delivered in a large variety of alloy combinations, clad ratios, sheet thicknesses and widths according to customer specifications.

Aluminium alloys are now well established materials for the manufacture of automotive heat exchangers. They offer properties that can be favourably utilised in various components:

- High thermal conductivity
- Low density
- Adequate strength (also at elevated temperatures)

- Good formability
- Excellent corrosion resistance.

Proper selection of aluminium alloys and product forms offers the possibility to develop and produce the various types of heat exchangers used in modern automobiles and to respond to the ever increasing market demands with respect to improved heat transfer performance, but also reduction of weight, size and cost.

For heat exchangers, different types of rolled as well as extruded aluminium products are used:

- Flat rolled materials, e.g.:
- Unclad fin stock for radiators, charge air coolers, heaters, etc.
- Clad fin stock for condensers
- Clad header plates and side plates for various types of heat exchangers
- Clad strip for welded or folded tubes for radiators, charge air cooler, heaters, etc.
- Clad plates for evaporators and oil coolers.
- Extruded material, e.g.:
- Extruded tubes for evaporators, radiators, condensers, etc.
- Extruded and drawn tubes for radiators, heater cores, evaporators and condensers
- Multiport extrusion tubes (MPE) for evaporators, condensers, charge air coolers, etc.
- Extruded shapes. [17]

9.1.4 Aluminium brazed heat exchangers material

The specific characteristics of aluminium heat exchanger materials differ depending on the product form and the envisaged application. Consequently, several aluminium alloy systems are used in heat exchangers and there are numerous alloy variants which have been developed for optimum performance during assembly (in particular depending on the applied brazing method: vacuum brazing or controlled atmosphere brazing utilizing potassium aluminofluorate fluxes) and in service (i.e. excellent corrosion resistance).

Non heat treatable – NHT (especially Al class 3000 – system Al-Mn) and heat treatable – HT (especially Al class 6000 – system Al-Mg-Si) aluminium alloys can be selected for the different heat exchanger components. In pure aluminium and NHT alloys, strain hardening by cold deformation increases the basic strength achieved through solid solution and dispersion hardening. Recovery and recrystallization processes during brazing, however, will eliminate any strength increase by strain hardening. HT alloys are strengthened by cold deformation as well, but offer in addition the possibility of precipitation hardening. Brazing processes carried out at approx. 600°C are ideal to dissolve the soluble alloying elements. Subsequent fast cooling will retain these elements in supersaturated solution. Precipitation hardening, i.e. the nucleation and growth of fine precipitates in HT alloys can then lead to a significant strength increase, both at room temperature (natural hardening) or by ageing in the temperature range 150-200°C either in a separate heat treatment step or – immediately after brazing - by controlled fast cooling and holding of the brazed component in the critical temperature range for a certain time.[18]

A. FIN

Fins require a high thermal conductivity, an advantageous strength-to-weight ratio and good corrosion resistance. Most important is also the ability of aluminium alloys to be formed into complex fin geometries. In mechanically joined heat exchangers, high formability is essential to the trouble-free production of collar fins. As a fins has a very small thickness (50 – 100 µm) so called sagging often occurs during brazing. As a sagging is marked the process which occurs during brazing (material recrystallization, fin deformation) which could leads to collapse of the heat exchanger assembly. In brazed heat exchangers, fin materials are typically based on the alloy EN AW-3003, but in general slightly modified compositions are used for optimum performance. Small additions of Cu and/or Mg (if allowed by the applied brazing technique) are made for increases strength. Other alloy variants contain higher amounts of Mn and sometimes also Si to ensure a higher strength after brazing, and a good sagging resistance during brazing. These alloy compositions favour the formation of large grains during brazing, which is beneficial for the sagging behaviour and hinders braze metal penetration into the core. Also low alloyed heat treatable alloy of the AlMgSi system (6xxx series alloys) are sometimes used (e.g. EN AW-6060 or EN AW-6063).

Additionally, fin stock alloys can be tailored for the cathodic protection of tubes or header alloys against corrosion by adding zinc in different levels (up to 2.5 % Zn). The range of the applied fin stock materials is further increased by clad fin variants where the clad composition is adapted to the composition of the core ally and to whether it is intended for vacuum brazing or brazing in controlled atmosphere with or without flux.[17]

Over the years, extensive alloy development activities and product-specific process optimization efforts have allowed a significant down gauging of the aluminium heat exchanger materials, enabling a considerable reduction of weight and cost.

B. Bare and clad rolled materials for headers, plates

The alloys (core alloys for clad variants) used for rolled strips and sheets for headers, side supports, tubes, etc., have essentially the same compositions as those listed above for fins (with the exception of the Zn-containing variants). For brazing applications, the core is clad with Al-Si alloy layers which act as the source for the filler metal during the brazing process. The thickness of the brazing clad layer is generally 5 - 20 % of the sheet thickness for one side clad variants, and 5 – 15 % if both sides are clad. Typical clad alloys for controlled atmosphere brazing are EN AW-4343 and EN AW-4045, for vacuum brazing EN AW-4004, EN AW-4045 and EN AW-4047. But there are also numerous modifications of these basic compositions in use.[17]

Aluminium brazing sheet is a highly engineered material consisting of multilayer composite materials of varying complexity. Depending on the requirements of the specific application, these materials can comprise 2, 3, 4 and even 5 layers. Each layer either serves a specific purpose during the production process or is used to meet a heat exchanger functional requirement while in service. For example, a 3XXX core alloy layer for post-braze strength can be clad with a modified 3XXX alloy layer for corrosion protection and a 4XXX alloy layer to provide the filler metal needed for the brazing process. Even more complicated version may be necessary for controlled atmosphere brazing (CAB). Magnesium additions significantly improve the mechanical properties of aluminium alloys. Unfortunately, magnesium interferes with the activity of many commercial fluxes (material improves the brazing). Nevertheless, multiple cladding layers can still permit the use of higher strength magnesium-bearing core alloys for CAB applications. Magnesium-free intermediate claddings serve as barriers to the diffusion of magnesium from the higher strength magnesium-bearing core alloy, and thereby reduce or eliminate any “poisoning” of the flux.

Clad aluminium tubes for brazing applications, adapted to the different brazing processes, are produced on roll forming lines from flat rolled strips in flat oval, rectangular and round profiles by longitudinal welding (generally using the high frequency welding process). Mostly, only a 2-layer composite consisting of the core alloy (typically EN AW-3003 or a modification of this alloy) and the brazing layer at the outer surface is used. If necessary, the core alloy can be covered on the other (inner) side for corrosion protection, e.g. with EN AW-1145 or EN AW-7072. [17]

C. Extruded tubes

Extruded tubes are available in various shapes, sizes and alloys. Apart from simple extruded tubes, heat exchanger tubes include in particular round or oval precision drawn tubes as well as multi-port extrusion (MPE) tubes. Although extruded aluminium tubes do not have the same performance characteristics as precision drawn tube, they can present a cost-efficient alternative in less demanding applications.

Round tubes are often smooth walled, but their performance may be also enhanced with axial, straight or helical micro-fins on the inner diameter surface to improve the refrigerant-side heat transfer by increasing the surface area. In case of precision drawn tubes, the calibration process ensures a high outer surface quality as well as narrow geometrical tolerances. Furthermore, precision drawn tubes offer highest quality and excellent processing capabilities for operations as bending, end forming, expanding, etc. Typically, aluminium alloys like EN AW-1050, EN AW-3003, EN AW-5049 and EN AW-6101 and modifications of these compositions are used both for extruded and precision drawn heat exchanger tubes. Long life (high corrosion resistant) alloys can also be used. Round tubes are found as header pipes in automotive heat exchangers such as condensers and as fluid lines in e.g. AC systems. MPE tubes are manufactured to meet specific requirements with respect to alloy, outside dimensions, wall and web thickness, hydraulic diameter, and other attributes. With their large internal surface area, the MPE profiles (or micro-channel tubes) achieve a more efficient heat transfer and are therefore ideal for use in highly effective heat exchangers. The tube material must have adequate strength (high pressure resistance) and fatigue resistance together with good air-side and waterside corrosion resistance. As more and more complex tube designs are used, the formability of the tube alloys becomes of greater importance. Thus MPE tubes are typically made from the alloys EN AW-1050, EN AW-3003 and modifications of these alloys.[17]

10 Task specification: Inner gas cooler requirements

The task of practical part of thesis is to design of heat exchanger – inner gas cooler (IGC) for R744 refrigerant which operates on high pressure side of cycle. As was described in theoretical chapter (chap. 4) this heat exchanger works as a heating in R744 heat pump system.

Heat pump system where to be heat exchanger used works under pressure from 50 – 170 bar (vehicle off / vehicle on – maximal possible pressure). Operating temperature range from -45 °C to 130 °C. max. Safety coefficient 2 for static pressure was set up – it means heat exchanger must withstand 340 bar at 130 °C. Heat exchanger must be able operate min 15 years for this was calculated 150 000 cycles of pressure change (vehicle off / vehicle on + discharge). As the Inner gas cooler operates either in winter where is low temperature and so low air humidity or in demisting mode when dehumidification of the air is secured by evaporator there is quite good corrosive environment. Anyway corrosion properties of heat exchanger must be demonstrated. Mechanical properties of heat exchanger could be influenced by sudden temperature change – this occasion must be tested too. As the heat exchanger operates under enhanced temperatures – influence of creep for HEX mechanical resistance must be checked. As the space of in the HVAC is limited dimension of heat exchanger could not exceed envelope 232 x 190 x 35 mm.

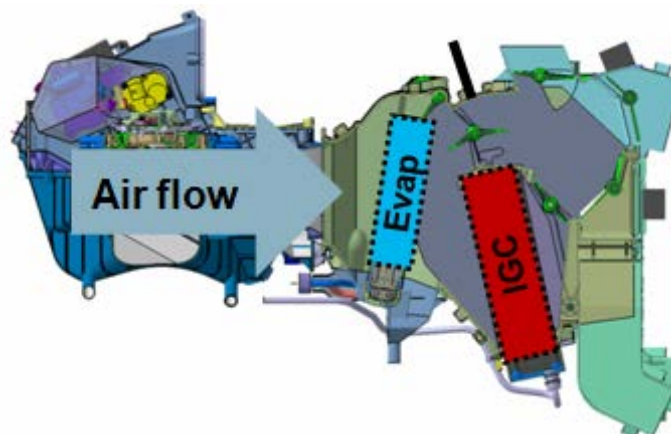


Figure 10-1: Position of IGC in the HVAC

Heating rejection performance must be the highest possible but minimum is 5,5 kW and to be assumed at following conditions:

- MA – Air mass flow through inner gas cooler = 390 kg /h
- TAIRI – Temperature Inner gas cooler inlet = 10 °C
- PRIGI – Pressure inner gas cooler inlet = 120 bar
- TRIGI – Temperature inlet = 120 °C
- M_ref- Ref. Mass flow = 82 kg / h

Due to reality that A/C is multi-zone (could be up to 3 zone) the zones are horizontally oriented and each section of IGC is used for one of the zone. Temperature of IGC body must be as much homogenous is possible.

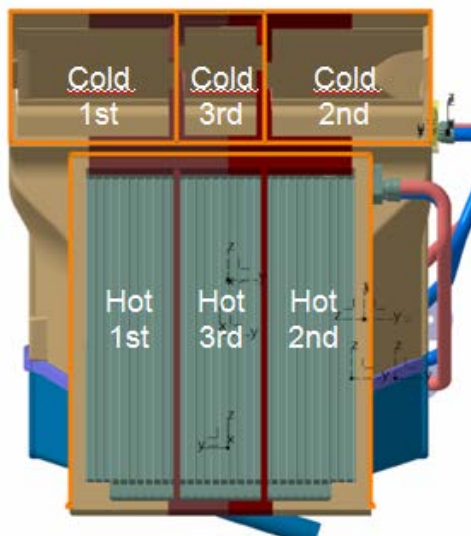


Figure 10-2 Zone distribution in the HVAC

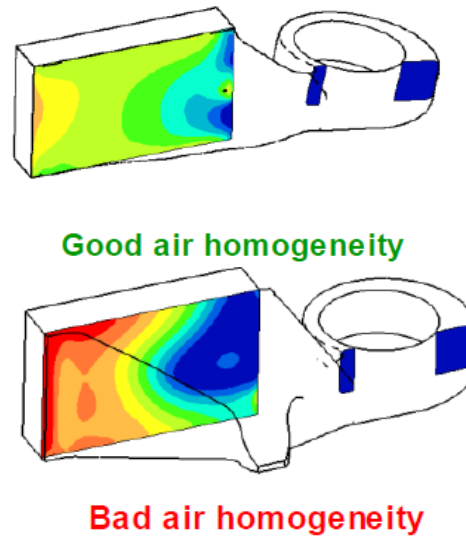


Figure 10-3 Good and bad temperature imbalance – HEX in HVAC

Tests	Values
Static mechanical test – Burst test	340 bar @ 130°C
Fatigue mechanical test – Pressure cycle	50-170 bar. @ 130 °C, 150 000 cycles
Temperature homogeneity	$dT - L/R < 3K$ a $dT - \text{min.} / \text{max.} < 10K$
Heat rejection power	5,5 KW @ MAE – 390 kg/h, TAIRI - 10°C, PRIGI – 120 bar, TRIGI – 120°C, MRIGI – 82 kg/h

Table 10-3 IGC test requirements

Design of IGC - heat exchanger should be based on already existing heat exchangers of Valeo Group. Firstly to avoid patent collision with competitors secondary to use already existing production capacities (production machines) of company.

11 Available Heat exchangers research

11.1 LUCIE - Evaporator

First heat exchanger is LUCIE (Light Ultra Cooling Innovative Evaporator) – evaporator. This heat exchanger is designed for low pressure side of R134a refrigerant however there is certain possibilities to make a redesign for R744 refrigerant.

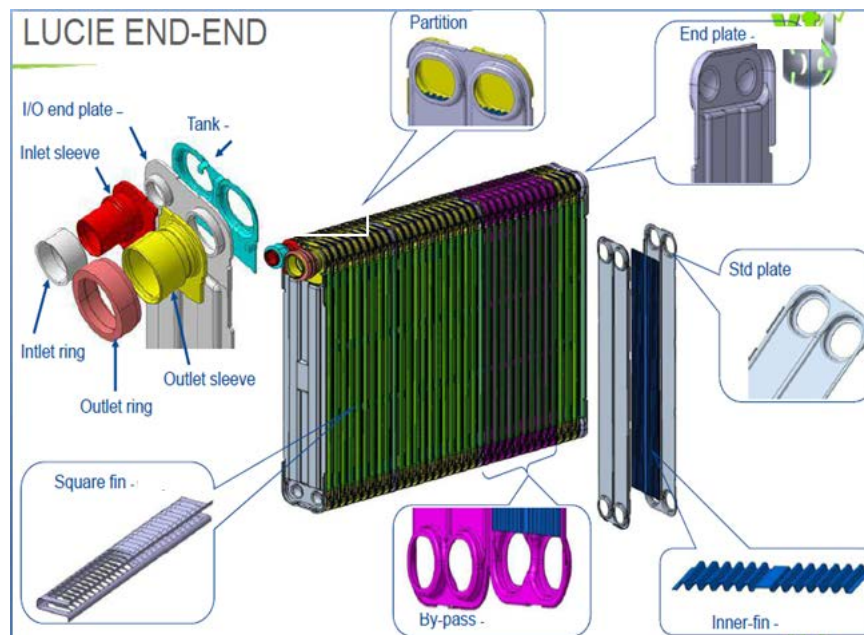


Figure 11-1: LUCIE - HEX

This is the fin plate heat exchanger where 2 plates assembled together with part inner fin creates (after brazing in furnace) tube where refrigerant flow through. The benefit of this solution is that thanks to inner fin there is enhanced heat exchange surface on refrigerant side and so improved heat flux from refrigerant side to air side. The disadvantage is that such a big surface cause enhanced fluid friction, increased of pressure drop and as a consequence decreases saturation temperature. Inner fin also noticeably improve mechanical resistance of tube as inner fin works like a rib. A square outer fin design secure better contact between fin and tube (which improves heat conduction).

In the heat exchanger there are several types of tubes (standard, partition, by-pass) which suitable positioning in heat exchanger core creates decided cooling circuiting. The circuiting of this heat exchanger is designed as the cross – counter flow 6 pass. It means that air inlet (hot) is oriented to heat exchanger refrigerant outlet (hot) and 6 pass improves heat exchanger temperature imbalance (heat map) – mechanism to be explained in following paragraph.



Figure 11-2: 6-pass

Although in most of circuiting length the evaporation process occurs and so only latent heat is absorbed by refrigerant and so no temperature increased. However on the certain evaporator length the evaporation ends (vapour quality: $x=1$). After this length vapours is superheated and so increase its temperature. This leads to temperature unbalance on HEX surface. Compensation is enabled that the coldest pass is covered by hottest pass on the opposite side. The second hottest by second coldest etc. (see figure 11-2).

As the plate material is very thin there is special focus to secure corrosion protection and are used even two anticorrosion mechanisms. Firstly material of plates is from so called Long life alloy (LLA). The function of this alloy is that during brazing Si diffuse from clad layer (Al-Si) to core layer (Al-Mn) and destabilise supersaturated solid solution of manganese in aluminium. This cause creation of Al-Si-Mn precipitation in small layer called Dense layer or Brown band. Electrical potential of this layer is lower than the rest of the material which cause that corrosion doesn't go directly throu (point corrosion) but is lateralised by this mechanism. Other properties of LLA is that due to alloy special manufacturing process are Al grains oriented and creates so called pancakes structure. Thanks to this undesirable intergranular corrosion is considerable limited. The second anticorrosion mechanism is that HEX fins are alloyed by Zn which decreases it's corrosion potential vs. tubes material and fins are sacrificed in favour for tubes.

From components manufacturing point of view the situation is favourable as only stamping technology is required.

11.2 R744 Evaporator

R744 evaporator has been developed recently. It operates on low pressure side of the cycle and hydraulic diameters of this HEX are designed for this. The base of heat exchanger is sub-assembly of 2 tanks (top, bottom). The tanks main function is to distribute refrigerants to flat tubes and to create desired circuiting. In case of R744 Evaporator is it 6 pass. The refrigerant inlet to right sleeve and flow through top (superior tank) and on parallel fills all flat tube during its way until is stop by barrier in top tank (marked green in circuiting schema – Figure 11-3) – pass 1. Refrigerant then continue flow in bottom (inferior) tank and on parallel fill flat tube till bottom tank barrier is reached – pass 2. Flow now continues from top tank toward to bottom tank – pass 3. On the bottom tank the refrigerant is redirected by by-pass section of bottom tank to left side of evaporator. Here the pass 4 copy pass 3, pass 5 copy pass 2 and pass 6 copy pass 1. Only difference is that flow is now on the left HEX side.

In each tank is presented header component to which are inserted flat tubes and which fix the other components (distribution, intermediate, cover). Distribution plate separate right and left side of HEX and allow its by-pass section refrigerant redirection. Cover plate is responsible for refrigerant distribution throu tank and creates passes by its barrier. Intermediate in fact works like a spacer to get sufficient hydraulic diameter as the manufacturing feasibility not allows creating sufficient cross section directly in cover.

Flat tubes has a 9 nine channel and are designed as a compromise between maximal possible hydraulic dimension (to keep refrigerant dP at minimum level) and it's mechanical resistance. Brazing process is secured by multi clad material (2 layers of Al 4343 on both

sides of plate components). Intake of refrigerant is secured by sleeves pressed to connector (brazing joint is created during brazing). Connector is extruded components with following machining (to create holes inside). These 2 operations make this component very expensive. Other extruded components are flat tubes. As for extruded components is not possible to apply mutli clad concept is solder applied by different way. On the flat surface is applied so called Silflux. Si during brazing temperature diffuse to tube material which locally decrease melting point of flat tube aluminium and so brazing joint between flat tube and fin is created. The circuiting of R744 evaporator is the same as LUCIE – means Cross counter-flow and 6 pass.

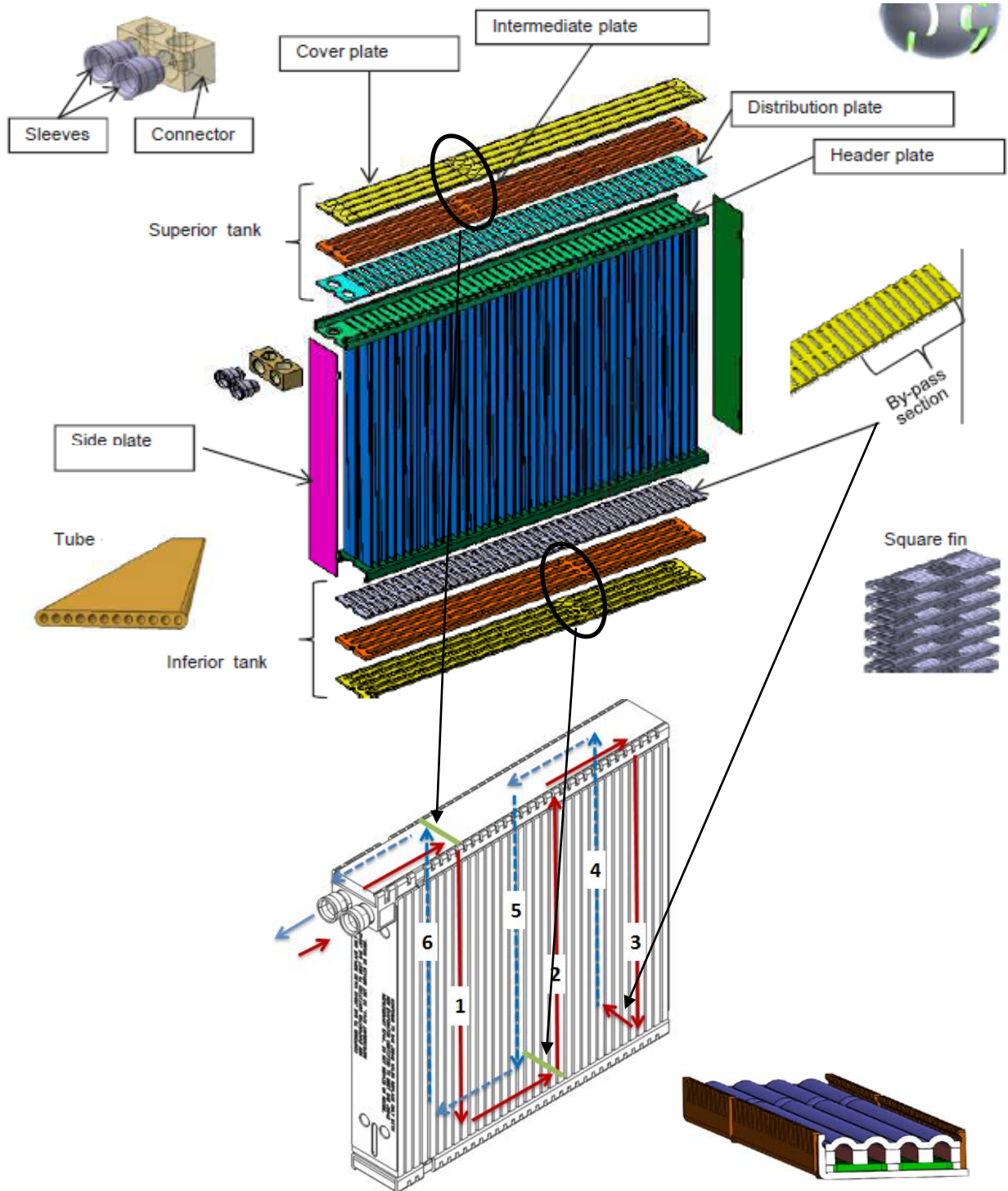


Figure 11-3: R744 - Evaporator

Figure 11-4: Tank cut view with details to channels

11.3 R744 – Outer cooler

This heat exchanger has been developed by Poland branch of company and so there is low availability of information. The benefit is that this heat exchanger works in high pressure side of R744 cycle. Disadvantage is that in this heat exchanger are many extruded components with following machining operation which makes heat exchanger a quite costly and its assembly requires new line equipment for its assembly.

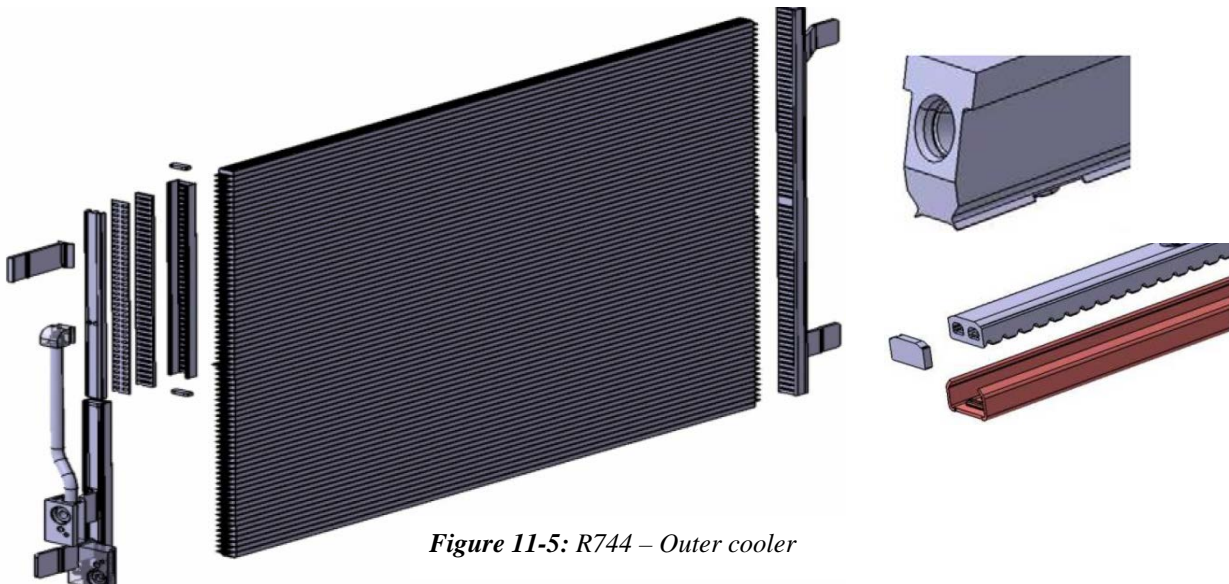


Figure 11-5: R744 – Outer cooler

11.4 Decision matrix

With all information about all 3 introduced heat exchangers weighted decision matrix was constructed and R744 Evaporator chosen as the most feasible for redesign.

Parameter	Weight	LUCIE		R744 Evaporator		Outer cooler	
Mechanical Robustness	5	1	5	3	15	5	25
Components in plant production feasibility	4	5	20	4	16	1	4
Manufacturing equipment possible to re-use	4	3	12	5	20	1	4
Corrosion resistance	2	2	4	4	8	5	10
Weight	2	5	10	3	6	3	6
Sume			51		65		49

Figure 11-6: Decision matrix

12 R744 – Evaporator redesign

In the previous part has been introduced heat exchanger feasible to be redesign for R744 – Inner gas cooler (IGC). Based on decision matrix has been chosen R744 – Evaporator. To understand where is the evaporator from mechanical resistance point of view vs. requirements demands for IGC main mechanical test has been launched.

1. Burst test

Burst test is static mechanical test mechanical test when heat exchanger is pressurised by test medium (Oil) till destruction (details below). Test was done on Burst machine - equipment of Zebrak laboratory. Test was not done according requirements at 130 °C but was done at room temperature of test medium (water) and components as the Valeo Zebrak testing machine is not equipped by heating device. 5 samples were tested. Burst values has been in range 324,6 bar – 332,5 bar. Analyses of parts after the test showed that there was one repetitive failure – crack in top tank in brazing joint between joined components: Intermediate and Distribution plate (Figure 12-2). Following metallographic analyses showed imperfections – porosities in these brazing joints. Figure 12-4 is detail photo of distribution plate where dark squares are relict of brazing joints. On these squares are visible white points – which are the porosities.

Testing conditions:

- Test medium and component temperature: 20 °C
- Initially HEX is pressurized by testing medium by speed 10 bar/s till pressure 120 bar is reached
- Than speed pressure is 1 bar/s until 320 bar is reached than HEX must withstand this pressure > 1 min. without any leakage
- Subsequently, the pressure is increased by max. 0,1 MPa/s until bursting.
- Sanction: HEX must withstand min 320 bar

NO.	Burst value [bar]
1	324,6
2	332,5
3	330,3
4	325,5
5	330,1

Figure 12-1: Burst test results

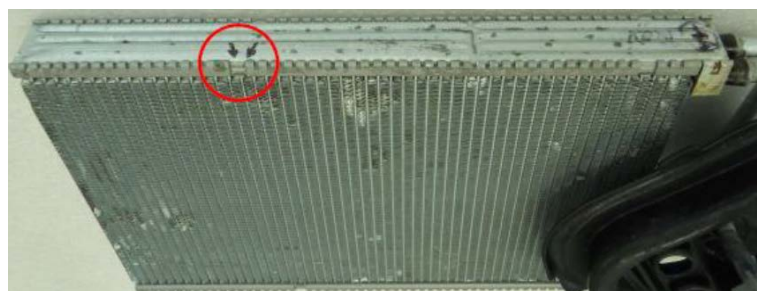


Figure 12-2: Sample after burst test – with marked failure area

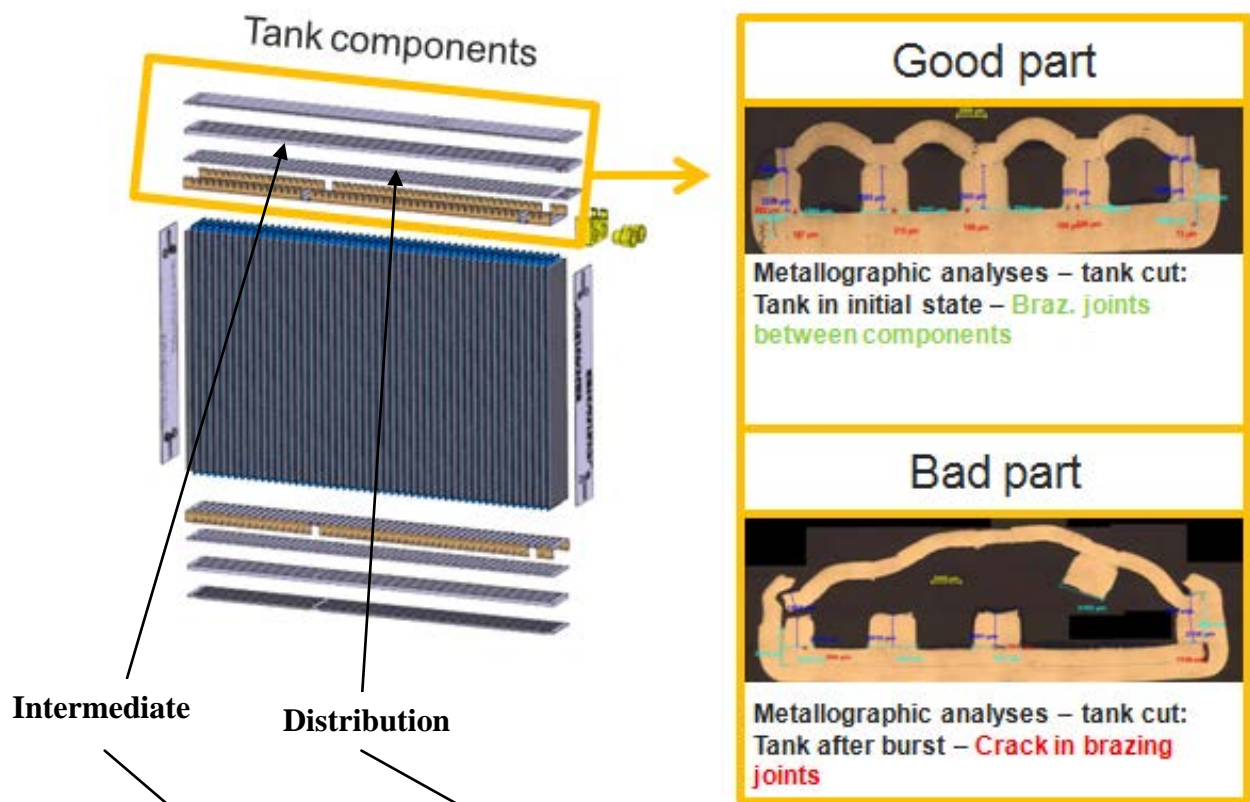


Figure 12-3: Metallographical analyses in failed area

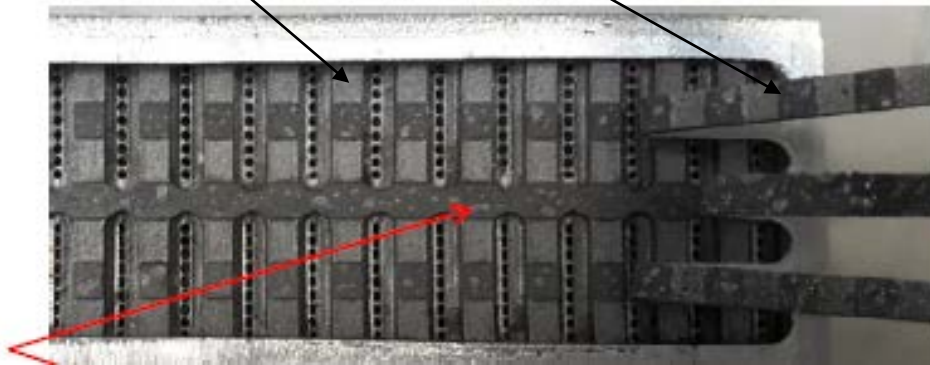


Figure 12-4: Detail of part after burst test

From this basic test was found that top tank must be strengthened as the requirements for IGC are resisting 340 bars @ 130 °C.

To determine dependency of Burst pressure on temperature the Burst pressure test at different temperature has been done at Czech aerospace research centre (VZLÚ) in Prague as this institute has necessary equipment. 8 evaporator samples were tested under different temperature to be able to determine dependency of burst pressure on temperature.

The failure mode remains the same for all tested parts– crack in the brazing joint between Distribution and Intermediate plate.

Temperature (°C)	Burst Pressure (bar)
25	322,8
70	320,8
100	305,2
125	294,4
135	291,5
145	285,6
155	281,7
165	277,8

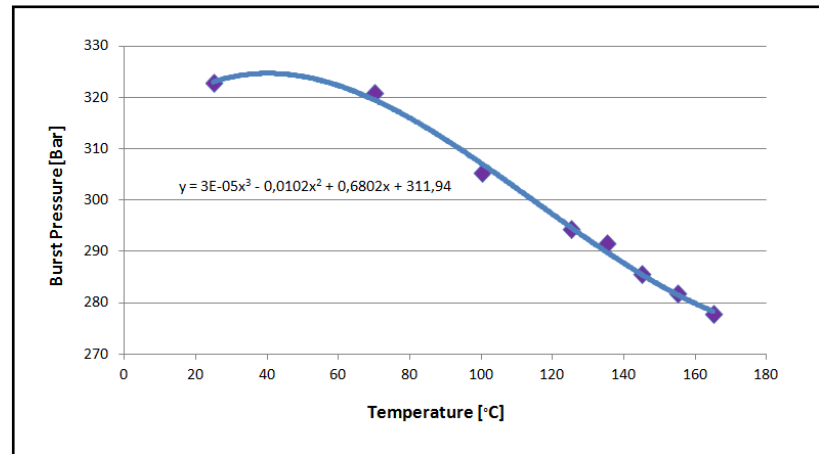


Chart 12-6: Dependency of Burst pressure on test temperature

From the results could be read that burst pressure of evaporator is 293 bar at 130 °C. If we compare the results at room temperature vs. Temperature at 130 °C we can observe mechanical degradation about 9%. From this consideration follows that to reach 340 bar at 130 °C is necessary to reach 370 bar at room temperature.

To see resistance of evaporator to fatigue, fatigue test – “Pressure change test” was launched. During this test is heat exchanger alternately pressurised.

Testing conditions:

- Test medium and component T: 130°C
- Pressure difference (dP): 50 – 170 bar
- Frequency: 1 Hz

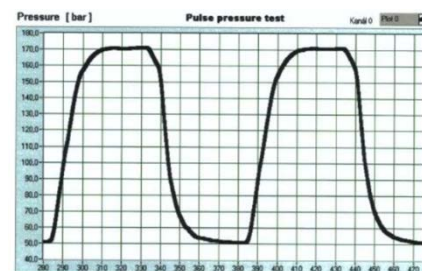


Chart 12-7: Pressure test frequency

Test was launched for 2 sample and 131 000 and 135 000 cycles was reached. Failure cause was the same as for static test - crack in top tank.

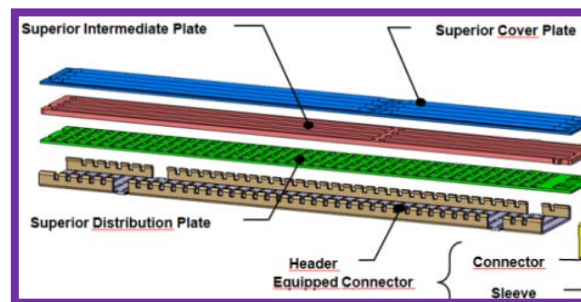
As the failure mode is for both test same and for static test there is bigger distance from desired values (Burst: 293 bar reached/340 bar desired vs. Pressure change test: 131K cycles reached / 150K cycles desired) implies that if static strength to be reached also fatigue requirements to be met.

From the test is known the „weakest“ component of assembly tank which should be reinforced by design change - however it tells anything about other components as during the test was not reach failure. To determine their ultimate strength FEM analyses to be done.

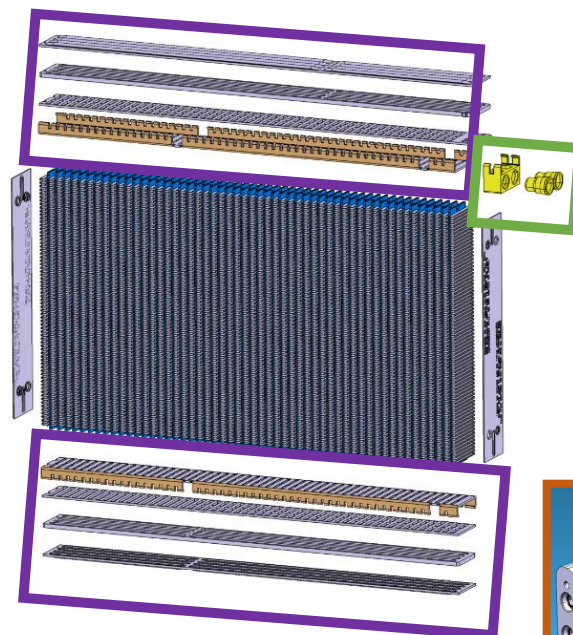
13 FEM – Mechanical robustness of R744 evaporator

The heat exchanger is made of 4 design groups: 1. Tank sub-assembly, 2. Flat tube, 3. Connector sub-assembly, 4. Pipes (Figure 12-8)). The materials of these groups are in table: xx. From the table is visible that heat exchanger consist from 3 Aluminium types - EN AW 3003 (Al-Mn) , AA 1197 (Al-Mn) and EN AW 6101(Al-Mg-Si).

1. Tank sub-assembly



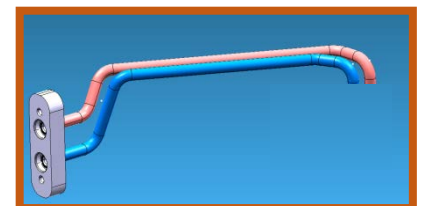
2. Flat tube



3. Connector sub-assembly



4. Pipes



Design groups material overview		
Group des.	Component	Material
Tank sub-assy.	Cover plate	EN AW 3003 – O, H20
	Header	
	Distribution plate	
	Intermediate	
Flat tube	-	AA1197
Connector sub-assy.	Connector	EN AW 6101
	Sleeve	EN AW 3003 - O
Pipes	Pipes	EN AW 6101 – T6

Table12-8: Design groups material overview

On the Table 13-1 is as example showed one of 6 received test report. On the table 13-2 is shown main material characteristics under given temperature reached by tensile test. From the table is visible that temperature 130 °C range has only small impact to yield strength (Rp0,2). However there is noticeable impact to ultimate strength (Rm) where is degradation from 7,5 % - 12,5 % in dependency of Al type. What is important these results are in line with results from Burst test where temperature 130 °C caused 9% HEX mechanical degradation vs. Burst under room temperature.

Material	Testing Temperature	Rp0,2 [Mpa]	Rm [Mpa]	A [%]	E [Gpa]	Rm degradation [%]
EN AW 3003	24 °C	66,2	113	10,4	53,6	10,6
	130 °C	63,9	100	14,4	78	
EN AW 6101	24 °C	90,4	200	26,7	59,6	12,5
	130 °C	91,6	175	27,4	59,5	
AA 1197	24 °C	18,3	73,2	17,1	37,3	7,5
	130 °C	18,8	67,7	17,2	29,6	

Table 13-2: Design groups material overview

13.2 Mechanical calculation

For mechanical calculation the following steps were taken:

1. Model creation + simplification – CATIA
2. Model mesh creation + material definition – NX NASTRAN
3. Boundary condition definition – NX NASTRAN
4. Linear static analyses – NX NASTRAN solver 101 (SOL 101 – lin. statics global constraints) – Inner pressure 170 bar (maximal possible pressure in car)
5. Nonlinear static analyses – NX NASTRAN solver 106 (SOL 106 – nonlinear static) – Pressure iteration till material Ultimate strength achieve

*Note: Von Mises stress (HMH theory) to be used

13.2.1 Tank sub-assembly

Simulation for tank sub-assembly was done on tank section to speed up calculation. Components in tank were merged by Boolean operation in Catia and brazing joint radius was added. Due to complex geometry of model tetrahedral mesh (CTETRA(10) with local mesh refinement were used. Model was fixed in grooves (blue) to represent real fixation by flat tubes in HEX. Pressure was applied to inner area of tank (red).

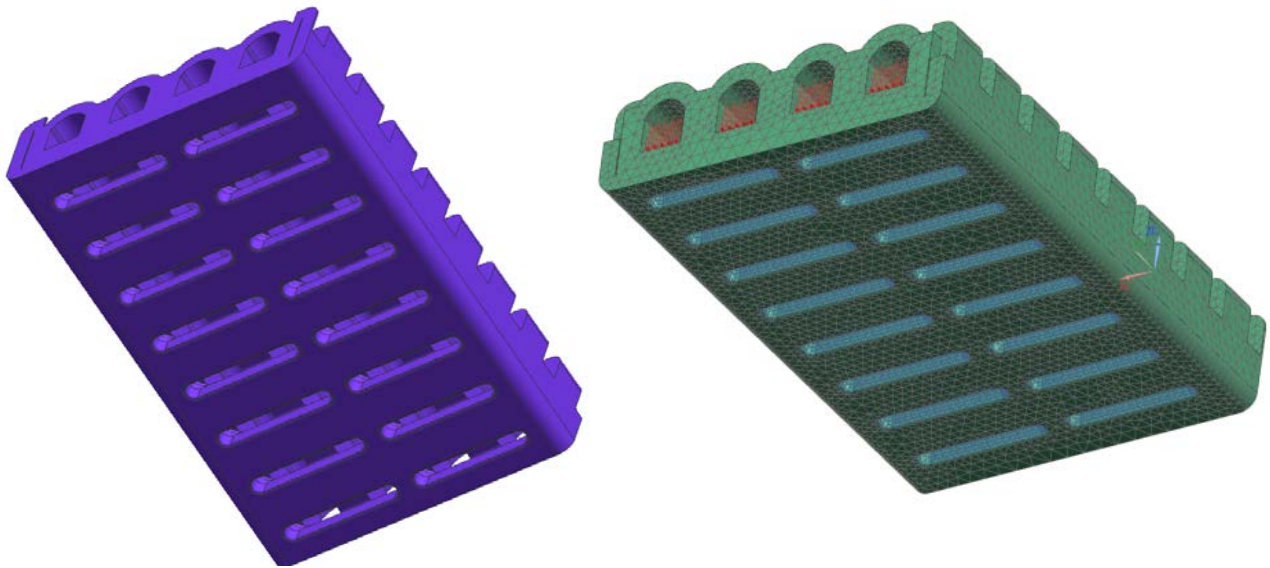


Figure 13-3: Model (left), Mesh model with boundary conditions and loads (right)

Linear static calculation (applied pressure: 170 bar) is in line with the real results as showed critical area between distribution plate and intermediate. $R_{p0,2}$ of material was in that area very overreached (however local stress their - 165MPa is non-realistic due to linear analyses). The rest of the component remains in elastic domain.

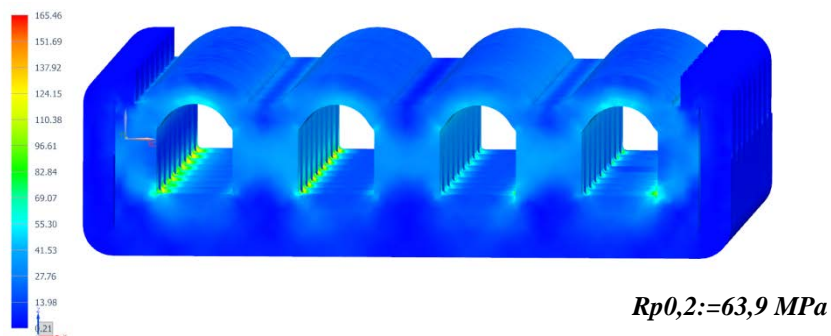


Figure 13-4: Load: 170bar, nonreal values due to linear analyses

For nonlinear static calculation was applied pressure increased to 340 bar where was reached material R_m limit for area between distribution plate and intermediate. The rest of model is far away from rupture.

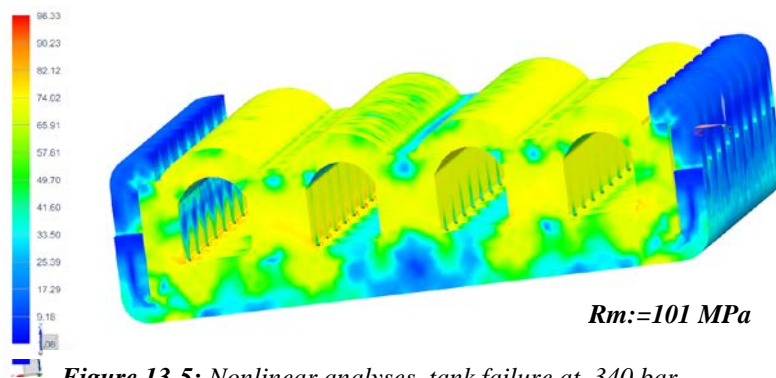


Figure 13-5: Nonlinear analyses, tank failure at 340 bar

To compare FEM results vs. results from real test (page 70) is visible that FEM indicates the same critical area however there is a gap between FEM crack prediction – 340 bar and real test crack – 293 bar (deviation of 16%). The reason is that real brazing joint was found as porous while FEM model is homogenous. During tank design modification must be taken 16% deviation to account.

13.2.2 Flat tube

The simple geometry of flat tube allow to use 3D swept mesh (chexa(8)). The prepared model was 1/2 of real pipe length. Fixation follows flat tube position in IGC tank. Inner pressure was applied to each of one hole.

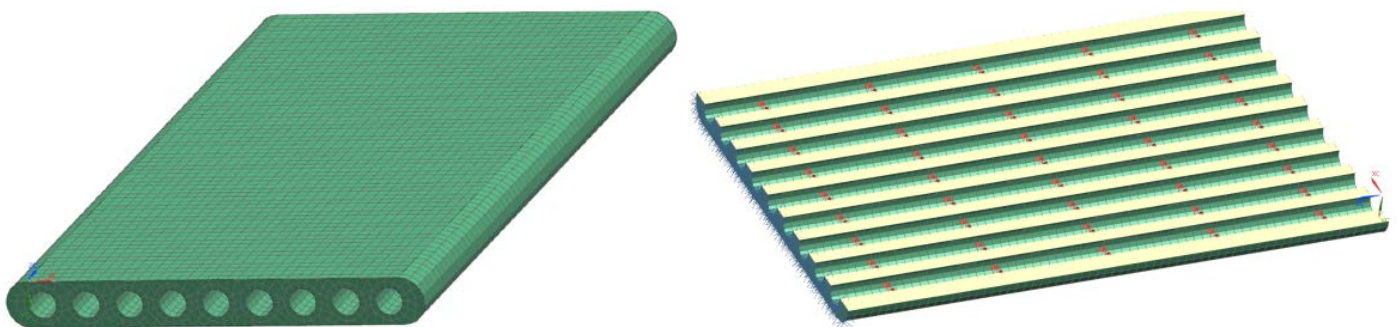


Figure 13-6: Model mesh (left), Boundary condition and loads (right)

Linear calculation showed that applied pressure 170 bar causes local stress which exceed material $R_{p0,2}$. Nonlinear calculation detected as 340 bar as pressure which lead to destruction and so also this component must be strengthen to be able to use it for IGC. While stress reaches its maximum on the side-wall between 2 channels / upper and lower wall has relatively low stress level.

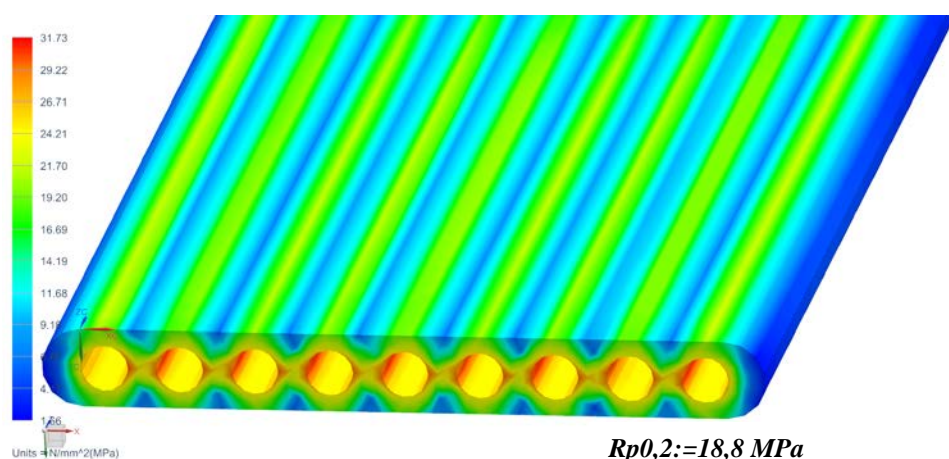


Figure 13-7: Linear analyses, load 170 bar

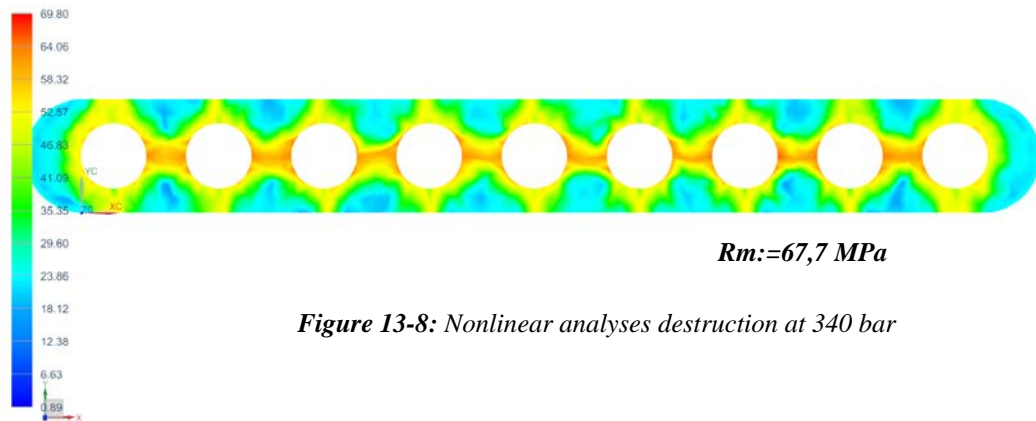


Figure 13-8: Nonlinear analyses destruction at 340 bar

To evaluate FEM results test on flat tube samples was done at 10 samples – results in range 331 to 347 bars was reached. The failure mechanism in crack tube was the one – firstly side wall crack which create “big pocket” and subsidiary overall destruction of flat tube. The failure mode is in line with FEM result.



Figure 13-9: Sample after the test

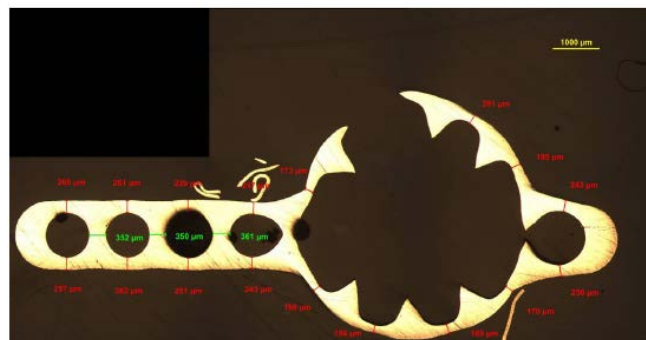


Figure 13-10: Metalanalyses of the sample after the test

13.2.3 Connector sub-assembly

This part consist of sleeve - pink (material: EN AW 3003) and connector - green (material: EN AW6101). As a mesh was chosen tetrahedral mesh (CTETRA(10)) with local refinement. As the model is symmetrical its $\frac{1}{2}$ was used to speed up the calculation. Boundary conditions took in to account the way of sub-assy. fixation to HEX tank and also its reduction to $\frac{1}{2}$. As in reality is to $\frac{1}{2}$ of sleeve (pink) inserted tube which considerable increase rigidity in this area was this fact simplified reflected by fixation in this area. The pressure was applied to inner area of part.

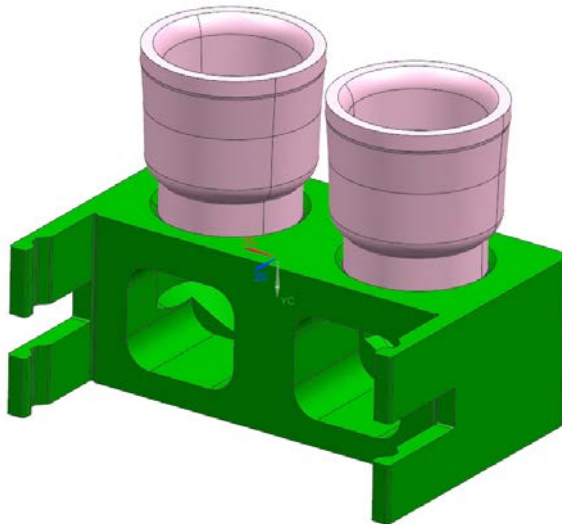


Figure 13-11: Original CAD model

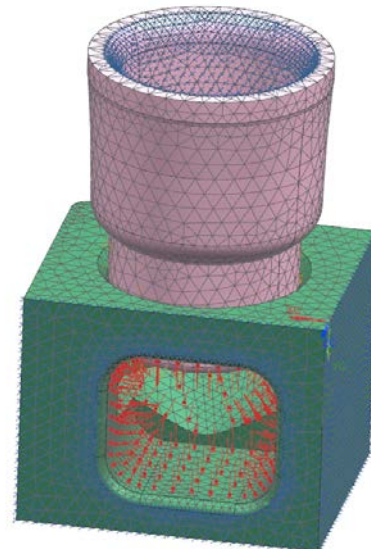


Figure 13-12: Meshed simplified model with applied loads and boundary conditions

The result of linear analyses showed that applied pressure 170 bar leads to exceeding of yield strength of sleeve. The connector is safe due to its better mechanical properties.

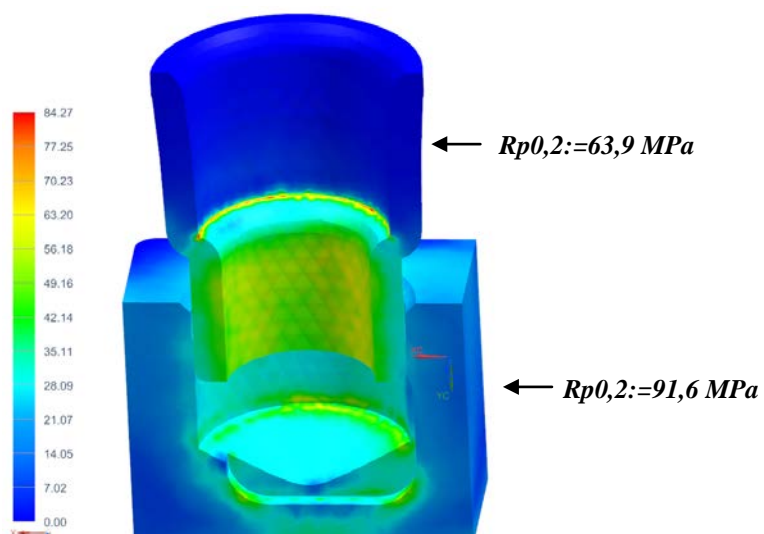


Figure 13-13: Linear analyses – sleeve $R_{p0,2}$ exceeding

The results of nonlinear analyses showed crack of sleeve at pressure 370 bar. The stress in connector is still away from crack.

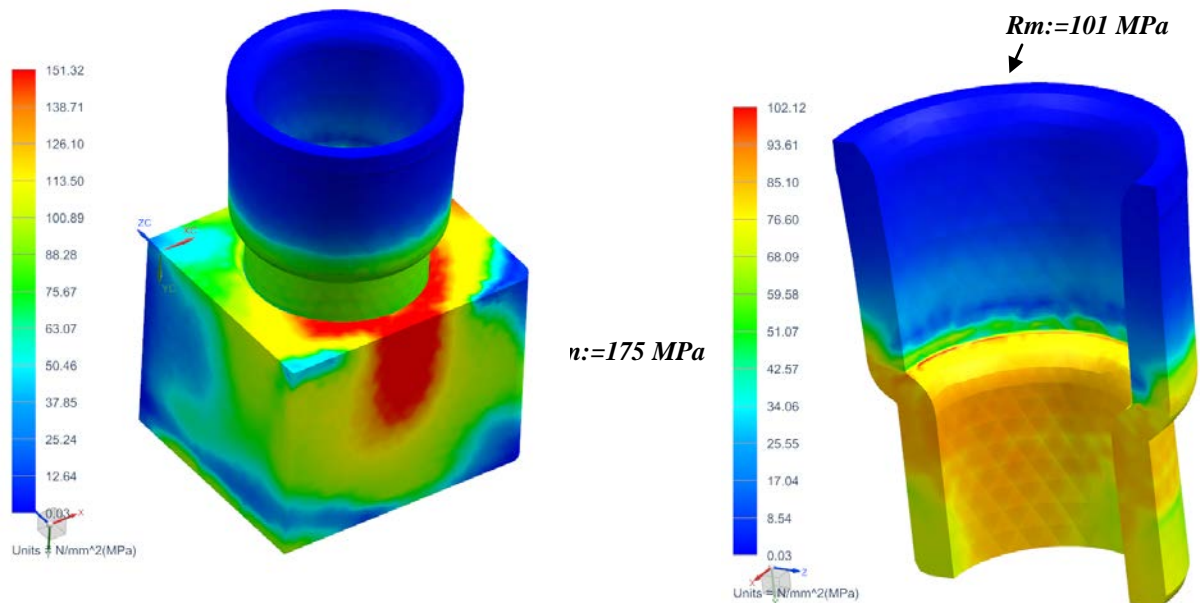


Figure 13-14: Nonlinear analyses – sleeve crack at 370 bar

The real test was done where prepared connector with closed square hole (to be able to pressurised part). 10 samples were tested. The failure mode of each one sample was crack in sleeve the same area as was predicted by FEM. The results were in range 375-403 bar.



Figure 13-15: 1. Sample before test, 2. Test failure, 3. Test failure

13.2.4 Pipe

For pipe 3D swept mesh (chexa(8)) was used. Fixation of pipe reflect reality, where one side is connect with HEX sleeve and second one to monoblock. Inner pressure was applied to pipe.

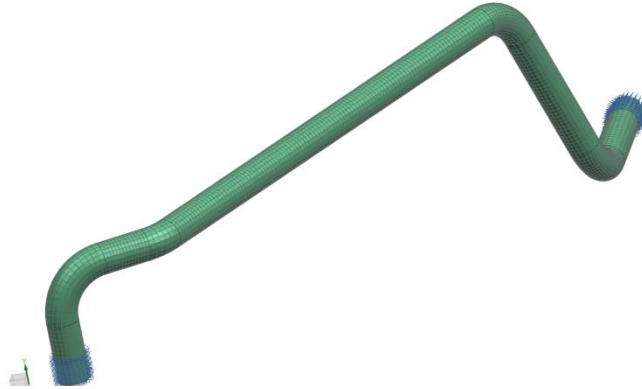


Figure 13-16: Pipe with applied mesh and boundary conditions

Linear analyses showed that during application 170 bar pipe remains safety in elastic domain.

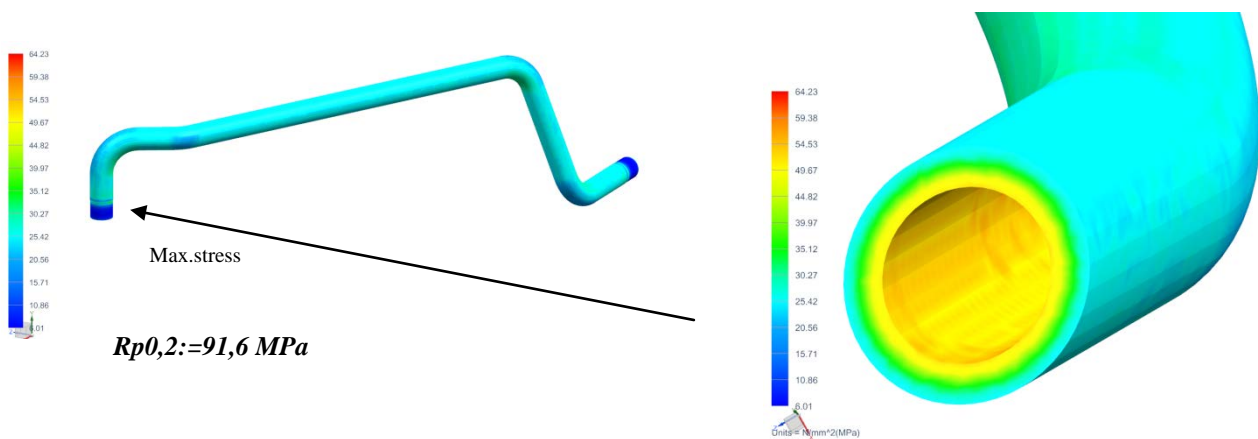


Figure 13-17: Linear statics analyses – load 170 bar

Nonlinear analyses showed crack pressure at 540 bar.

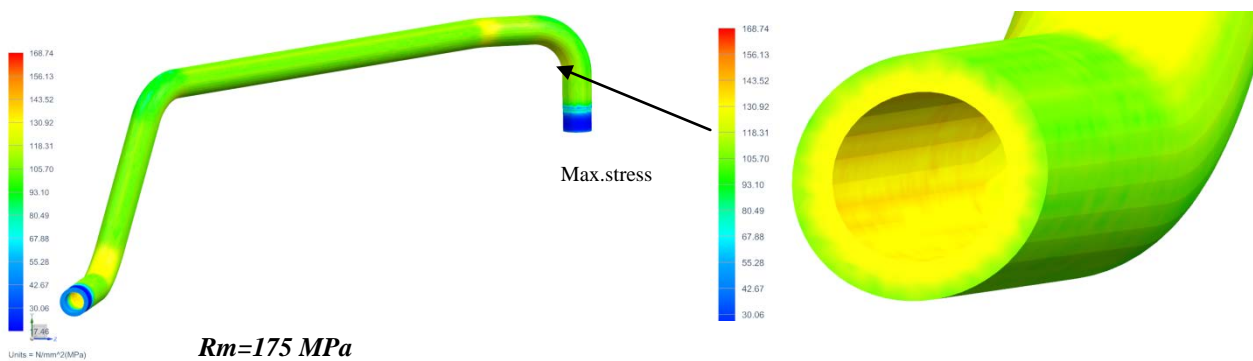


Figure 13-18: Nonlinear static analyses crack at 540 bar

Test was on 10 parts and burst values in range 502 – 520 bar were measured.



Figure 13-19: Tested pipes

13.2.5 FEM summary

On the table is summary of FEM study and test on real components. As tank and flat tube are not able to withstand required pressure 340 (confirmed by FEM + real test) must be strengthened. Sleeve not crack before 370 bar but at maximal possible pressure at car - 170 bar plastic deformation occurs which could lead to noticeable degradation of component fatigue resistance properties. Fatigue resistance of sleeve must be verified by a fatigue test.

Component	FEM		Real test - Burst pressure [bar]	To be strengthened
	Pressure 170 bar - Rp0,2 exceed	Burst pressure [bar]		
Tank	YES	340	296	YES
Flat tube	YES	340	331-347	YES
Connector	NO	No crack at 370 bar	-	NO
Sleeve	YES	370	375-403	Based on fatigue test
Pipe	NO	540	502-520	NO

Figure 13-20: FEM and real test summary

14 IGC design

In the previous chapter was with help of FEM and real testing determine that tanks and flat tube must be strengthened and sleeve verified by fatigue test. However assignment regarding HEX refrigerant circuiting (IGC must be 2pass) will affect final design.

14.1 Tank design

As the IGC refrigerant circuiting should be 2 pass the tanks must be modified accordingly. On the Figure 14-1 are shown differences between original 6-pass heat exchanger and desired 2-Pass heat exchanger.

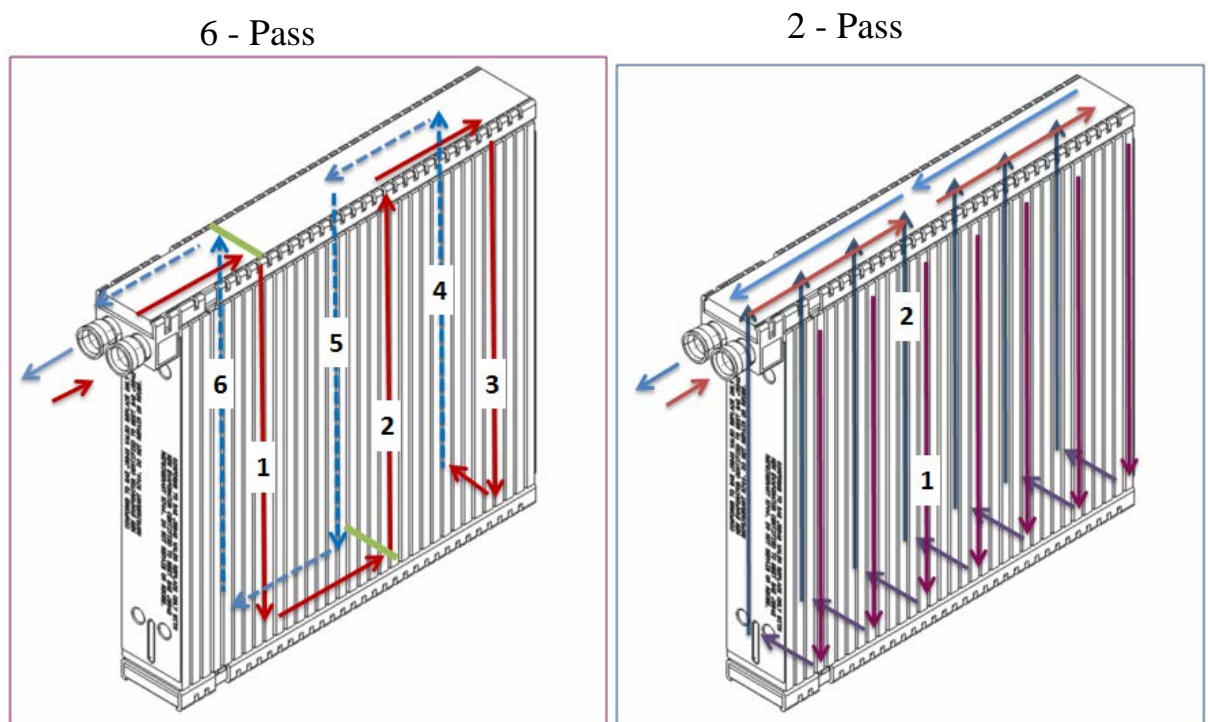


Figure 14-1: 6 pass vs. 2 pass circuiting

To reach 2 pass design and desired mechanical properties following design features was applied:

1. To enable refrigerant flow through complete length of top tank the barriers design features from top tank must be removed (barriers marked green).
2. The bottom tank must enable transfer of refrigerant from IGC right side to left side in whole length – bottom tank must be complete by-pass.
3. As the bottom tank works as by-pass only - the refrigerant is in fact transfer from right side flat tube to left side flat tube. The flat tube cross section to be reduced - to resist to height pressure. The intermediate component could be removed from bottom tank.
4. As IGC works at supercritical phase (refrigerant density is close to liquid, but with low viscosity) the lower ref. dP vs. evaporator is supposed and due to this the lower tank cross

section could be (carefully) used. As the lower cross section is required Superior and inferior cover plate to be designed as flat. This makes its mass production more effective regarding component price

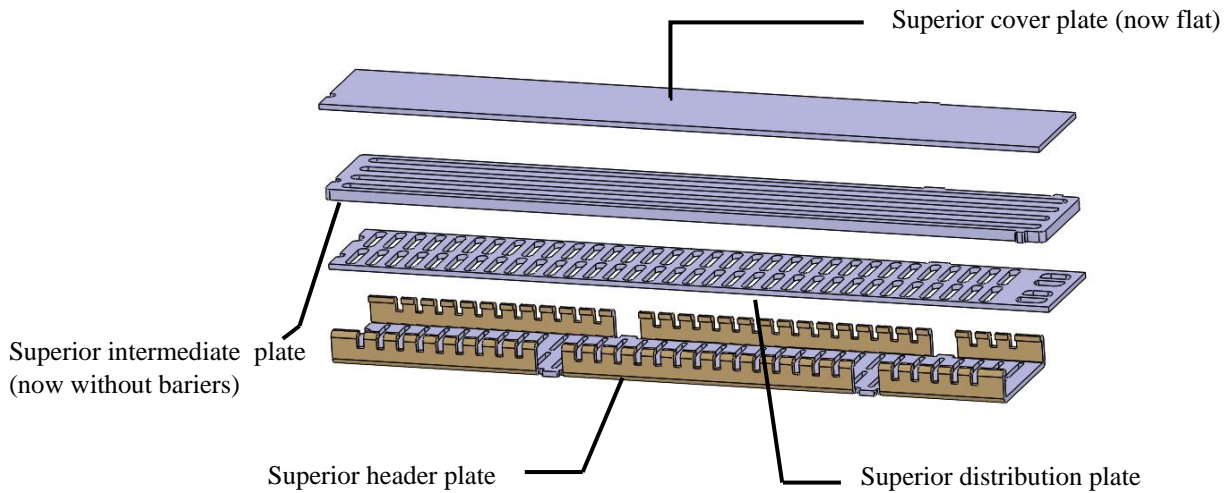


Figure 14-2: IGC Top tank assembly

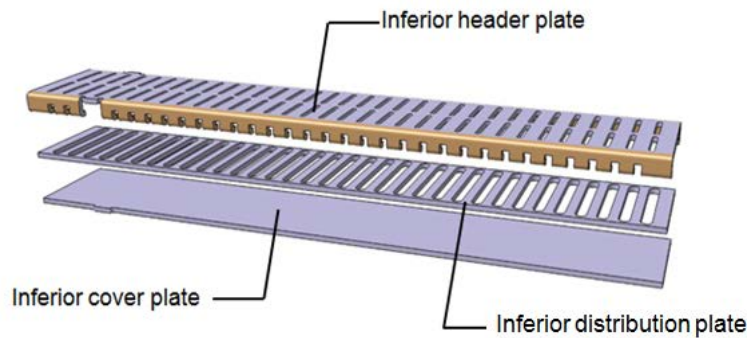


Figure 14-3: IGC Bottom tank assembly

The top tank was strengthened by increasing width of the (intermediate) ribs in sense to decrease local stress in critical area. It must be found good balance as the rib width increase lead to reduction of channel cross section which consequently cause additional refrigerant dP.

As in the initial FEM analyses of evaporator tank there was a gap 16% between FEM and real test (caused by porosity in a real part) this gap to be taken into account for optimisation. As the goal for real component is burst > 340 bar so the goal for FEM to be reach Rm for 400 bars. Several design and calculation was launched to reach this value. On the picture is stress of top tank final definition at Load 380 bar. The maximal stress remains on the same area (intermediate-distribution). However the stress is quite high also on cover – which is now flat due to low cost for manufacturing. This area must be focused during real test and in case of problem thicker core, better material or “arc” design must by applied.

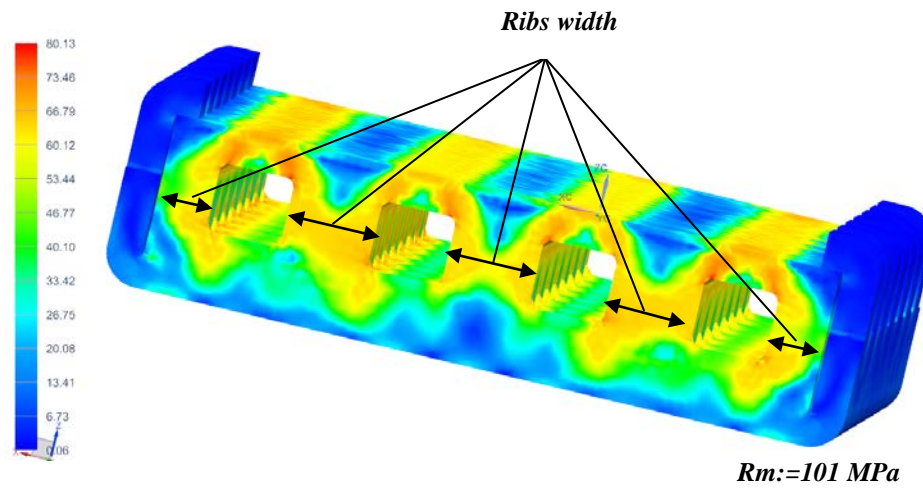


Figure 14-4: IGC Top tank, stress at load 380 bar

Calculation was done also for bottom tank which is now different ws. Top tank. The FEM showed that bottom tank is more robust and will not be failure mode during real test.

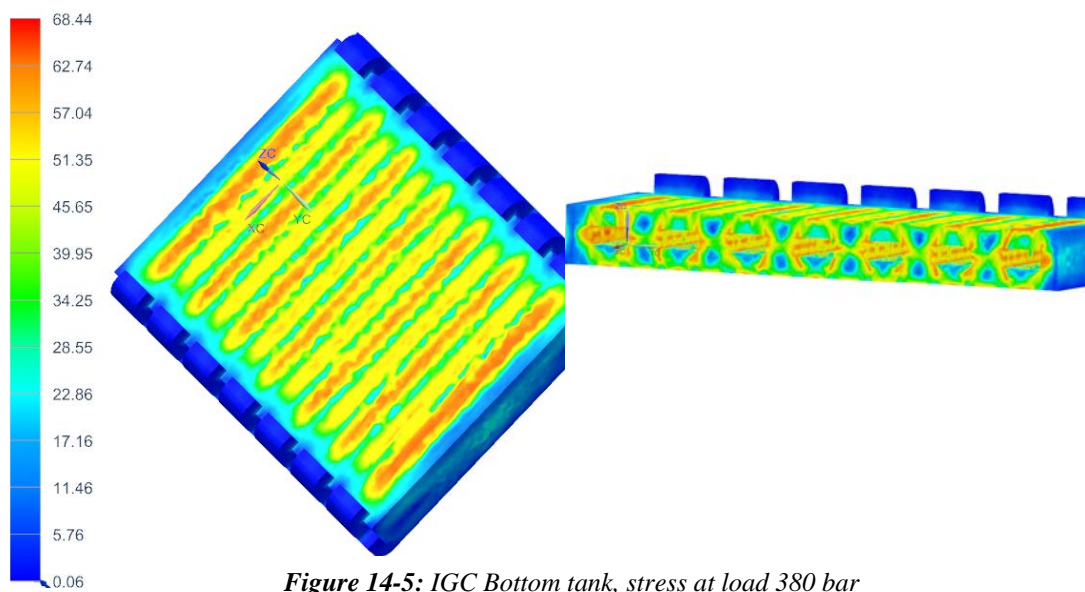
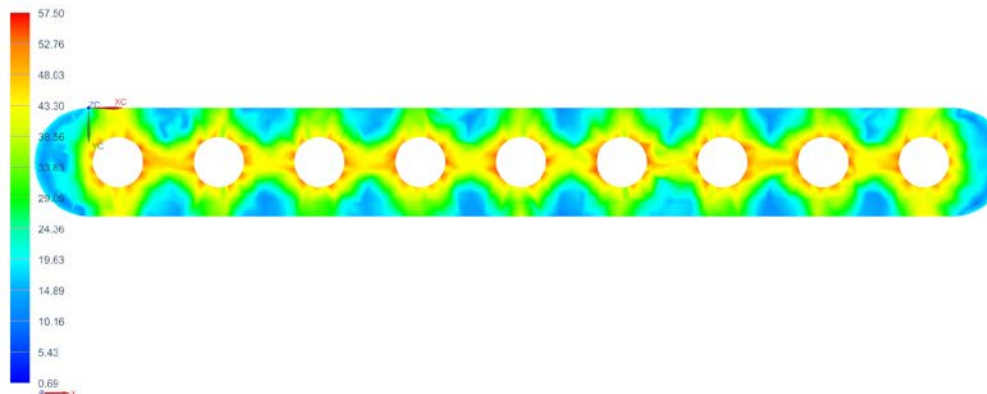


Figure 14-5: IGC Bottom tank, stress at load 380 bar

14.2 Flat tube design

For flat tube was as the FEM goal set up to reach Rm at 400 bar. This “oversized” is due to fact that flat tube is the most exposed component from corrosion point of view and corrosion could decrease mech. properties of flat tube. The FEM burst for 400 bar is reached if the channel diameter is reduced from 0,81 mm to 0,65 mm. Also several iteration calculations were launched till this diameter was selected.



14.3 Real mechanical test

To confirm new design of components - prototypes drawing have been prepared and components produced. For the tanks components the parts were machined from desired cladded material. For flat tube new extruded tool at supplier was ordered. 11 complete Inner gas cooler heat exchanger prototypes were built in the company prototype shop by prototype shop technicians and tested by tightness test in Helium chamber. 5 samples for static test: Burst test, 6 samples for fatigue test - Pressure cycle (change) test. The both test was done again in VZLÚ Prague at temperature 130 °C



Figure 14-7: IGC prototypes



Figure 14-8: Leak tightness test in helium chamber

14.3.1 Burst test

Result from burst test confirmed FEM as the failure area was again crack in top tank. The burst results were in range from 373,5 to 428,7 bar. The average is 391,4 bars (FEM 400 bar predicted). As the requirement for IGC is to pass pressure 340 bar the IGC sample demonstrated their mechanical robustness.

<i>Burst test sanction:</i>	Sample No.	Burst pressure [bar]	Failure
<i>340 bar min.</i>	1.	373,5	Top tank
	2.	380,0	Top tank
	3.	377,0	Top tank
	4.	428,7	Top tank
	5.	397,9	Top tank
	Average	391,4	N/A

Figure 14-9: IGC burst test results

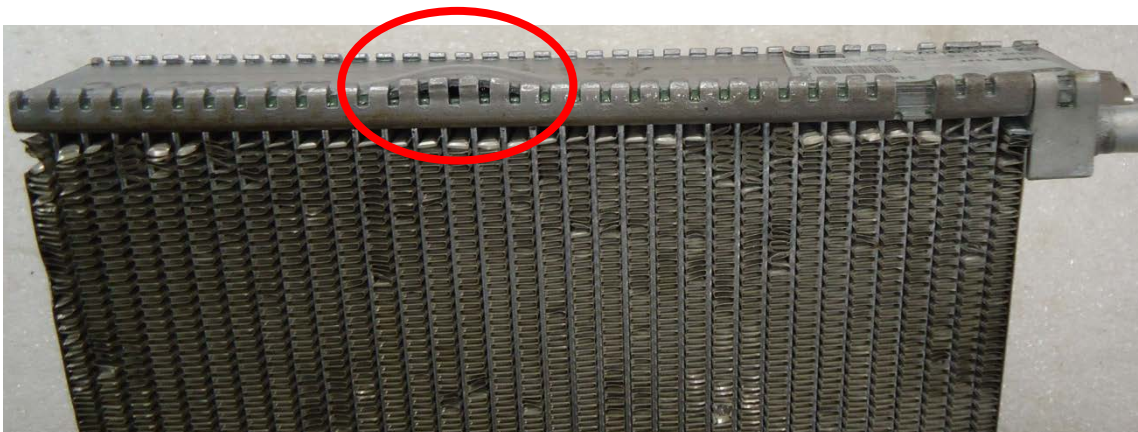


Figure 14-10: Sample No.3 crack in the top tank

14.3.2 Pressure cycle test

The first batch of 2 samples was tested at VZLÚ at desired conditions:

- Test medium and component T: 130°C
- Pressure: 50 – 170 bar (Pressure range: 120 bar)
- Frequency: 1 Hz
- Sanction: To reach at least 150 000 cycles

The values: 731 422 cycles and 759 855 cycles was reached. The failure mode was again crack in top tank. As was brightly demonstrated the IGC robustness the next samples was tested at higher Pressure range (140 and 160) in sense to check if the failure mode will not change. As the failure mode remains the same the fatigue curve (Delta pressure – Cycles number to failure) was constructed (Figure 14-12).

Test	Pmax	Pmin	P range	P ampli	N	Avg.
Test1	170	50	120	60	731422	745638,5
Test1	170	50	120	60	759855	
Test2	180	40	140	70	393242	404039,5
Test2	180	40	140	70	414 837	
Test3	200	40	160	80	139010	155058
Test3	200	40	160	80	171106	

Figure 14-11: Fatigue test results

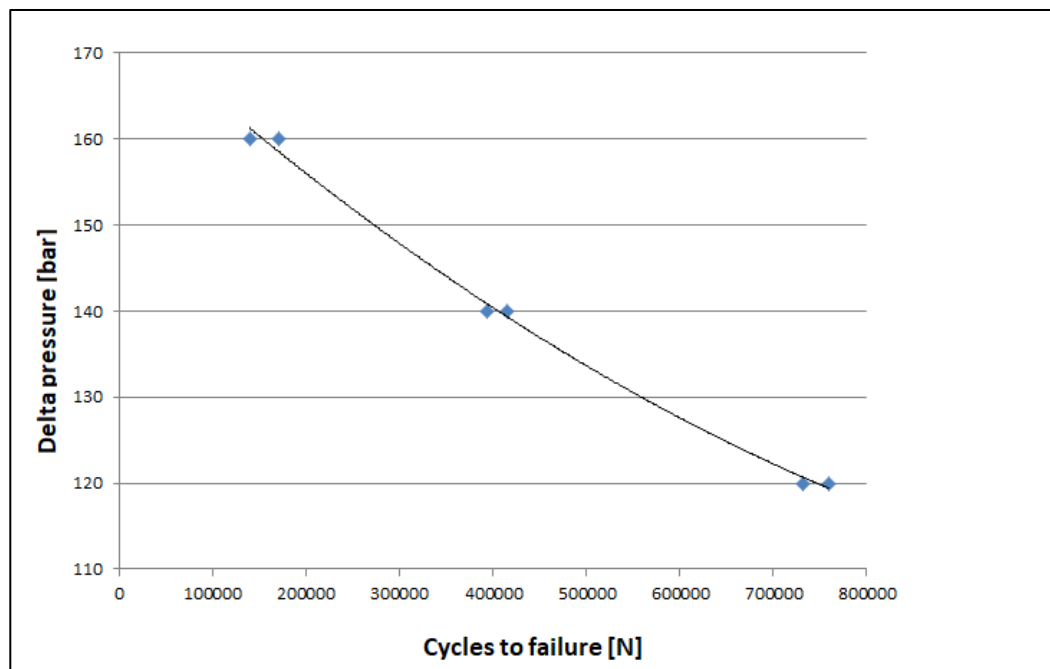


Figure 14-12: IGC Fatigue curve

14.3.3 Mechanical test conclusion

For burst test (static test) was on 5 tested samples reached values in range 373,5 – 428,5 bar (min. 340 bar required by specification). For pressure cycle (fatigue test) was reached at over 750 000 cycles (150 000 cycles min. required by specification). The failure mode for both test remains the same – crack in top tank and so it seems that sleeve is resistant vs. fatigue at given pressure although FEM detected $R_{p0,2}$ exceeding at 170 bar. However the robustness of IGC HEX in this definition must be confirmed by test on more samples with statistics evaluation (Weibull distribution). Then could be full validation launched.

15 Inner gas cooler geometry optimisation in terms of heating performance

15.1 Dymola Interface and inputs definition

For inner gas cooler geometry optimisation was used software DYMOLA developed by the Dynasim company. The Air Conditioning library is one from many libraries which could be open in Dymola. This Air condition library is used for the steady-state and transient simulation of air conditioning systems using modern, compact heat exchangers and actually it is mostly used by car makers and its suppliers. The Air Conditioning library works with basic correlations for heat and mass transfer and pressure drop for A/C components the same which are described in chapter 7 and 8 in this thesis. Actually by this software is possible to simulate even also some dynamic behaviour of A/C loops.

The Dymola user interface is close to component real connection to test bench and so the input parameters are following: A. Air and Refrigerant inlet are given by specification (table: 15-2). B. Inner gas cooler geometry – this geometry is described in details in following page together with initial values.

The desired outputs are: Air pressure drop inside evaporator [dP], Heating power [kW], Temperature refrigerant outlet [°C], Refrigerant pressure drop [bar].

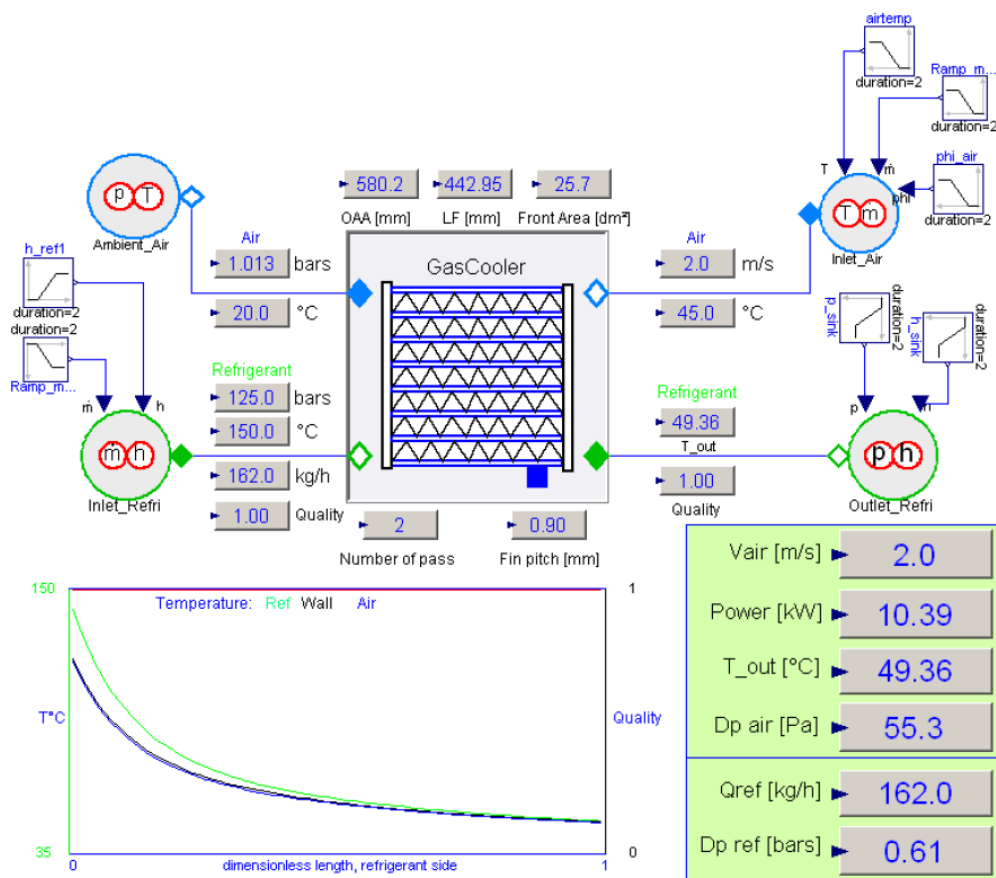


Figure 15-1: Dymola interface of Gas cooler with inputs and outputs

A. Air and Refrigerant inlet (given by specification)

Air - Input	Unit	Value	Refrigerant - Input	Unit	Value
Air velocity	m/s	3,12	Refrigerant inlet pressure	Bar	120
Temperature of the air on the inlet side	°C	120	Refrigerant inlet temperature	°C	120
			Refrigerant mass flow	kg/h	90
			Refrigerant quality	-	1

Table 15-2: Inputs: Air – inlet, Refrigerant inlet

B. Inner gas cooler geometry inputs (given by IGC design)

Dymola term	Description	Value
General dimensions		
flowscheme	IGC circuiting	[2;1]
flattubes	Number of flat tubes in pass	[33;33]
depth	-	32
height	To height is counted only active area (finned area), not tanks	213,5
width	To height is counted only active area (finned area), not side plate	188
Flat tubes Geometry		
h_flattubes	Flat tube thickness	1,44
z_flattubes	Flat tubes pitch in Heat exchanger	5,59
dp	Flat tube thickness under the channel	0,495
pipes	Number of channel in one flat tube	9
pipedsign	Type of channel design	1
rp	Channel radius (in ase of design 1)	0,41
u_1pipe	Flat tube channel perimeter	2,54
area_1pipe	Flat tube channel surface	0,52
Dhyd	Flat tube channel hydraulic diametr	0,81
Louvered fin geometry		
fins	Number of fins per 100 mm tube length	74,07
findesign	Fin design type - 1) Sinusoidal fin, 2) Square fin	2
L_l	Louvers (fin cut) length	3,15
L_p	Louvers (fin cut) pitch	1,25
L_alpha	Louvers angle opening	35
F_d	Fin thickness	0,07

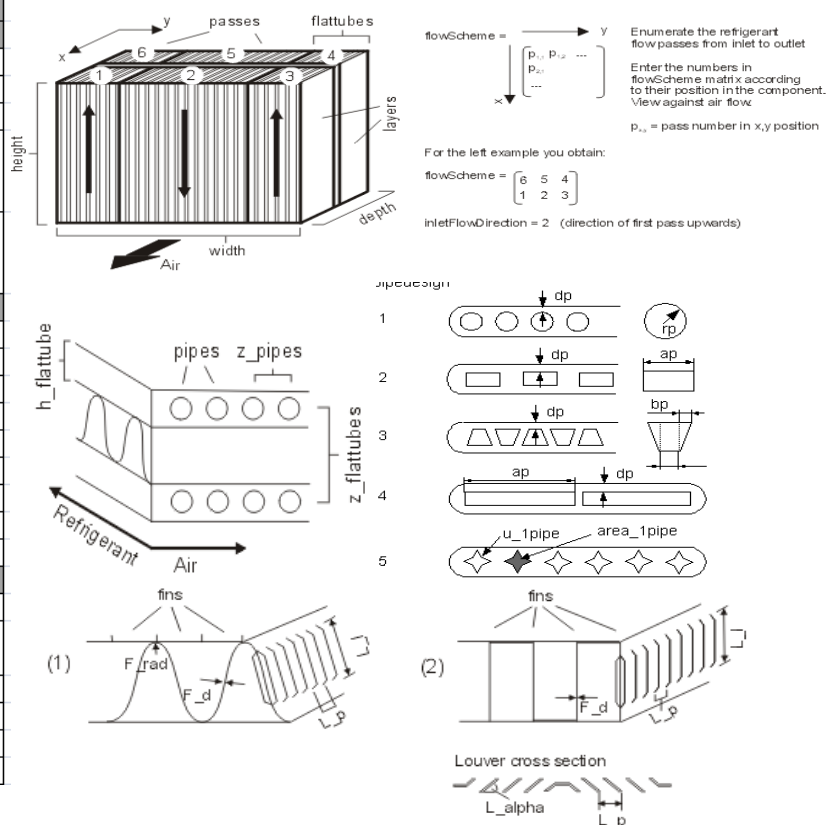


Figure 15-3: Inputs: Inner gas cooler geometry

15.2 Dymola Calculation

First calculation was done in sense to determine impact flat tubes channels diameter reduction as from calculation and real test was observed that diameter 0,81mm is too high in terms of burst resistance. In sense to this all variable inputs was fixed as initial acc. Figure 15-3 and only some parameters of flat tubes was modified. The thickness of flat tube, number of channels and the type 1(circle) remained but the parameters d_p and r_p has been change in sense to reflect channel diameter change. For initial simulation flat tube diameter was calculated in range 0,81mm – 0,7mm. The results from simulation are visible in Figure 15-5.

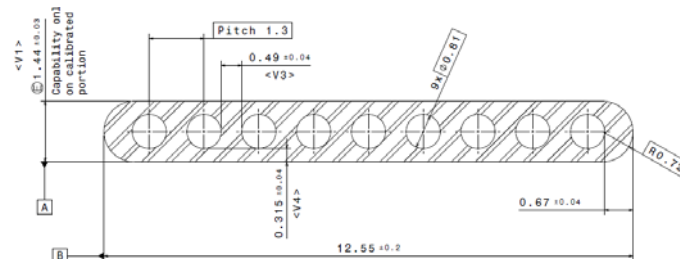


Figure 15-4: Flat tube – channel dia. 0.81 mm

Channel diameter [mm]	Power [kW]	Gap power [%]	R744 pressure drop [bar]
0,81	5,12	-7	0,12454
0,8	5,12	-6,86	0,12456
0,79	5,13	-6,72	0,12459
0,78	5,14	-6,57	0,12463
0,77	5,15	-6,44	0,12467
0,76	5,15	-6,31	0,12473
0,75	5,16	-6,17	0,12479
0,74	5,17	-6,04	0,12487
0,73	5,18	-5,91	0,12495
0,72	5,18	-5,78	0,12505
0,71	5,19	-5,66	0,12517
0,7	5,20	-5,53	0,12530

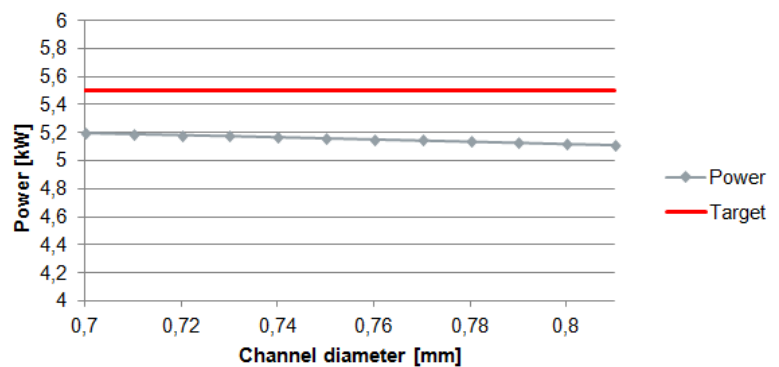


Figure 15-5: Performance dependency on flat tube diameter (9 channels)

From the results is visible that channel diameter reduction change has only negligible impact to refrigerant pressure drop which was expected because of high refrigerant density due to high pressure. But what was not expected is that simulation results showed positive impact of channel reduction for heating performance which raised about 80 W for channel in diameter 0,7 mm vs. 0,81 mm. Regarding overall performance: 5,12 kW / 0,81 mm – 5,2 kW/ 0,7 mm was observed that is insufficient vs. required - specification: 5,5 kW and must be improved by additional design change.

As the heat exchanger exchange the heat between refrigerant side and the air side – the design solution has been searching accordingly: a) on the refrigerant side, b) on the air side.

A. Refrigerant side

Previous calculation showed benefit of channel diameter reduction in terms of heating performance. In chapter 14 was channel diameter reduction confirmed as a benefit for mechanical resistance of flat tube. However this reduction has its limits from heat exchanger assembly (brazing) point of view. As was explained in theoretical chap. 9.1.3 during the brazing – clad is in liquid state and migrate on the surface while capillary effect occurs. The channel diameter reduction promotes this capillary effect and so there is a risk of channel block by clad which lead to channel dysfunction and as a result heating performance decrease. Due to this was channel diameter 0,65 mm confirmed as channel diameter for 9 channels flat tube – this is safe solution from mechanical and clogging point of view.

The stress in the flat tubes has its maximum in the side wall between neighbouring channels and contrary this is stress at minimum level on the tip of flat tubes (radius). Due to this is possible move first and last channel closer to the tips which brings space for one additional channel. Due to this the channel pitch is only slightly decrease and small mechanical degradation of 10 channels 0,65 mm vs. 9 channels 0,65mm confirmed by FEM. The benefit of this solution is additional heat exchange surface. Calculation to be done also for this event.

If to be neglected the clogging phenomena significantly lower diameter 0,55mm allows have 12 channels in flat tubes – from mechanical point of view. More channel means higher heat exchange surface which should bring benefit from heating performance point of view. For 3 mentioned definitions (picture) has been launched calculation – the results from calculations are in Table 15-7.

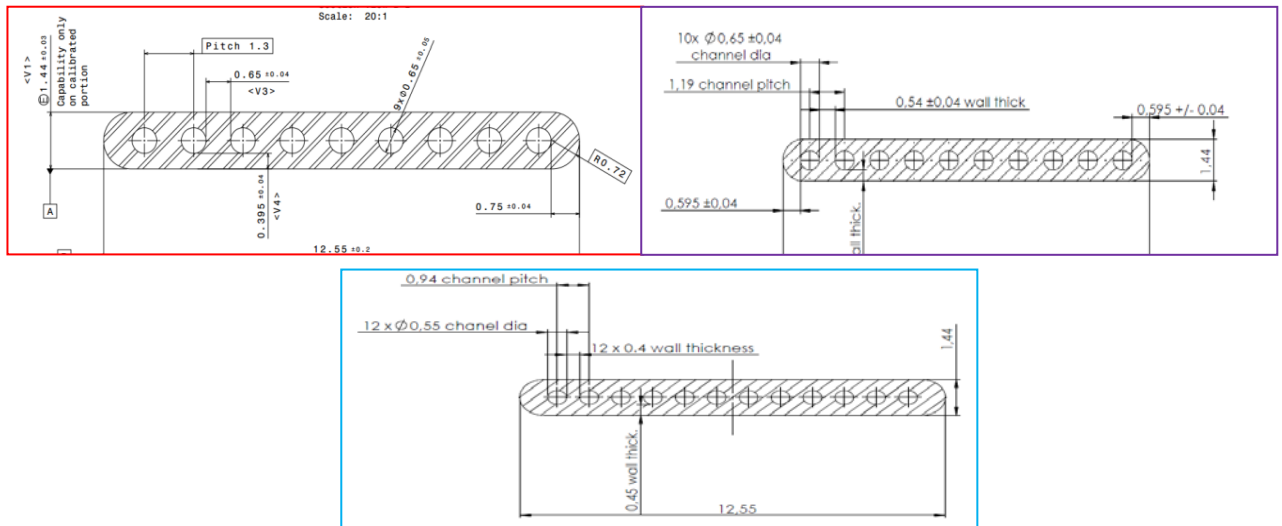


Figure 15-6: Flat tubes definition for second simulation

Flat tubes			
Number of ports by tube	9x0.65	10x0.65	12x0.55
Power [kW]	5,23	5,24	5,31
Dp R744 [bar]	0,126	0,125	0,127
Dp air [Pa]	72,67	72,67	72,67

Table 15-7: Results of second simulation

From the calculation is visible benefit 110 W of IGC with flat tube with flat tube at diameter 0,65 mm and 9 channels tube vs. Initial diameter 0,81 mm and again negligible increase of ref. dP. No impact of 10 channels flat tube vs. 9 channels to performance. But 12 channels tube with diameter 0,55 mm brought additional 80 W to heating performance reached with 9 x 0,65 flat tube and so performance of IGC with pipe with definition is 5,31 kW. 12 channels flat tube with diameter 0,55 mm seems to be best option, however with this definition still 200W missing to reach specification.

B. Air side

Optimisation of air side is very important because heat resistance on the air side is cca. 10x higher vs. heat resistance on the refrigerant side (see chap. 7.1.2 and 7.2). The key component for air side optimisation is fin. Unfortunately fin is very expensive in term of production (production tool is costly) and was decided to keep current fin feature (evaporator state) for IGC. Due to this only option is to increase heat exchange surface of heat exchanger by add more fin material to flat tube. This is quite easy in term or production as more fin convolution is added to tube by reduction fin characteristic dimension: Fin pitch. For this fin dimension change is not necessary to buy new forming tool as it's possible to reach this by production machine adjustment. Fin pitch is loaded to soft as a „fin parameter”. FP: 1,35, FP:1,2, FP:1,1 and FP: 1,0 was tested. Best of IGC geometry was acc. to Figure: 15-3 (Flat tube 9x0.81mm)

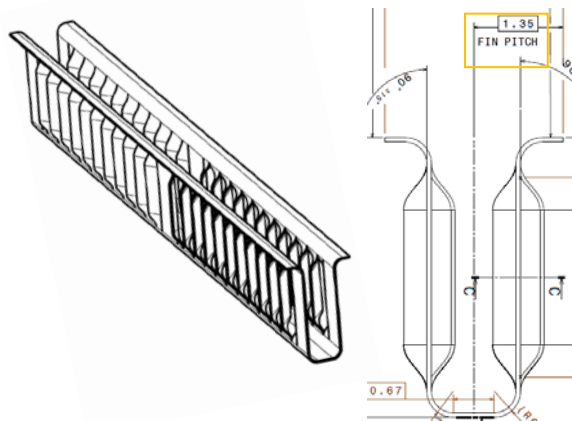


Figure 15-8: Fin pitch

Fin pitch (mm)	Dp _{air} (Pa)	Power (kW)	ΔPower target (%)
1	104,84	5,31	-3,40
1,1	92,06	5,27	-4,22
1,2	82,12	5,20	-5,40
1,3	72,66	5,12	-7,00

Figure 15-9: FP calculation results

From the simulation results is visible rule the lower FP the higher performance (which was expected by heat exchange surface increase). But there was observed negative trend air pressure drop which increase very dramatically with lower FP. The limit of air pressure drop was not given by specification but the air pressure drop is every time negative phenomenon as the air energy lost in heat exchanger must be compensates by higher performance of fan which brings the air to cabin and so high air dP could be claim by car makers.

In order to determine if „works“ combination of flat tube modified and FP modified was launched final simulation acc. to key: each FP in combination with each flat tube design (see Figure: 15-10). From this simulation is visible that target 5,5 kW should be reached for FP 1,0 with flat tubes 12 channel with diameter 0,55 mm. From the graph „Power“ is visible positive impact of FP reduction and 12 ports flat tube design. From the graph „Dp air“ is visible negative impact of FP reduction to air dP (which increase). From the graph „dP R744“ is visible the negligible impact of flat tube design and even „more negligible“ impact of FP to refrigerant dP as graph differences are caused mainly by very fine scale of graph and on real product not to be noticed. However these differences are explicable. 9 channel flat tubes have the lower cross section and so the highest fluid velocity cause highest friction vs. 10 channels.

Fin pitch	1,3 mm			Fin pitch	1,1 mm		
Number of ports by tube	9	10	12	Number of ports by tube	9	10	12
Power [kW]	5,23	5,24	5,31	Power [kW]	5,39	5,40	5,48
Dp R744 [bar]	0,126	0,125	0,127	Dp R744 [bar]	0,125	0,124	0,126
Dp air [Pa]	72,67	72,67	72,68	Dp air [Pa]	92,07	92,07	92,08

Fin pitch	1,2 mm			Fin pitch	1 mm		
Number of ports by tube	9	10	12	Number of ports by tube	9	10	12
Power [kW]	5,32	5,33	5,41	Power [kW]	5,44	5,45	5,53
Dp R744 [bar]	0,125	0,125	0,126	Dp R744 [bar]	0,125	0,124	0,125
Dp air [Pa]	82,13	82,13	82,13	Dp air [Pa]	104,85	104,85	104,86

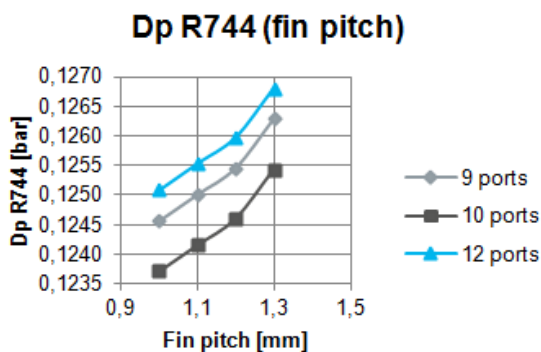
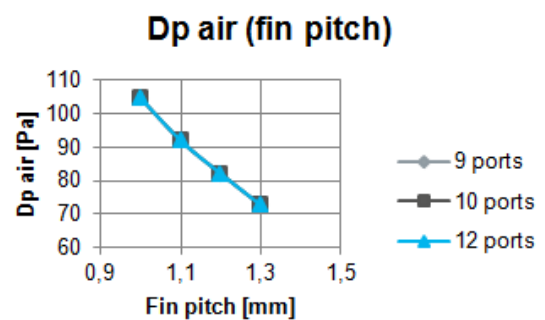
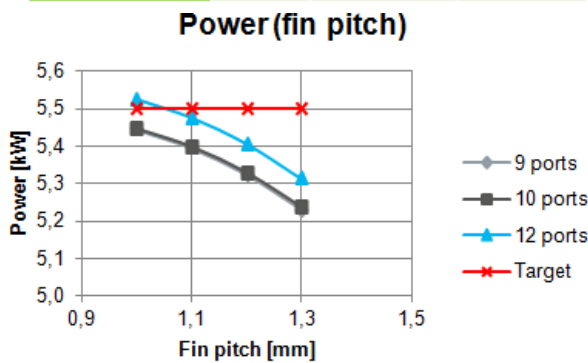


Figure 15-10: FP calculation results

15.3 Prototypes build

To confirm results from Dymola calculation the following prototypes was built in sense to test them on Performance test bench measurement device. For all prototypes were used new tanks designed and confirmed by mechanical test for IGC as these tanks were used for all definitions in Dymola. 4 prototypes were built. The prototype marked as 0. is a reference against which to be improvements compared. For each one following prototype was implemented one improvement vs. def. 0 to see its direct impact to performance. Each improvement is highlighted by blue colour and it's calculated written. For sample A. was implement flat tube 9 channels – diameter 0.65 where was calculated benefit +110 W vs. Sample 0. For sample B. was implemented improvement 12 channel flat tube with channel diameter 0.55 mm. From simulation the best heating performance reached fin pitch 1.0 but this fin pitch was not able to produce on current fin manufacturing machine. The closest fin pitch which was able to produce is 1.1 which was used for prototype C.

Sample mark.	Tanks	Fin pitch	Flat tubes	Calculated heating performance	Calculated benefit vs. design 0
0.	NEW - IGC	1.3	9 x 0.81 mm	5.12 kW	-
A.	NEW - IGC	1.3	9 x 0.65 mm	5.23 kW	+ 110W
B.	NEW - IGC	1.3	12 x 0.55 mm	5.35 kW	+ 230W
C.	NEW - IGC	1.1	9 x 0.81 mm	5.27 kW	+ 150W

Table 15-11: Prototypes for heat rejection definition

16 Heat performance and air temperature unbalance measurement

16.1 Testing device description

The measurement of the prototype samples has been done in Valeo Bad Rodach where is located development test bench able to work with R744 refrigerant. The test was done with cooperation with test engineers from Valeo Bad Rodach which has great experience whit the measurement device.

The test bench consist in fact from two independent units (Figure 16-1) .The first one is the air unit (produce the air flow) and the second one is A/C system with components.

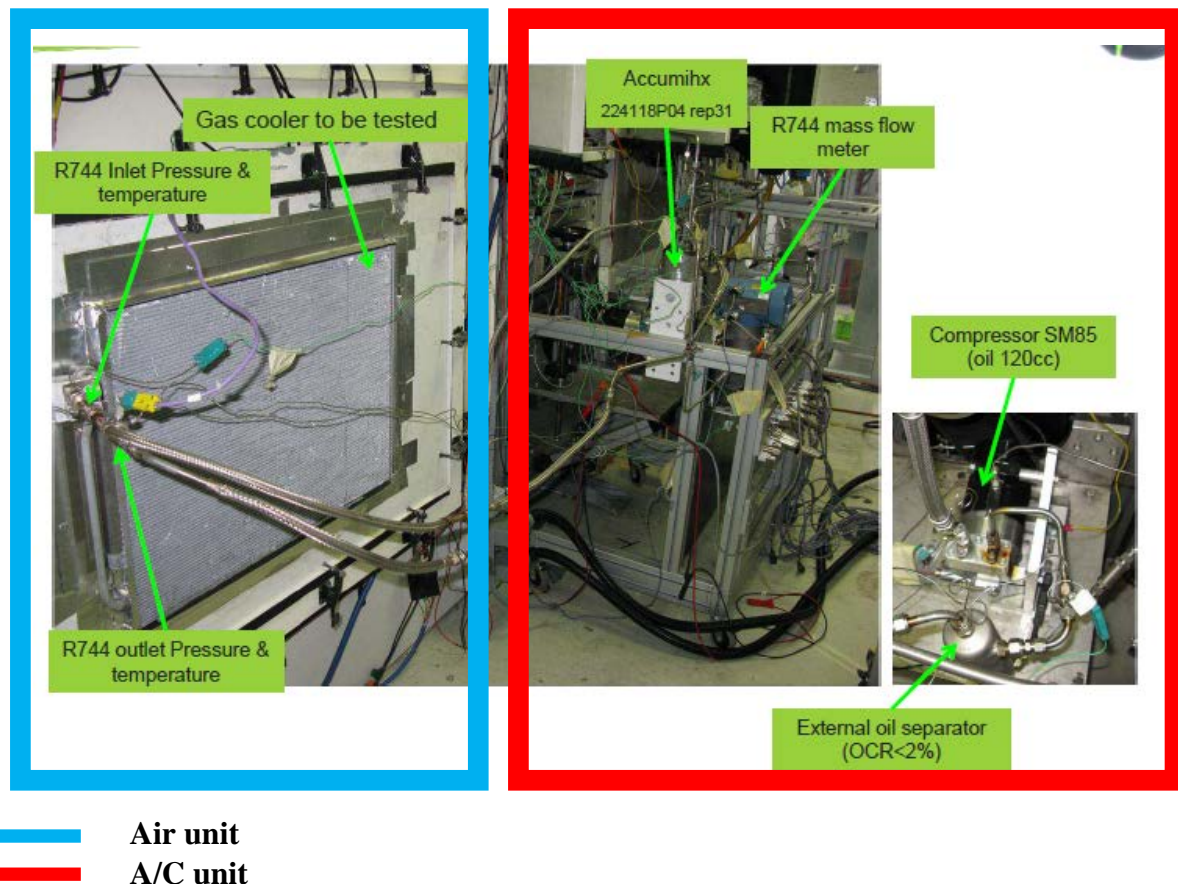


Figure 16-1: Testing device – performance test bench

Air unit serves for production the air under desired quality (temperature, humidity), desired air mass flow and inlet temperature homogeneity. This homogeneity is important for right measurement of heat exchanger temperature imbalance (dT) and to reach perfect homogeneity in front of heat exchanger - air mixing chamber is used. The air temperature – TA as well as air mass flow – MA is set up on test bench. The air flow is fed by air tunnel to measured heat exchanger. The air flow is heated by heat exchanger. Before heat exchanger there is grid with 2×3 thermocouples which measure air temperature inlet to Inner gas cooler – $TAIGI$. On the air outlet side of heat exchanger other thermal grid is presented with 6×4 thermocouples which measure air inner gas cooler outlet temperature – $TAIGO$.

A/C system consists from components which enable to set up required refrigerant (gas) inlet conditions for Inner gas cooler. Temperature of Inner gas cooler on inlet – $TRIGI$,

Pressure of Inner gas cooler inlet - PRIGI and refrigerant mass flow – M_Ref. Refrigerant flows through Inner gas cooler body – exchange its temperature with the air and on the outlet of Inner gas cooler are measured following values. Refrigerant outlet temperature of Inner gas cooler – TRIGO, pressure of refrigerant Inner gas cooler outlet – PRIGO. All these values are measured by sensors.

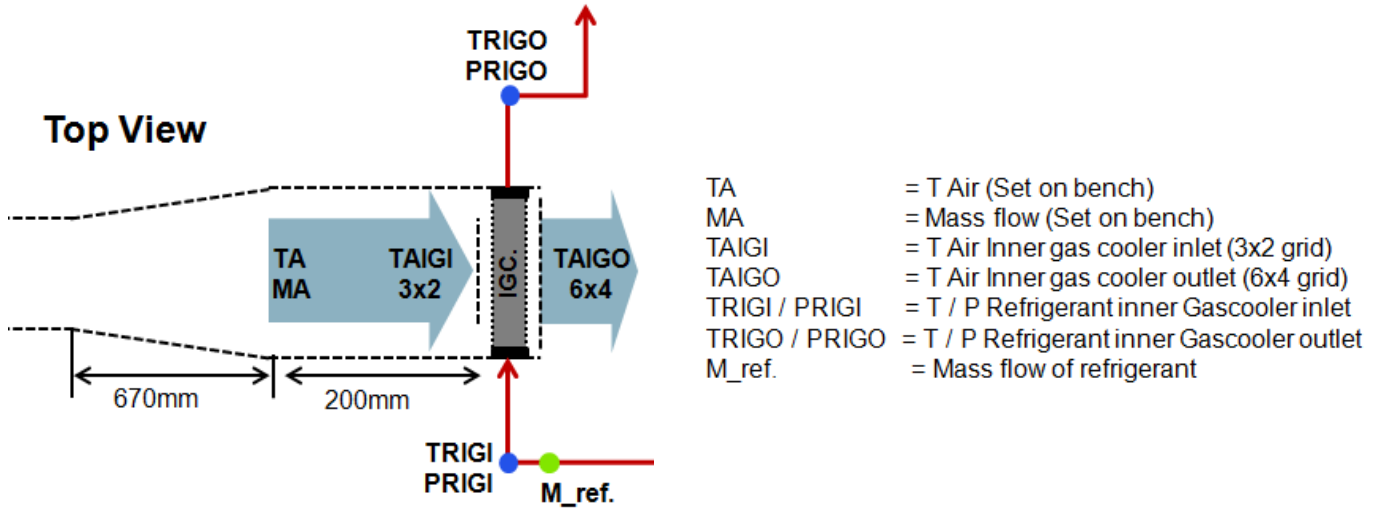


Figure 16-2: Scheme of integration of Inner gas cooler to the test bench

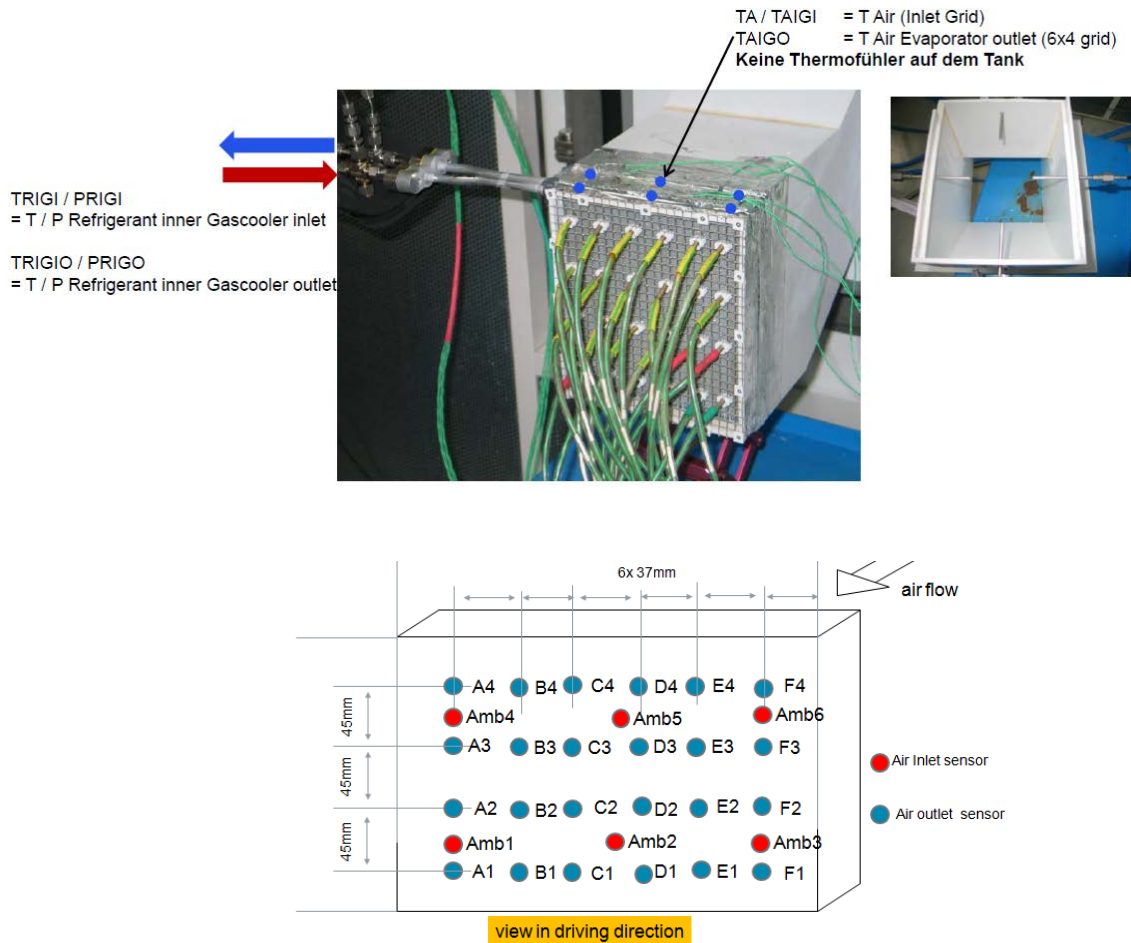


Figure 16-3: Outlet grid – thermocouples layout

16.2 The measurement procedure

Every sample was installed to the test bench with both thermal grids. On the test bench was set up required inlet conditions see Table 16-4. And it's values were checked on the test bench monitor which displays the values from all connected sensors.

TAIR [°C]	MAir [kg/h]	PRIGI [bar]	TRIGI [°C]	M_ref. [kg/h]
10	390	120	120	90

Table 16-4: Test conditions- inlet values

During the measurement was observed that is required certain time when all input parameters to be closest to desired – time of stabilisation took 1 – 15 minutes. However there was every time some deviations on inlet conditions vs. desired conditions and so actual inlet values was recorded and take into account for performance calculation. Then was noticed all output values (TRIGO, PRIGO, T from outlet grid thermocouples.).

16.3 Heat rejection performance evaluation

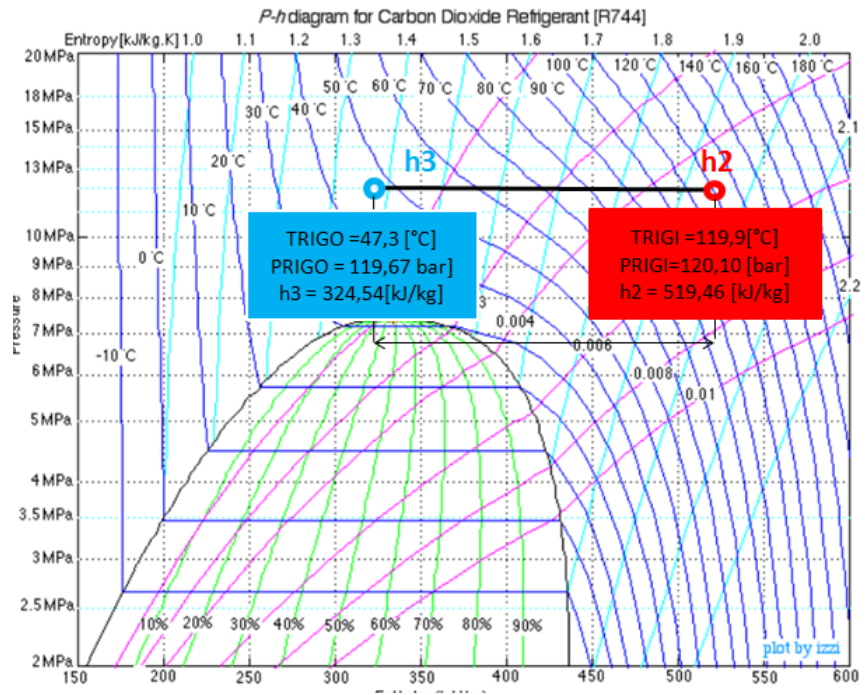
The heat rejection performance was calculated on refrigerant side based on equation given in chapter 3.4.3. This equation has been redesigned to match with measurement record:

$$\dot{Q}_{IGC} = M_{ref} \cdot (h_2 - h_3) [W]$$

M_ref. is fixed by given conditions and varied around desired value 90 kg/h. Also specific enthalpy on the inlet – h₂ is fixed by inlet conditions – PRIGI and TRIGI. The enthalpy h₂ could be easily read from R744 log P – h diagram (see table: 16-5) or could be used some R744 enthalpy calculator in this case was used Dymola soft. (R744 library). The outlet specific enthalpy h₃ is given by outlet pressure and outlet temperature of refrigerant – TRIGO, PRIGO measured by sensors.

On the picture below is described heating performance calculation of one of the samples where following values has been measured:

TRIGI = 119,9 [°C]
PRIGI = 120,1 [bar]
TRIGO = 47,3 [bar]
PRIGO = 119,67 [°C]
M_ref = 90,27 [kg/h]



$$\dot{Q}_{IGC} = (90,27/3600) \cdot (519,46 - 324,54) \cdot 1000 = 4,89 [kW]$$

Table 16-5: Heating performance calculation example

16.4 Air temperature unbalance (dT) evaluation

The information about air temperature unbalance is given by 24 thermocouples placed in such way to cover whole active surface of Inner gas cooler. Two main required parameters were evaluated: 1. dT Min/Max, 2. dT L/R.

1. dT Min/Max is the difference between hottest and coldest point on IGC active surface and is calculated as a simple difference of highest and lowest value measured by single thermocouple.

2. dT L/R is temperature difference of left side and right side of IGC (reflect zone in HVAC). This division is made by vertical plane in the middle of IGC. Calculation of dT is given by differences of mean temperature left side (3x4 thermocouples) and right side (3x4 thermocouples). On the example one the table below is example of one measured IGC sample.

		Grid - IGC: Air outlet						
	MW	72,4	71,3	68,5	66,0	60,8	53,1	
dT U/D	60,9	60,8	60,5	61,0	58,0	52,0	46,3	MW
8,8	MW	56,2	57,7	54,3	54,4	48,4	44,7	56,51
	52,1	54,7	56,6	54,7	53,2	46,6	44,1	
	MW	60,7			52,3			dT (Min/Max)
	Min/Max	18,1			21,9			28,35
		dTL/R		8,4				

Table 16-6: dT Min/Max and dT L/R example

16.5 Prototype samples measurement results

In the blue table below (Table 16-7) are values measured on the test bench and in the row Q_{IGC} is heating rejection calculated from measured values. In the green table below - Power are values which were reached during 1D Dymola calculation (described in chapter 14.2). Comparison of blue and green table to be visible how much precise Dymola calculation was.

To focus on Heat rejection is clear that no one sample reached the target 5,5 kW (max. 5,2 kW). However the improvement of Samples A. B. C. in comparison with sample 0 is visible. The 9 flat tubes diameter reduction from 0,81mm (sample 0) to 0,65mm (sample A.) brought the benefit 50W (100W was predicted by Dymola calculation). 12 Channel flat tube (sample B.) brought benefit 190W vs. definition 0 (230W was calculated by Dymola). The fin pitch change from 1,3 (sample 0) to 1,1 (sample C) brought benefit of 100W (150W was calculated by Dymola). If stay at evolution of preciseness of Dymola calculation is visible that accuracy is very high when only increments (between measured and Dymola calculated) are compared. In absolute scale are calculated value shifted about cca. +100W against measured on test bench.

Phys. quantity	Unit	Samples			
		0	A.	B.	C.
TAIGI	°C	10.0	9.71	10.4	10.2
TAIGO**	°C	57.4	57.6	58.5	58.8
MAir	Kg/h	390	390	390	390
TRIGI	°C	120.0	120.1	119.9	120.0
PRIGI	bar	120.5	119.9	120.4	119.9
M_R	kg/h	89.6	89.7	90.1	90.2
dT min-max	°C	22.7	24.9	22.0	24.4
dT L/R	°C	3.4	4.4	3.6	4.4
Q_{IGC}^*	kW	5.01	5.06	5.20	5.11
Power	kW	5.12	5.23	5.35	5.27

* Calculated using enthalpy differences

** TAIGO is represented by the mean temperature at the flow (4x6 grid)

Table 16-7: Measured values – blue table / Calculated Power green table

dT min.-max. was measured in range from 22.0 °C till 24.4 °C. This is caused that refrigerant inlet temperature 120 °C is during flow through IGC cooled down very intensively to outlet temperature cca.57.4 – 58.8 °C (temperature gradient 62 °C) which creates very hot and vice versa very cold areas on heat exchanger surface. dT L/R is on the other way quite good 4.4 °C max. On the Figure 1-8 took by thermal camera is visible thermal unbalance of Sample 1.

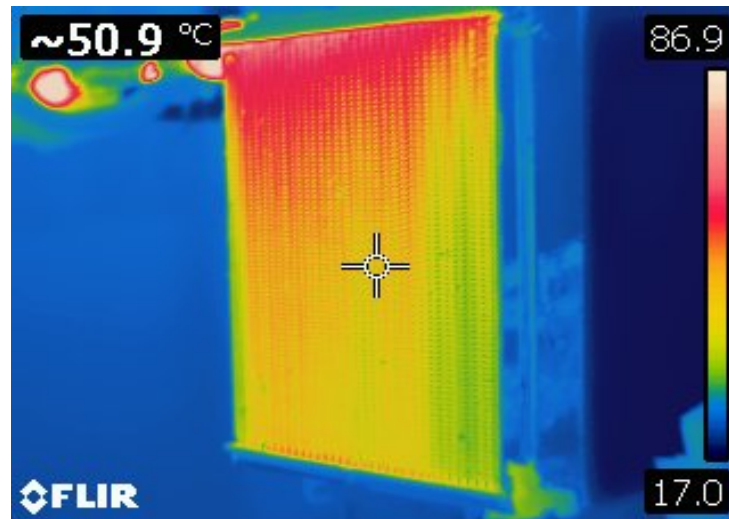


Figure 16-8: Sample 1 – thermal camera photo

From the picture is visible that temperature gradient decrease in sense from beginning (HEX inlet) top tank to the end of top tank. From this is visible that mas flow in each of flat tube decrease in this sense.

16.6 Measurement conclusion

From the results conclude that every improvement bring benefit regarding heating performance however no one of them reached the target 5.5 kW (the best improvement - 12 channels tube reached 5.2 kW). If to be superposed benefit of 12 channel flat tube and fin with Fin pitch 1.1 the performance 5.3 kW should be reached however this must be confirmed by measurement of prototype in this definition.

Current temperature homogeneity of tested sample is pure and should be improved by other development.

17 Possible steps of other development

Regarding heating performance the easiest way how to increase performance is other fin pitch reduction. Deeper analyses will take fin shape optimisation with help one of CFD software in regime flow with heat transfer.

During investigation was also detected that in the top tank is hot stream on the inlet influenced by cold stream on the outlet of tank as there is heat conduction threw wall. This heat exchange in fact steals the performance as the heat is not exchange with the air. This phenomenon was confirmed with one prototype sample with air gap between hot stream and cold stream (to prevent heat conduction). This prototype brings benefit + 350W vs. the same prototype with tank in without this gap.

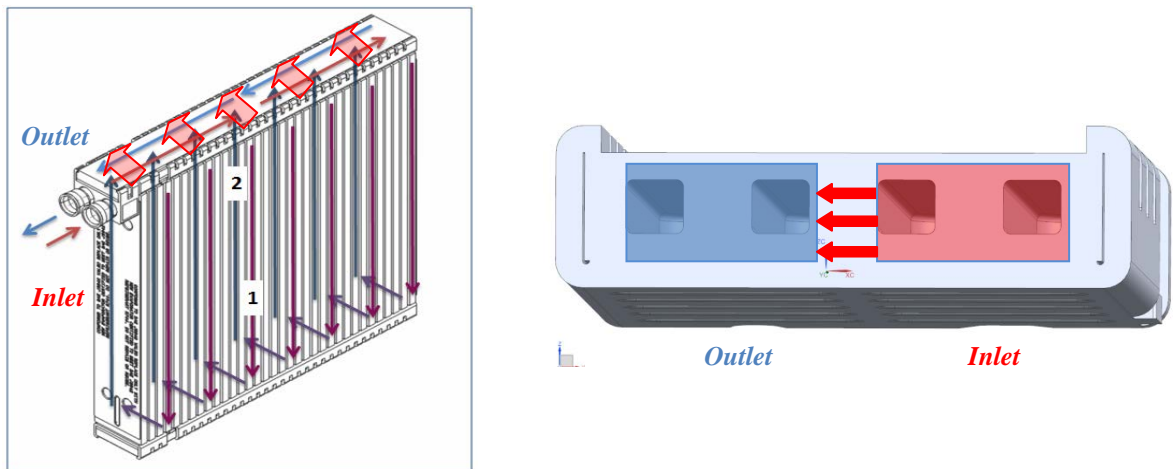


Figure 17-1: Heat conduction through wall

The temperature unbalance - dT of inner gas cooler could be improved by mass flow unification in each tube. This could be easily realised by restriction of refrigerant flow per each single tube. This restriction could be realised by additional component, where diameters of holes are variable and does (feed) the right refrigerant amount to each single flat tube – „Feeding plate”. To find optimal restriction the CFD calculation must be launched. The prototypes must be built and tested.

However all this design change must be optimised from mechanical point of view by FEM and their robustness must be confirmed by real tests.

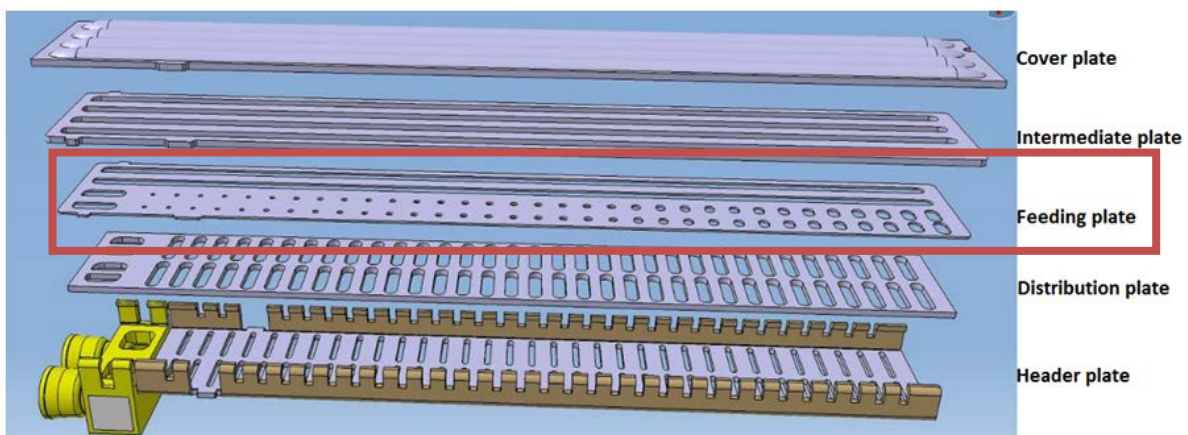


Figure 17-2: Top tank assembly with feeding plate allows right refrigerant distribution

18 Conclusion

In the theoretical part of this thesis was firstly described the cooling cycle and basic calculation of this cycle. The chapters explain differences and benefits of R744 (CO₂) vs. conventional refrigerant used in automotive follows. As the Inner gas cooler (IGC) is component for R744 heat pump system was this system and role of IGC inside described also. As for right function and performance of heat exchanger must be thermodynamics principal taken in to account - the chapters about mass and heat transfer related to design of heat exchangers are incorporated to this thesis. The physical principles are further used during design itself. In the last theoretical chapter the aluminium heat exchangers were described. It was focused to their main features, materials and manufacturing technology.

In the practical part of the thesis were firstly introduced IGC requirements given by Valeo Company. The IGC design should outcome from heat exchangers which are currently in company portfolio as some of their components could be used in Inner gas cooler design. As the most suitable for redesign was selected "R744 evaporator". By the static and fatigue test were determined mechanical the weakest point of this Evaporator – top tank. To determine robustness of other components in evaporator the FEM analyses was done. For material inputs tensile test at 130 °C (maximal possible temperature in IGC) was realised. The FEM result was confirmed by real mechanical test on the components. Unsatisfactory components were detected and strengthened by optimal design. Tanks components were fully redesign to meet requirements regarding IGC circuiting (to be 2 pass). The Inner gas cooler prototypes were built and tested by static and fatigue tests. These prototypes meet the mechanical requirements are ready for full validation.

1D calculation was launched to determine heating performance of IGC definitions. The outputs of initial calculation were that heating performance of definition (already validated mechanically) does not meet heating performance requirements. To reach this performance requirements several design modifications (optimisation of refrigerant side and air side) was proposed and calculated. According to calculation the best design definition should reached heat performance target 5.5 kW

To evaluate simulation results the prototypes of heat exchangers were built and measured with support of test engineers on the test bench in Bad Rodach. The simulation results were confirmed with some deviations vs. calculation (max. 170 W). However it was determined that if to be built the prototype where to be implemented all improvements - 5.3 kW to be measured and target 5.5 kW will not be reached. From measurement was also known that all IGC definitions were very temperature inhomogeneous. In the last chapter are mentioned other possible future improvements which should be deeper investigated. With these improvements the requirement should lead to achievement of heating performance target and considerably improvement of temperature homogeneity of heat exchanger.

Sources:

- [1] Holeček, M.: Materials for course: "Termomechanika", FST ZČU ac. year: 2014/15, unpublished
- [2] Lehocký, M.: Automobilová klimatizační jednotka [online]. 2016 [cit. 2016-10-02]. Downloaded from: <<http://stc.fs.cvut.cz/pdf/LehockyMarek-335939.pdf>>
- [3] Kalčík, J.: Technická termodynamika. Praha, ČSAV, 1963
- [4] Mareš, M.: Kapitoly z termomechaniky. Plzeň, 2008
- [5] SWEP: The refrigerant handbook [online]. 2017 [cit. 2017-08-03]. Downloaded from: <<https://www.swep.net/refrigerant-handbook/refrigerant-handbook/>>
- [6] Petrák, M: Chladicí technika [online]. 2017 [cit. 2017-08-03]. Downloaded from: https://www.ib.cvut.cz/sites/default/files/Studijni_materialy/CHTC/Petrak_Chladici_technika_cviceni.pdf
- [7] Watson, K.: ENERGY CONVERSION - THE EBOOK [online]. 2017 [cit. 2017-13-05]. Downloaded from: <<http://www.personal.utulsa.edu/~kenneth-weston/>>
- [8] Team of authors: Thermodynamics 3 – trainings material of THS – Valeo, 2015, unpublished
- [9] Žitek, P.: Materials for course: „Základy stavby energetických strojů“ na FST ac. year: 2014/2015, unpublished
- [10] Carbon Dioxide (R744) - The Newefrigerant 2017 [cit. 2017-08-03]. Downloaded from: https://www.ohio.edu/mechanical/thermo/Intro/Chapt.1_6/Chapter4c.html
- [11] Fuks, J.: Analýza závislosti chladícího faktoru, hmotnostní a objemové chladivosti transkritického oběhu s oxidem uhličitým na teplotě okolí a na tlaku ve vysokotlakém výměníku tepla, bacalor thesis [online]. 2016 [cit. 2016-10-02]. Downloaded from: https://alfred.uk.zcu.cz/F/L3RJGC1NGBRY4NPCHGM9ADPG1NF3TPNCNAMNXLC8AXV N5Y44K9-02825?func=full-set set&set_number=000875&set_entry=000006&format=999
- [12] Materials for course: „Aplikovaná termomechanika“, ČVUT ac. Year: 2011/2011, [online] 2017 [cit. 2017-08-03]. Downloaded from: <http://tzb.fsv.cvut.cz/files/vyuka/125yatm/prednasky/125yatm-06.pdf>
- [13] Cengel, Y et Ghajar, A.: Heat and mass transfer, New York, McGraw-Hill Education, 2015
- [14] Mayer, J. Course: Heat transfer, lecture 35 [online]. 2018 [cit. 2018-01-01]. Downloaded from: <https://www.youtube.com/watch?v=R9fpOcwLlLoA>
- [15] Cengel, Y et Boles, M.: Thermodynamics and engineering approach, New York, McGraw-Hill Education, 2015
- [16] Garcia et. Al.: Braz3 – internal training material, Valeo THS – nonpublished, 2005
- [17] Applications–Power train – Heat exchangers 2017 [cit. 2017-13-05]. Downloaded from: <https://european-aluminium.eu/media/1583/aam-applications-power-train-7-heat-exchangers.pdf>
- [18] Michna et al.: Encyklopedie hliníku. Prešov. Adin s. r. o., 2005
- [19] Controlled Atmosphere Aluminum Brazing Systems – downloaded from: <https://www.secowarwick.com/wp-content/uploads/assets/Documents/Brochures/Controlled-Atm-Alum-Brazing-Systems.pdf>
- [20] Cengel, Y et Cimbala, J.: Fluid mechanics, New York, McGraw-Hill Education, 2014
- [21] A. J. Ghajar, C. C. Tang, and W. L. Cook. "Experimental Investigation of Friction Factor in the Transition Region for Water Flow in Minutubes and Microtubes." Heat Transfer Engineering, Vol. 31, No. 8 (2010), pp. 646–657.

List of appendices:

Appendix NO. 1: Assembly drawing - Inner gas cooler assembly

Appendix NO. 2: Assembly drawing – Inner gas cooler core assembly

Appendix NO. 3: Assembly drawing – Inner gass cooler top tank assembly